Universidade de Aveiro Departamento de Química
2021

ANA MIGUEL DA SILVA LOUREIRO

Removal of albumin from platelet lysates for the fabrication of hydrogels for 3D cell culture

Remoção de albumina de lisados de plaquetas para a fabricação de hidrogéis para cultura 3D de células

Universidade de Aveiro Departamento de Química
2021

ANA MIGUEL DA SILVA LOUREIRO

Removal of albumin from platelet lysates for the fabrication of hydrogels for 3D cell culture

Remoção de albumina de lisados de plaquetas para a fabricação de hidrogéis para cultura 3D de células

Dissertação apresentada à Universidade de Aveiro para cumprimento dos requisitos necessários à obtenção do grau de Mestre em Bioquímica, realizada sob a orientação científica da Doutora Mara Guadalupe Freire Martins, Investigadora Coordenadora do Departamento de Química da Universidade de Aveiro e da Doutora Catarina de Almeida Custódio, cofundadora e investigadora da empresa METATISSUE.

Aos meus pais

o júri

presidente	Prof. Doutor Francisco Manuel Lemos Amado Professor associado com agregação da Universidade de Aveiro
vogal – arguente principal	Doutora Sandra Cristina da Silva Bernardo Investigadora do Centro de Investigação em Ciências da Saúde da Faculdade de Ciências da Saúde da Universidade da Beira Interior
vogal - orientador	Doutora Catarina de Almeida Custódio Co-fundadora e investigadora na spin-off Metatissue

agradecimentos

Gostaria de começar por agradecer ao Professor Doutor João Mano e à Doutora Catarina Custódio a oportunidade que me deram de poder fazer parte do seu projeto, a METATISSUE. Um obrigada especial à Cátia, que me foi acompanhando mais de perto, pelos ensinamentos e pela disponibilidade.

Gostaria também de agradecer à Doutora Mara Freire por ter aceite o desafio proposto pela METATISSUE e por me ter recebido no seu grupo de investigação. Um obrigada especial ao Emanuel pelos ensinamentos, acompanhamento e motivação, à Ana pelo companheirismo, à Marguerita pelas trocas de ideias e à Rita pela boa disposição.

À minha família e amigos o maior agradecimento de todos. Aos meus pais um agradecimento muito especial, pois foram eles que me guiaram até aqui, na esperança de me darem um futuro melhor e foi por eles que me esforcei por manter o rumo. Ao meu irmão por me distrair e fazer rir. À Beatriz pelas chamadas para fazer o balanço da situação e à Francisca pela empatia. Por último, o meu maior agradecimento ao Rodrigo por todo o apoio nestes últimos tempos.

palavras chave Cultura 3D, hidrogéis, lisados de plaquetas, sistemas aquosos bifásicos, sistemas de partição de três fases, remoção de albumina, proteínas

resumo A transição da segunda para a terceira dimensão é crucial para melhorar a fiabilidade e a capacidade de previsão dos ensaios celulares, motivando o desenvolvimento de plataformas capazes de recapitular o microambiente celular fisiológico *in vitro*. As proteínas naturalmente presentes no corpo humano têm atraído atenção como biomateriais para o fabrico de plataformas, devido à sua semelhança bioquímica com os tecidos nativos e a sua potencial origem alogénica. Neste contexto, a METATISSUE desenvolveu um novo hidrogel fotopolimerizável baseado em proteínas de lisados de plaquetas humanas (PL). Apesar do grande desempenho nos testes de encapsulação celular, as células cultivadas na superfície não aderem, e a remoção da albumina de soro humano (ASH) foi proposta como uma estratégia para melhorar este aspeto. Sendo assim, o objetivo do presente trabalho foi a remoção de ASH dos PL usando sistemas de partição de três fases à base de sistemas aquosos bifásicos (SAB). Estes sistemas foram estudados seguindo duas abordagens, nomeadamente pela precipitação seletiva da ASH na interfase do sistema ou migração para uma das fases. Para isso, avaliaram-se oito SAB compostos por diferentes componentes formadores de fase. O sistema PEG 1000/tampão citrato apresentou o melhor desempenho, sendo que 53% da massa total de ASH dos PL fica retida na fase rica em PEG, enquanto que as restantes proteínas precipitam na interfase. Esta fração precipitada pode ser facilmente isolada e utilizada como uma fração de PL com um conteúdo de albumina reduzido (AD-PL). Este sistema foi aumentado em termos de escala (até cerca de 50 g) e a AD-PL obtida foi modificada com anidrido metacrílico (AD-PLMA), permitindo a formação de hidrogéis derivados de AD-PLMA.

keywords 3D cell culture, hydrogels, platelet lysates, aqueous biphasic systems, three-phase partitioning, albumin removal, proteins

abstract The transition from the second to the third dimension is crucial to improve the reliability and predictive ability of cell-based assays, motivating the ongoing research on scaffold development to develop *in vitro* systems that could recapitulate the physiological cellular microenvironment. Proteins naturally occurring in the human body have been attracting attention as biomaterials for scaffold fabrication, due to their biochemical similarity with native tissues and potential allogenic source. In this context, METATISSUE has developed a novel photopolymerizable hydrogel based on human platelet lysates (PL) proteins. Despite the great performance in cell encapsulation tests, seeded cells do not adhere properly and the removal of human serum albumin (HSA) was proposed as a reliable approach to overcome this drawback. Herein, the goal of the presented work was the removal of HSA from PL using three phase partitioning (TPP) systems based on aqueous biphasic systems (ABS). These systems were investigated following two approaches, namely by the selective precipitation of HSA at the interphase or by the selective migration of the protein to one of the phases of ABS. A screening of eight ABS composed of different phase-forming components was performed. The ABS composed of PEG 1000/citrate buffer presented the best performance, being 53% of the total HSA mass of PL retained at the top phase, while the remaining PL proteins precipitate at the interphase. These precipitated proteins can be easily isolated and used as an albumin-depleted PL (AD-PL) fraction for hydrogel fabrication. This system was then scaled-up (up to ca. 50 g) and the AD-PL obtained was modified with methacrylic anhydride (AD-PLMA), allowing the successful AD-PLMA hydrogel formation.

Contents

List of tables

List of figures

List of abbreviations

[Bu_3NC_4]Br	tri(n-butyl)[4-ethoxy-4-oxobutyl]ammonium bromide
[Bu_3PC_2]Br	tri(n-butyl)[2-ethoxy-2-oxoethyl]phosphonium bromide
[P_{4444}]Br	tetrabutylphosphonium bromide
2D	two-dimensional
3D	three-dimensional
ABS	aqueous biphasic systems
AD-PL	albumin-depleted platelet lysates
AGB-IL	glycine-betaine analogue ionic liquid
BM-MSCs	bone-marrow mesenchymal stem cells
BMP-2	bone morphogenetic protein 2
BSA	bovine serum albumin
CA	cellulose acetate
ChCl	cholinium chloride
CMa	collagen membranes with aligned fibers
CMr	collagen membranes with radomnly orientated fibers
CMs	collagen membranes
DHT	dehydrothermal treatment
ECM	extracellular matrix
EDC	ethyl-3(3-dimethylamino) propyl carbodiimide
ELPs	elastin-like polypeptides
FBS	fetal bovine serum
FK	feather keratin
GAG	glycosaminoglycan
GelMA	methacrylated gelatin
GFs	growth factors
GMA	glycidyl methacrylate
GTA	glutaraldehyde
HA	hyaluronic acid
HAp	hydroxyapatite
hASCs	human adipose stem cells

HHK	human hair keratins
HPA	hydroxyphenylacetic acid
HSA	human serum albumin
I-2959	Irgacure 2959
IL	ionic liquid
ILTPP	ionic liquid-based three phase partitioning
KeratATE	keratin allyl thioether
MA	methacrylic anhydride
MMP	matrix metalloproteinase
mTGase	microbial transglutaminase
NB	norbornene
OVA	ovalbumin
PBS	phosphate buffered saline
PCL	polycaprolactone
PDAC	pancreatic ductal carcinoma
PEG	polyethylene glycol
PL	platelet lysates
PLMA	methacrylate platelet lysates
PPG	polypropylene glycol
PRF	platelet-rich fibrin
PRP	platelet-rich plasma
PSA	porcine serum albumin
RCP	ruthenium catalyzed photocrosslinking
SDS-PAGE	sodium dodecyl sulfate polyacrylamide gel electrophoresis
SE-HPLC	size-exclusion high-performance liquid chormatography
SMCs	smooth muscle cells
TE	tissue engineering
TGase	transglutaminase
THPC	tetrakis(hydroxymethyl)phosphonium chloride
TPP	three-phase partitioning
UV	ultra-violet
VEGF	vascular endothelial growth factor

Chapter I

Background

Background

Abstract

Cell-based assays have been proven to be an indispensable tool either to further our knowledge on the physiological mechanisms underlying cell behavior and tissue development, as also to the development of new drugs. Traditionally, these studies have been conducted on two-dimensional (2D) substrates, however, the oversimplified conditions under which cells are cultured lead to misleading data. Therefore, on an attempt to bridge the gap between *in vitro* cell culture and *in vivo* tissues and thus increase the reliability and predictive ability of cell-based assays, three-dimensional (3D) cell culture models have emerged, and scaffold-based models have been attracting particular attention since they can recapitulate several biochemical and biophysical aspects of the native extracellular matrix (ECM). In this sense, METATISSUE developed a novel photopolymerizable hydrogel derived from platelet lysates (PL) proteins and currently aims at the improvement of its biochemical properties, which involves the removal of HSA from PL. Aqueous biphasic systems (ABS) have been widely reported for the extraction of biomolecules and more recently have also demonstrated the ability to behave as three-phase partitioning (TPP) systems. Therefore, in the present work, various ABS will be explored aiming to find the best ABS-based TPP system for the removal of HSA from PL.

1. Cell culture: from the second to the third dimension

In vitro cell culture constitutes a fundamental tool for the investigation of complex cellular processes that occur *in vivo,* by allowing the maintenance of living cells outside the organism and, therefore, their study. Cell-based assays are at the foundation of the current knowledge on fundamental cellular and molecular biology and are indispensable for the biotechnological and pharmaceutical industries. In traditional cell culture methods, cells are typically grown as a monolayer on a rigid and flat artificial substrate, like Petri dishes or culture flasks, supplemented with a nutritious medium, and maintained at body temperature[1]. These two-dimensional (2D) cell culture methodologies present some attractive features, such as the ease of handling, well-established protocols, low-cost, and the continuous improvements made in 2D cell culture platforms and functional tests, that have been

contributing to their widespread[2]. However, the conditions of the monolayer systems are very unnatural and several studies clearly evidence that due to the confinement to a planar environment, 2D growing cells lack complex morphological processes and present forced polarity, whereby only a segment of the cell membrane can interact with the extracellular matrix (ECM) and neighboring cells, while the rest of the cell is exposed to a homogeneous concentration of nutrients and soluble factors present in the culture media (Figure I.1)[3,4]. Those alterations in cell morphology, polarity, cell-cell and cell-ECM interactions, and access to nutrients and signaling molecules, ultimately influence numerous fundamental cellular processes, including differentiation, proliferation, apoptosis, numerous signaling pathways, and expression of genes and proteins, resulting in abnormal cell function and behavior[5,6]. As a result, the data obtained from such experiments could be misleading and non-predictive regarding what happens *in vivo*, thus contributing to the gap in our understanding of mammalian tissue cell biology and, in part, to the low success rate of preclinical assays to predict *in vivo* drug responses[7]. Therefore, the development of cell culture platforms that better mimic the native ECM is fundamental to overcome the limitations of 2D cell culture assays and thus increase the reliability and predictive ability of cell-based studies.

The ECM of mammalian tissues is a complex and dynamic structure, that comprises a 3D network of fibrillar proteins, like collagen, elastin, fibronectin, and laminin, surrounded by a highly hydrated matrix of proteoglycans, glycoproteins, and glycosaminoglycans, that is constantly remodeled by cells during tissue morphogenesis, homeostasis, and regeneration[8]. Besides the physical support to the cellular constituents of tissues, the ECM also contributes with important biochemical cues, such as gradients of nutrients, cytokines, growth factors, and other signaling molecules, that regulate cell behavior. The ECM-cell crosstalk is therefore pivotal for the maintenance of tissue function. Changes in ECM's chemical and mechanical properties have been reported to be associated with the development and progression of several pathologies, such as cancer, muscular dystrophies, cardiomyopathies, and atherosclerosis, highlighting the importance of this structure in tissue functionality[9].

Three-dimensional (3D) cell culture systems have emerged as an alternative to shorten the gap existing between the traditional 2D models and *in vivo* tissues[10,11]. 3D cell culture models recreate important biochemical gradients as well as cell interaction with the

surrounding extracellular environment and neighboring cells. 3D cell culture models represent a more physiologically relevant and better *in vitro* representation of native tissues when compared to their conventional 2D counterparts[12,13] (FigureI.1). Due to the reported increased predictive ability of cell-based drug and toxicity assays conducted on 3D platforms, these models may constitute a reliable alternative to the use of experimental animals in pre-clinical research, addressing the 3Rs (replacement, reduction, and refinement) policy for the use of animals in biomedical research and diminishing the costs associated with the drug discovery process[14]. Moreover, by enabling the manipulation of the chemical composition, biological cues, and physical properties of the cell microenvironment, 3D culture systems can be employed to study the ability of cells to sense and decode the surrounding information and for tissue engineering (TE) applications[15,16].

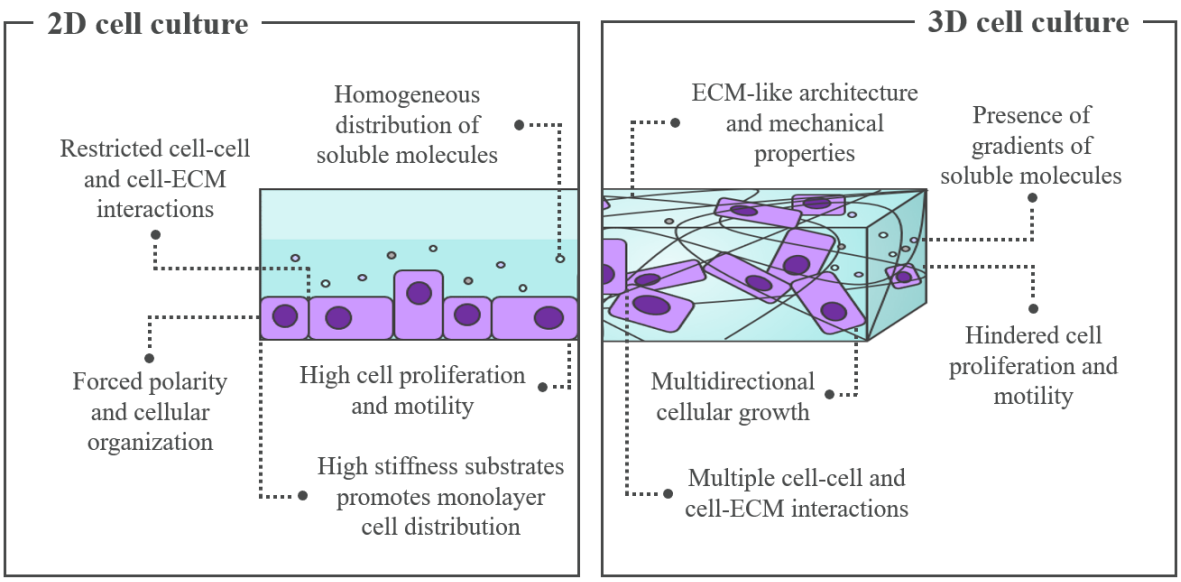

Figure I.1 Schematic representation of the differences between cell culture in 2D and 3D platforms.

2. *In vitro* 3D cell culture models

3D cell culture techniques can be divided into two main categories: scaffold-free and scaffold-based systems. Scaffold-free models rely on the inherent ability of some cells to aggregate in specific conditions and form spheroids. Monoculture or co-culture techniques employed on the development of such models include round-bottom ultra-low attachment

plates, magnetic levitation, pellet culture, hanging drop, spinner culture, rotating wall vessels, and microfluidics[17,18]. Cellular spheroids with high cell densities can recreate the *in vivo*-like microenvironment regarding cell-cell communication, and as cells synthesize their own ECM, they can also mimic cell-ECM interactions[19,20]. The oxygen and nutrients gradient established across the spheroid resemble what happens in solid avascular tumors, a necrotic/hypoxic core surrounded by a proliferative zone. Diffusion barriers established on spheroids are also interesting for drug-related assays and, for that reason, such systems have been particularly explored in cancer-related research. Regardless of the potential applications and the advances made on spheroid culture procedures, there is still room for improvement, since the current methods for spheroids' production can be time-consuming, labor-intensive, expensive, and not scalable[21]. Furthermore, spheroids are limited to low cell numbers and certain cell-types, restricting their versatility.

In scaffold-based models, cells are cultured in 3D scaffolds that are designed to recreate the extracellular microenvironment provided by the ECM in native tissues and thus recapitulate cell processes that are driven by cell-ECM and cell-cell interactions. Scaffold-based models are essential not only for *in vitro* cell-based studies but also make part of TE' triad, providing the structural support and cell guidance needed for the development of functional tissues *in vitro*[22]. Scaffolds for cell culture and TE should match some fundamental properties such as biocompatibility, biodegradability, bioactivity, mechanical stability, and a molecular architecture that provides space for cell growth and that facilitates the exchange of nutrients and waste metabolites[23]. Such properties play a crucial role in cell behavior and are highly dependent on the materials and production techniques employed in scaffold fabrication. Among the myriad of available scaffold-based platforms, hydrogels have attracted particular attention. Consisting of a 3D network of hydrophilic polymeric chains formed by intermolecular or supramolecular crosslinking, hydrogels present tissue-like mechanical properties, structural organization, and gradients of soluble molecules, like nutrients, oxygen, and metabolites, recapitulating several key aspects of native ECM[24].

Synthetic and natural polymers are the preferred materials for the fabrication of 3D scaffolds, due to the ease of tunability of their chemical and structural properties. On one hand, synthetic polymers present some attractive features, like the well-defined, tunable, and reproducible mechanical and physicochemical properties[25]. However, their low biocompatibility, lack of biofunctionality, and potential cytotoxicity may limit their

applicability. On the other hand, naturally-derived polymers usually grant great biocompatibility, biodegradability, and bioactivity, due to the chemical similarity with biological constituents of tissues and the presence of biological motifs on their structure that can be recognized by cell surface receptors, promoting cell adhesion and proliferation, and of enzyme binding sites, enabling biological degradation[26]. However, the batches' variability and the risk of immunogenicity, commonly associated with polymers from natural sources, may affect the reproducibility of experimental outcomes and restrict their biomedical applications. Furthermore, natural scaffolds are usually mechanically weak and exhibit fast degradation rates. In this regard and in an attempt to combine the well-defined tunable physicochemical properties of synthetic polymers with the intrinsic biological properties of natural polymers, semisynthetic polymers have emerged, that can be obtained either by adding chemical moieties to natural polymers or bioactive motifs to synthetic ones[27].

3. METATISSUE

The growing evidence of the potential of 3D cell culture platforms to bridge the gap between the traditional 2D cell culture and *in vivo* animal models and to engineer tissue-like constructs for TE has contributed to the exponential growth of the 3D cell culture market in the past years. Protein-based hydrogels and ECM-derived substrates, as is the case of type I collagen (e.g., RAFT, PureCol, and RatCol) and solubilized basement membrane of Engelbreth-Holm-Swarm mouse sarcoma cells (e.g., Cultrex, ECM Gels, Geltrex, and Matrigel) respectively, are currently considered the gold standards for 3D cell culture, holding the largest market share. However, despite their great biological performance, the difficulty of handling, inability to modify their mechanical properties to match that of native tissues and their animal origin restrict their application. Therefore, there is still a need to develop advanced platforms that combine the bioactivity of natural materials and the tunability of synthetic ones. This has motivated the continuous search for alternatives and opened opportunities for novel companies, as is the case of METATISSUE, a start-up founded in 2018 by researchers from the University of Aveiro, which focus is the design and development of protein-based materials for 3D cell culture derived from human fluids and tissues donated by hospitals and clinical institutions. Their human-derived products promise to increase the accuracy of in vitro studies by providing realistic microenvironments to cells,

addressing the needs of life science researchers, biotechnological and pharmaceutical companies, and diagnostic centers, aiding in the development of living tissue constructs and furthering our knowledge in cell's biology.

The R&D team of METATISSUE developed and patented a 3D cell culture platform derived from human platelet lysates (PL). This novel material was recognized for its ability to support cells function *in vitro*, while maintaining the desirable stability, as well as for its tunable mechanical and biochemical properties, which renders it a user-customizable character. Although platelet rich plasma (PRP) and PL-based hydrogels have already been explored as 3D cell culture platforms, they have poor mechanical properties and poor stability *in vitro*[28]. METATISSUE's product overcomes these limitations, through the methacrylation of PL (PLMA), producing PL-based photopolymerizable materials whose properties can be tailored by varying the degree of functionalization and/or PLMA concentration[29]. In the present year, the company is focused on introducing this product to the market, while maintaining the laboratory research work, so that new, equally innovative and efficient products are developed.

A specific research line in the company is focused on the optimization and control over the biochemical properties of the PL based hydrogels. PL are a cocktail of proteins, comprising multiple growth factors (GFs), cytokines, and other bioactive molecules that are involved in numerous cellular processes and are the major contributors to the bioactivity of PL-based hydrogels[28,30]. However, despite the good results obtained with encapsulated cells, seeded cells did not adhere properly to the hydrogel. Looking at PL biochemical composition, the high amounts of humans serum albumin (HAS) (approximately 41% of the total peptides found in PL[30]) may explain this phenomenon, since poor cell attachment is commonly observed in albumin-based scaffolds[31]. Therefore, it was hypothesized that decreasing the HSA content on PL, and hence the relative increase in bioactive molecules, will result in PL-based photopolymerizable hydrogels with superior ability to promote cell adhesion.

4. Aqueous biphasic systems-based three-phase partitioning

Aqueous biphasic systems (ABS) are ternary mixtures composed of water and non-volatile solutes, typically two polymers, a polymer and a salt, or two salts, that above a certain concentration undergo separation and form two coexisting immiscible phases, each one enriched in one of the phase-forming components, and thus providing a selective

environment that favors the preferential partition of a target biomolecule[32]. First proposed by Albertson[33] as alternative liquid-liquid extraction/purification techniques, ABS have been attracting considerable attention as alternative methods for the purification and extraction of proteins due to the highly biocompatible environment that they offer, since they are mainly composed of water and once the majority of the polymers used on their formation have a stabilizing effect over proteins' ternary structure. Moreover, since the use of hazardous volatile organic solvents, common to more traditional liquid-liquid methods, is avoided in ABS preparation, this technique has been considered as a cost-effective and environmentally friendly alternative[34]. Additionally, ABS allow the extraction/purification and concentration in a single-step, are relatively simple to use, and can be easily scaled-up.

The selective partitioning of a target protein in an ABS is a complex process that is not yet fully understood, but is known to be influenced by multiple factors, including proteins' physicochemical properties (molecular weight, conformation, and surface charge and hydrophobicity), ABS' parameters (type and concentration of the phase-forming components, ionic strength, pH, and temperature), and the interactions established between the proteins and the phase-forming components[35]. The manipulation of ABS parameters has therefore been investigated to achieve desired partition profiles and different types of systems have emerged. Among the myriad of ABS studied, polyethylene glycol (PEG)-dextran and PEG-salt systems are the most widely used for protein separation. Between them, PEG-salt systems present some advantages such as the lower viscosity and lower cost of the salts used as phase forming components comparatively to dextran[36]. Carbonate, phosphate, and sulfate anions have been commonly used as the salting-out inducing salts in the formation of PEG-based ABS; however, their accumulation in effluent streams raise some environmental issues[37]. Hence, citrates have been proposed as more biodegradable and non-toxic substitutes for phosphate and sulfate salts in PEG-salt ABS formation.

More recently, in addition to the widely investigated polymer-based and polymer-salt systems, Rogers *et al.*[38] reported the formation of ABS by mixing inorganic salts with ionic liquids (ILs) aqueous solutions. ILs are salts with melting points below 100°C that are usually composed of a large organic cation and an organic/inorganic anion[39]. Due to their ionic nature, most ILs present negligible volatility and non-flammability at atmospheric conditions, high thermal and chemical stabilities, and strong solvation ability for a variety of compounds. Nevertheless, one of the most advantageous features of ILs is their tailorable

polarity, hydrophobicity, and viscosity, resulting from the numerous anion-cation design possibilities, which is further extended for IL-based ABS, overcoming the restricted polarity range associated with more traditional polymer-based systems and thus increasing the selectivity and extraction efficiencies for a target protein[40].

Within the field of IL-based ABS, Alvarez *et al.*[41] proposed for the first time the concept of IL-based three-phase partitioning (ILTPP). TPP has been previously reported as a simple technique for protein purification and concentration through the precipitation of a target protein at the liquid-liquid interface between an organic phase of *tert*-butanol and an aqueous solution of ammonium sulfate that can be easily isolated, do not requiring back-extraction steps[42]. Nevertheless, traditional TPP approaches make use of traditional organic solvents. The use of IL-based ABS in ILTPP approaches overcome this disadvantage and therefore ILTPP presents as a promising alternative for protein recovery, combining the advantages of IL-based ABS and TPP, and has been extended to other ABS[41]. Herein, the concept of TPP using different types of ABS will be explored to obtain albumin-depleted PL (AD-PL) fractions through two possible mechanisms: a) by the precipitation of HSA and subsequent recovery of the remaining proteins in one of the ABS' phases or b) by the preferential retention of HSA in one of the ABS' phases and recovery of the remaining proteins in a solid third layer (Figure II.2).

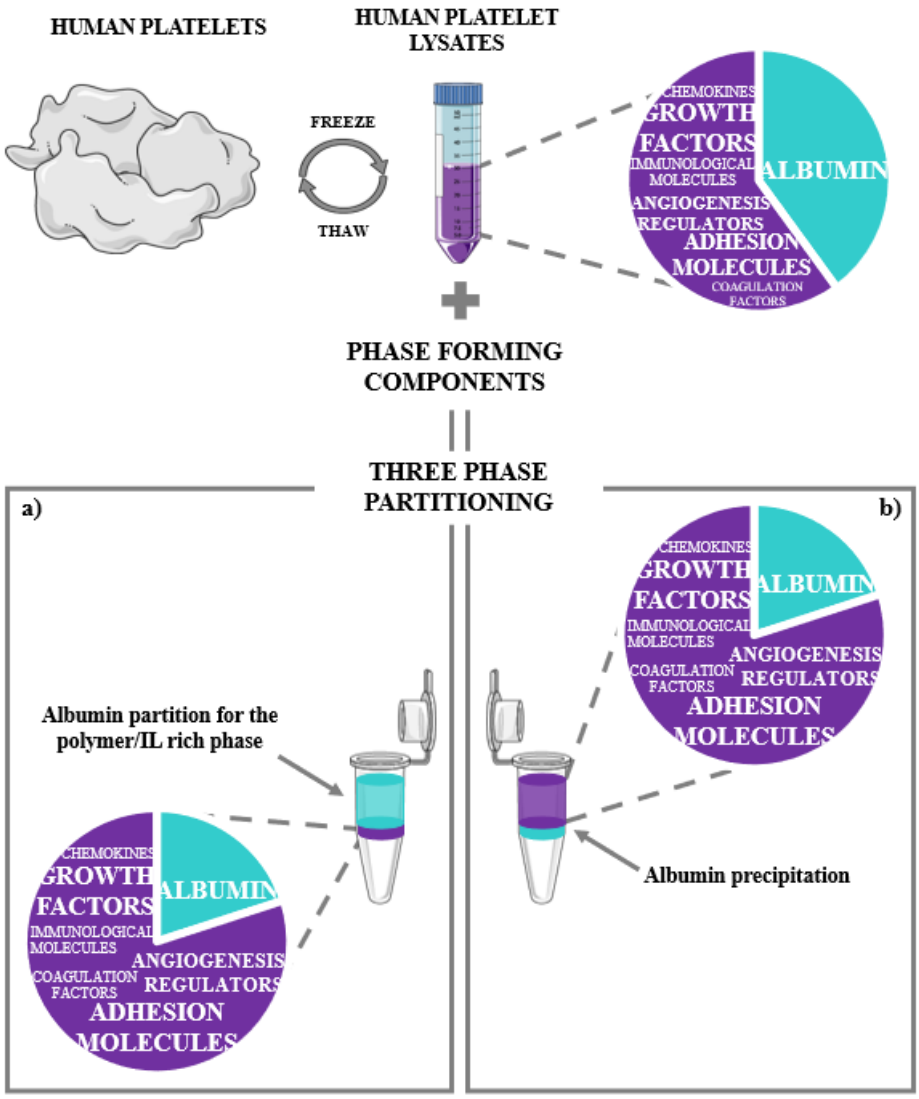

Figure II.2 Schematization of albumin removal from PL following an ABS-based TPP approach, either by a) albumin partition for the polymer/IL rich phase and precipitation of the remaining PL proteins at the interphase, or b) albumin precipitation at the interphase and partitioning of the remaining PL proteins for the polymer/IL rich phase.

References

1. Breslin, S. & O'Driscoll, L. Three-dimensional cell culture: The missing link in drug discovery. *Drug Discovery Today* **18**, 240–249 (2013).
2. Edmondson, R., Broglie, J. J., Adcock, A. F. & Yang, L. Three-Dimensional Cell Culture Systems and Their Applications in Drug Discovery and Cell-Based Biosensors. *Assay Drug Dev. Technol.* **12**, 207–218 (2014).
3. Cukierman, E., Pankov, R., Stevens, D. R. & Yamada, K. M. Taking cell-matrix adhesions to the third dimension. *Science (80-.).* **294**, 1708–1712 (2001).
4. Kapałczyńska, M., Kolenda, T., Przybyła, W., Zajączkowska, M., Teresiak, A., Filas, V., Ibbs, M., Bliźniak, R., Łuczewski, Ł. & Lamperska, K. 2D and 3D cell cultures – a comparison of different types of cancer cell cultures. *Arch. Med. Sci.* **14**, 910–919 (2018).
5. Birgersdotter, A., Sandberg, R. & Ernberg, I. Gene expression perturbation in vitro - A growing case for three-dimensional (3D) culture systems. *Seminars in Cancer Biology* **15**, 405–412 (2005).
6. Weaver, V. M., Petersen, O. W., Wang, F., Larabell, C. A., Briand, P., Damsky, C. & Bissell, M. J. Reversion of the malignant phenotype of human breast cells in three-dimensional culture and in vivo by integrin blocking antibodies. *J. Cell Biol.* **137**, 231–245 (1997).
7. Hay, M., Thomas, D. W., Craighead, J. L., Economides, C. & Rosenthal, J. Clinical development success rates for investigational drugs. *Nat. Biotechnol.* **32**, 40–51 (2014).
8. Hynes, R. O. The Extracellular Matrix: Not Just Pretty Fibrils. *Science (80-.).* **326**, 1216–1219 (2009).
9. Bonnans, C., Chou, J. & Werb, Z. Remodelling the extracellular matrix in development and disease. *Nature Reviews Molecular Cell Biology* **15**, 786–801 (2014).
10. Custódio, C. A., Reis, R. L. & Mano, J. F. Engineering Biomolecular Microenvironments for Cell Instructive Biomaterials. *Adv. Healthc. Mater.* **3**, 797–810 (2014).
11. Pampaloni, F., Reynaud, E. G. & Stelzer, E. H. K. The third dimension bridges the

gap between cell culture and live tissue. *Nature Reviews Molecular Cell Biology* **8**, 839–845 (2007).

12. Mabry, K. M., Payne, S. Z. & Anseth, K. S. Microarray analyses to quantify advantages of 2D and 3D hydrogel culture systems in maintaining the native valvular interstitial cell phenotype. *Biomaterials* **74**, 31–41 (2016).
13. Baker, B. M. & Chen, C. S. Deconstructing the third dimension-how 3D culture microenvironments alter cellular cues. *Journal of Cell Science* **125**, 3015–3024 (2012).
14. Fang, Y. & Eglen, R. M. Three-Dimensional Cell Cultures in Drug Discovery and Development. *SLAS Discov. Adv. Sci. Drug Discov.* **22**, 456–472 (2017).
15. Drury, J. L. & Mooney, D. J. Hydrogels for tissue engineering: scaffold design variables and applications. *Biomaterials* **24**, 4337–4351 (2003).
16. Fisher, M. B. & Mauck, R. L. Tissue Engineering and Regenerative Medicine: Recent Innovations and the Transition to Translation. *Tissue Eng. Part B Rev.* **19**, 1–13 (2013).
17. Timmins, N. E., Harding, F. J., Smart, C., Brown, M. A. & Nielsen, L. K. Method for the generation and cultivation of functional three-dimensional mammary constructs without exogenous extracellular matrix. *Cell Tissue Res.* **320**, 207–210 (2005).
18. Achilli, T. M., Meyer, J. & Morgan, J. R. Advances in the formation, use and understanding of multi-cellular spheroids. *Expert Opinion on Biological Therapy* **12**, 1347–1360 (2012).
19. Ekert, J. E., Johnson, K., Strake, B., Pardinas, J., Jarantow, S., Perkinson, R. & Colter, D. C. Three-dimensional lung tumor microenvironment modulates therapeutic compound responsiveness in vitro - Implication for drug development. *PLoS One* **9**, (2014).
20. Doublier, S., Belisario, D. C., Polimeni, M., Annaratone, L., Riganti, C., Allia, E., Ghigo, D., Bosia, A. & Sapino, A. HIF-1 activation induces doxorubicin resistance in MCF7 3-D spheroids via P-glycoprotein expression: A potential model of the chemo-resistance of invasive micropapillary carcinoma of the breast. *BMC Cancer* **12**, (2012).
21. Mehta, G., Hsiao, A. Y., Ingram, M., Luker, G. D. & Takayama, S. Opportunities and challenges for use of tumor spheroids as models to test drug delivery and efficacy. *J.*

Control. Release **164**, 192–204 (2012).

22. O'Brien, F. J. Biomaterials & scaffolds for tissue engineering. *Materials Today* **14**, 88–95 (2011).
23. Slaughter, B. V., Khurshid, S. S., Fisher, O. Z., Khademhosseini, A. & Peppas, N. A. Hydrogels in regenerative medicine. *Advanced Materials* **21**, 3307–3329 (2009).
24. Nguyen, K. T. & West, J. L. Photopolymerizable hydrogels for tissue engineering applications. *Biomaterials* **23**, 4307–4314 (2002).
25. Zhu, J. & Marchant, R. E. Design properties of hydrogel tissue-engineering scaffolds. *Expert Review of Medical Devices* **8**, 607–626 (2011).
26. Jose, G., Shalumon, K. T. & Chen, J.-P. Natural Polymers Based Hydrogels for Cell Culture Applications. *Curr. Med. Chem.* **27**, 2734–2776 (2019).
27. Tibbitt, M. W. & Anseth, K. S. Hydrogels as extracellular matrix mimics for 3D cell culture. *Biotechnology and Bioengineering* **103**, 655–663 (2009).
28. Santos, S. C. N. da S., Sigurjonsson, Ó. E., Custódio, C. de A. & Mano, J. F. C. da L. Blood Plasma Derivatives for Tissue Engineering and Regenerative Medicine Therapies. *Tissue Eng. Part B Rev.* **24**, 454–462 (2018).
29. Santos, S. C., Custódio, C. A. & Mano, J. F. Photopolymerizable Platelet Lysate Hydrogels for Customizable 3D Cell Culture Platforms. *Adv. Healthc. Mater.* **7**, 1800849 (2018).
30. Santos, S. C., Custódio, C. A. & Mano, J. F. Photopolymerizable Platelet Lysate Hydrogels for Customizable 3D Cell Culture Platforms. *Adv. Healthc. Mater.* **7**, 1800849 (2018).
31. Ong, J., Zhao, J., Levy, G. K., Macdonald, J., Justin, A. W. & Markaki, A. E. Functionalisation of a heat-derived and bio-inert albumin hydrogel with extracellular matrix by air plasma treatment. *Sci. Rep.* **10**, 12429 (2020).
32. Freire, M. G., Cláudio, A. F. M., Araújo, J. M. M., Coutinho, J. A. P., Marrucho, I. M., Lopes, J. N. C. & Rebelo, L. P. N. Aqueous biphasic systems: a boost brought about by using ionic liquids. *Chem. Soc. Rev.* **41**, 4966 (2012).
33. Asenjo, J. A. & Andrews, B. A. Aqueous two-phase systems for protein separation: A perspective. *Journal of Chromatography A* **1218**, 8826–8835 (2011).
34. Rosa, P. A. J., Ferreira, I. F., Azevedo, A. M. & Aires-Barros, M. R. Aqueous two-phase systems: A viable platform in the manufacturing of biopharmaceuticals.

Journal of Chromatography A **1217**, 2296–2305 (2010).

35. Chow, Y. H., Yap, Y. J., Tan, C. P., Anuar, M. S., Tejo, B. A., Show, P. L., Ariff, A. Bin, Ng, E.-P. & Ling, T. C. Characterization of bovine serum albumin partitioning behaviors in polymer-salt aqueous two-phase systems. *J. Biosci. Bioeng.* **120**, 85–90 (2015).
36. Rito-Palomares, M. Practical application of aqueous two-phase partition to process development for the recovery of biological products. in *Journal of Chromatography B: Analytical Technologies in the Biomedical and Life Sciences* **807**, 3–11 (2004).
37. Perumalsamy, M. & Batcha, M. I. Synergistic extraction of bovine serum albumin using polyethylene glycol based aqueous biphasic system. *Process Biochem.* **46**, 494–497 (2011).
38. Gutowski, K. E., Broker, G. A., Willauer, H. D., Huddleston, J. G., Swatloski, R. P., Holbrey, J. D. & Rogers, R. D. Controlling the Aqueous Miscibility of Ionic Liquids: Aqueous Biphasic Systems of Water-Miscible Ionic Liquids and Water-Structuring Salts for Recycle, Metathesis, and Separations. *J. Am. Chem. Soc.* **125**, 6632–6633 (2003).
39. Seddon, K. R. A taste of the future. *Nat. Mater.* **2**, 363–365 (2003).
40. Pereira, J. F. B., Rebelo, L. P. N., Rogers, R. D., Coutinho, J. A. P. & Freire, M. G. Combining ionic liquids and polyethylene glycols to boost the hydrophobic–hydrophilic range of aqueous biphasic systems. *Phys. Chem. Chem. Phys.* **15**, 19580 (2013).
41. Alvarez-Guerra, E. & Irabien, A. Ionic Liquid-Based Three Phase Partitioning (ILTPP) for Lactoferrin Recovery. *Sep. Sci. Technol.* **49**, 957–965 (2014).
42. Dennison, C. & Lovrien, R. Three Phase Partitioning: Concentration and Purification of Proteins. *Protein Expr. Purif.* **11**, 149–161 (1997).

Chapter II

Proteins: versatile platforms for 3D cell culture

Proteins: versatile platforms for 3D cell culture

Abstract

Protein-based scaffolds hold great potential for the recreation of the complex extracellular matrix (ECM) *in vitro*. Therefore, the combination of different proteins and fabrication techniques have been widely reported in the last years and have been contributing to the advances made on scaffold design. This review focus on the recent advances on scaffolds fabrication using proteins naturally occurring in the human body.

1. Introduction

In vivo, cells are surrounded by a three-dimensional (3D) complex and dynamic network, the extracellular matrix (ECM), that not only gives physical support as also provides essential biochemical and biomechanical cues that guide cell adhesion, proliferation, and differentiation[1]. ECM is an heterogeneous fiber network comprising approximately 300 different proteins, including collagens, elastin, proteoglycans, and cell-biding glycoproteins, which are crucial for the maintenance of ECM structure, mechanical properties, and biological activities of tissues and organs[2]. Besides being the major ECM constituents, proteins can also be promptly degraded by enzymatic or hydrolytic cellular processes allowing cell-mediated matrix remodeling[3,4], and some of them inherit bioactive sequences, such as cell binding motifs, that promote cell adhesion and proliferation[5,6]. Therefore, due to their inherent bioactivity, biocompatibility, biodegradability, low toxicity, and abundance on native ECM, proteins hold great potential as biomaterials and have been commonly employed on the fabrication of scaffolds for 3D cell culture and TE applications[7]. Some of the most recent works using proteins naturally occurring in human tissues to fabricate 3D scaffolds, including collagen, keratin, and elastin, or blood plasma, like albumin, fibrinogen, and platelet concentrates, are described in the following sections.

2. Collagen

Collagens are the main constituents of ECM, being the most abundant proteins in the mammalian body, and accounting for around 20-30% of the total protein content[8]. This protein superfamily is essential for the maintenance of the structural integrity and mechanical strength of organs and tissues[9], and the control over cell adhesion, migration, and chemotaxis[10]. Up to date, there are 28 structurally different types of collagen identified among vertebrates[11]. Despite the variability, all types of collagen share a common structural motif, as all of them consist of a supercoiled right-handed triple helix, composed of three parallel left-handed polypeptide α-chains intertwined, also known as tropocollagen. In turn, these individual triple helices self-assemble in a sophisticated, hierarchical manner, giving rise to macroscopic structures such as fibers and intricate networks, typical of tendons and basement membranes, providing mechanical and structural support to the ECM[9]. This typical molecular architecture is strongly related to the characteristic amino acid composition of α-chains. Each α-chain is composed of Gly-Xaa-Yaa repeating units, where proline and hydroxyproline residues, respectively, predominantly occupy X and Y positions[12]. The short side chains of glycine allow the tight packaging of the polypeptide chains in the triple helix, while proline and hydroxyproline residues stabilize the triple helix structure, due to their ability to establish inter-chain hydrogen bonding and electrostatic interactions.

Due to its natural occurrence in human tissues, collagen is an attractive biopolymer for the development of 3D cell culture scaffolds, not only for its abundance but also for the inherent biochemical and structural activity that this biomolecule presents on tissue formation. Collagen-based biomaterials can be separated into two different groups in what concerns their origin. In one group are the biomaterials derived from decellularized tissues and organs, like porcine dermis, intestine or bladder submucosa, or human dermis[13]. This approach resorts to physical, chemical, or enzymatic treatments to remove cells while preserving ECM composition and architecture[14]. In the second group are the biomaterials developed from purified collagen that has been isolated and extracted by tissue solubilization with proteolytic enzymes or salt solutions. Bovine and porcine skin, and bovine and rat tail tendons are among the primary sources of purified collagen for biomedical applications, and, more recently, marine-derived collagen has also been explored as an alternative source[15]. Animal-derived collagen presents, perhaps, some drawbacks such as potential biological

contamination and composition variability from batch to batch. To circumvent these drawbacks, recombinant human collagen has been synthesized since 2004, with reduced variability and immunogenicity when compared to the one derived from animal sources[16]. However, the low yields and the control over posttranslational modifications remains a challenge, limiting their wider application.

Collagen hydrogels can be simply fabricated from colloidal suspensions of collagen in water. Such aqueous-based colloidal gels preparation typically starts with the addition of phosphate buffer and a NaOH solution to the collagen suspension at 4ºC, to neutralize acidic collagen monomers and promote the alignment and aggregation of collagen molecules into fibrils[17]. Subsequently, the mixture is warmed up to physiological temperatures, inducing the self-assembled fibrillogenic gelation of collagen[18]. The mild conditions under which the process occurs renders collagen hydrogels the possibility of incorporation of cell and bioactive compounds during the assembling process. Taking advantage of that, Shahin-Shamsabadi *et al*[19]. have recently proposed a technique that combines matrix- and cell-directed self-assembly processes to form collagen-based multicellular tissue constructs in a rapid, scalable, controllable, and simple manner. By allowing a sequential assemble of the collagen into fibrils followed by the cells binding and force exertion, this method enables the fabrication of homogenous and heterogenous multicellular constructs with complex shapes and precise spatial positioning of cells. The described method can be of particular interest for the development of realistic *in vitro* models for drug discovery and bioassays that aim at the study of cell migration and cell-cell interactions.

Despite the bio-inductive profile that collagen-based hydrogels can offer, their weak mechanical properties, contraction upon gel formation, difficult handling, and rapid *in vivo* degradation susceptibility limit their applications. Inter- and intramolecular crosslinking approaches have been commonly employed as a strategy to improve collagen-based biomaterials' physicochemical properties, usually by the modification of carboxyl and amine groups of proteins to allow the formation of covalent bonds, that ultimately leads to the stabilization and strengthening of collagen' molecular structure[20]. Crosslinking techniques can be grouped into three major categories: chemical, physical, and biological crosslinking. Chemical crosslinking is mostly achieved by the covalent amine/imine linkage promoted by crosslinkers such as cinnamaldehyde, ethyl-3(3-dimethylamino) propyl carbodiimide (EDC), genipin, glutaraldehyde (GTA), hexamethylene diisocyanate, or N-

hydroxysuccinimide[21,22]. Regardless of the improvements in the mechanical properties and degradation susceptibility achieved with the application of chemical crosslinking to collagen-based biomaterials, the toxicity of residual chemical agents may compromise cell encapsulation and affect incorporated growth factors (GFs). Photochemical crosslinking has also been widely explored to prepare collagen hydrogels with improved stability and gained substantial interest in the development of cell-laden hydrogels for TE applications, as a more biocompatible strategy[23]. Yang *et al.*[24] developed a photo cross-linkable type II collagen hydrogel, by the synthesis of type II collagen functionalized with a photo-active group through an amidation reaction between the amino groups of lysine residues of collagen and methacrylic anhydride (MA), and further exposure to an external source of ultra-violet (UV) light in the presence of the photoinitiator 2-hydroxy-1-[4-2-hydroxyethoxy)phenyl]-2-methyl-1-propanone, also known by is trade name Irgacure 2959 (I-2959). The obtained hydrogels showed improved mechanical properties and the ability to induce the chondrogenic differentiation of bone marrow mesenchymal stem cells (BM-MSCs), making them suitable candidates for cartilage TE. Besides that, these photo cross-linkable system enables spatial control over the polymerization reaction, an attractive feature for micro-TE. Applying a similar photo cross-linkable approach, Zhang *et al.*[25] fabricated a collagen-based BM-MSC-encapsulating hydrogel in a single step, for application in bone TE. The hydrogel was obtained by the exposure to UV light, in the presence of the I-2959 photoinitiator, of a mixture containing BM-MSCs and functionalized collagen and hyaluronic acid (HA) with glycidyl methacrylate (GMA) and MA, respectively. BM-MSCs encapsulated within the collagen-based hydrogel showed good adhesion and proliferation, proving that the system developed is suitable for cell culture. Besides, the osteogenic differentiation of BM-MSCs encapsulated within the hydrogel was also demonstrated, suggesting that the collagen composite system could be developed for bone TE purposes.

Physical crosslinking procedures include dehydrothermal treatment (DHT), UV, and γ-radiation, and are the least used for the fabrication of collagen-based cell culture platforms, mainly due to their impact on collagen structure. Dehydrothermal crosslinking makes use of high temperatures under vacuum conditions to promote condensation reactions among the carboxyl and amino groups of collagen amino acid residues[26]. Nakada *et al.*[27] showed that by varying the temperature and time of DHT to prepare a collagen scaffold allows to optimize its biocompatibility and durability. In the case of UV crosslinking, the incidence of

UV light leads to the generation of free radicals on the aromatic groups of phenylamine and tyrosine residues that interact between them and form chemical bonds, in a process known as radical polymerization[26]. However, the use of UV light alone is not enough to achieve high crosslinking densities and, therefore, currently are added photosensitizers, such as riboflavin, to potentiate the crosslinking efficacy. Zhao *et al*.[28] optimized the conditions of riboflavin-UV crosslinking to prepare a collagen-based artificial cornea with the desired biological and mechanical properties.

Biological crosslinking makes use of enzymes, like transglutaminase (TGase) and horseradish peroxidase, with the major advantage of diminished cytotoxic risk once no chemical residues or by-products are present in the final material[29,30]. TGase, a monomeric protein found in animals, plants, and microorganisms, catalyzes the acyl transfer reaction between the γ-carboxamide and ε-amino groups of glutamine and lysine residues, respectively, resulting in the formation of intra- and intermolecular ε-(γ-glutamyl)-lysine covalent crosslinked proteins[31]. The high cost of mammalian derived TGase have limited its application in the past. Nowadays, TGase has been extracted from microorganisms with high yields and low costs, making it more suitable to be used as a crosslinking agent[32]. Jiang *et al.*[33] describe the combination of microbial TGase (mTGase) with collagen to prepare a self-catalytic crosslinked collagen fibril hydrogel. Besides the crosslinking activity, mTGase also demonstrated the ability to promote the self-aggregation of collagen into aligned fibrils. Furthermore, the native triple helical structure of collagen is not affected during the process and its thermal stability is markedly enhanced, resulting in a matrix material with improved biological function and mechanical stability. The developed collagen fibril hydrogel crosslinked by mTGase promotes L929 fibroblasts adhesion and proliferation *in vitro* and skin wound healing *in vivo*, rendering to the developed material great potential for skin tissue regeneration.

The combination of collagen with other compounds is also a common strategy to improve the mechanical and/or biological functions of collagen-based scaffolds. The incorporation of hydroxyapatite (HAp), the primary mineral constituent of human bone tissue, into collagen scaffolds confers them osteoinductive and osteoconductive features, resembling what happens in natural bone ECM[34]. Therefore, collagen-HAp composite scaffolds have been attracting considerable attention for bone-related applications. By applying a "layer-by-layer" freeze-drying technique, Chen *et al*.[35] fabricated a collagen-

HAp porous scaffold with a dual-gradient in pore size and HAp content. Besides mimicking the chemical composition of the normal bone tissue, the collagen-HAp composite scaffold also mimics its inherent gradient structure. Furthermore, it was demonstrated that the fabricated scaffold was able to promote the BM-MSCs proliferation and differentiation into osteoblasts. Therefore, the herein presented collagen-HAp scaffold holds attractive features to be applied as an advanced strategy for bone TE.

The fibrillar conformation of collagen is crucial for the mechanical properties of ECM and cell-ECM interactions[28]. *In vivo*, fibrillogenesis is carried out by cells, and the local requirements of the tissue dictate the suprafibrillar architecture that could vary from highly aligned fibers in tendons[38] to a cholesteric arrangement in the bone[39]. Therefore, the induction of fibrillogenesis and the ability to control suprafibrillar architecture *in vitro* are essential tools in the development of biomimetic collagen scaffolds. Several studies describe the application of different techniques to produce collagen fibrils and manipulate their suprafibrillar architecture for the development of scaffolds for cell culture and TE. For example, Elamparithi *et al*.[40] first described the fabrication of collagen nanofibers by electrospinning that retains their native triple-helical structure. The crosslinking of electrospun collagen nanofibers with EDC resulted in a porous matrix with mechanical properties similar to human myocardium. Myoblasts cultured in these systems showed reasonable proliferation rates and prominent expression of muscle-specific proteins, such as actin and desmin, indicating that the scaffold is suitable for muscle cell culture. Besides that, the developed 3D collagen nanofibrous scaffolds also demonstrate the ability to support cardiomyocytes' contractility *in vitro*, suggesting that they could be further developed as 3D models and for cardiac TE applications. More recently, Yang *et al.*[41] developed two types of collagen membranes (CMs) with different fiber orientations by counter-rotating extrusion of insoluble collagen fibers at different speeds for the first time. Rat BM-MSCs cultured on the fabricated CMs with randomly orientated (CM_r) and aligned (CM_a) fibers presented two distinct morphologies, highlighting the ability of cells to sense and respond to the fiber orientation. The well-aligned fibers on CM_a were able to induce an elongated morphology on BM-MSCs and, therefore, promote their tenogenic differentiation *in vitro*. Furthermore, the tensile mechanical properties of CMa were similar to those from rat Achilles tendon. Besides, the *in vivo* application of CM_a-BM-MSCs constructs on a rat Achilles tendon defect

model presented good healing quality, indicating that the biomimetic collagen scaffolds developed are, therefore, promising candidates for tendon TE.

2.1. Gelatin

Gelatin consists of a hydrosoluble proteinaceous mixture of denatured and partially hydrolyzed collagen, majorly type I[42]. The processing of collagen to obtain gelatin consists of a two-step procedure, where collagen is first subjected to an acidic or alkaline pretreatment, to promote the breakdown of non-covalent bonds, and then heated, to cleave hydrogen and covalent bonds. Depending on the pretreatment, two types of gelatin are obtained, namely, type A and type B, for acidic and alkaline hydrolysis pretreatment, respectively. Gelatin B presents a higher content of carboxylic acid than gelatin A, due to the conversion of asparagine and glutamine residues into aspartic acid and glutamic acid, correspondingly, resulting from the high pH conditions during the pretreatment. Therefore, gelatin A and B present distinct isoelectric points of 7.0-9.0 and 4.7-5.2, respectively, which confers to gelatin-based biomaterials the ability to form ionic complexes with both positively and negatively charged factors and, therefore, to be developed as retention and delivery platforms for GFs[43]. Furthermore, the high temperatures applied to collagen during the denaturation process leads to loss of its tertiary conformation, conferring to gelatin diminished antigenicity and batch-to-batch variation. Gelatin owns the superior cell-adhesion, proliferation, and differentiation performance of collagen, since the bioactive sequences, like matrix metalloproteinase (MMP)-sensitive degradation sites and integrin-cell binding motifs, such as Arg-Gly-Asp (RGD) peptide, are retained on the gelatin backbone[44]. In addition to all the aforementioned, gelatin is also easy to manipulate and presents as a cost-effective alternative source of collagen, making it one of the most useful biomaterials for creating cellular scaffolds[45].

Thermo-reversible transparent gelatin hydrogels can be prepared by simply heating gelatin solutions above 35^{o}C, and then allowing them to cool down and establish a physically crosslinked network of collagen molecules[46]. However, this type of physical hydrogels has low mechanical strength, is not stable at body temperature, and does not allow control and fine-tune of its properties. Hence, the modification of gelatin or the combination with other materials is essential for the preparation of gelatin-based hydrogels with suitable mechanical

properties for 3D cell-culture and TE applications. Similar to the previously reported mechanisms for collagen-based biomaterials, physical, chemical, and enzymatic cross-linking methods are described in the literature for gelatin preparations. A comparative study performed by Yang *et al.*[47] tested the influence of some of the commonest crosslinking agents, namely GTA, EDC, genipin, and mTGase, on the properties of gelatin sponge scaffolds. Among the four tested crosslinkers, mTGase was identified as the most biocompatible and effective crosslinker for the fabrication of gelatin sponges. mTGase-crosslinked material showed the best overall performance, with good compressive modulus, porosity, anti-degradation capability, *in vitro* cell compatibility, and *in vivo* biocompatibility. On the other hand, GTA- and EDC-sponges presented the weakest performance, exhibiting certain cytotoxicity and fast degradation rates, respectively. Due to the superior features of mTGase as a covalent crosslinker, several researchers have been focusing their work on the design, development, and characterization of mTGase crosslinked gelatin scaffolds. Echave *et al.*[48] prepared 3D porous structures using gelatin from bovine skin with different concentrations of mTGase by freeze-drying technique. The results demonstrate that the swelling degree of the scaffolds is conversely proportional to enzyme concentration, being observed that for lower enzyme proportions, materials with a higher degree of swelling were obtained. Furthermore, the mTGase crosslinked gelatin sponges were able to retain and release vascular endothelial growth factor (VEGF) and bone morphogenetic protein 2 (BMP-2), following a first-order release kinetic, and induce the osteogenic differentiation of MSCs, suggesting that the prepared scaffolds could be useful for bone regenerative purposes. More recently, Yu-Ju Sun *et al.*[49] made use of mTGase to stabilize an A549 cell-laden gelatin microbubble structure with uniform pore size and cell distribution fabricated by microfluidic, that mimics the lung alveoli. A non-small-cell lung cancer proof-of-concept chemotherapeutic drug, gemcitabine, was then introduced to demonstrate the potential of the scaffold to be used as a drug-screening platform. The findings show that the 3D gelatin scaffold exhibits superior mimicking ability of the physiological lung conditions and predicts drug efficacy more faithfully than 2D cell culture models. By offering more accurate preclinical predictions, the developed platform seems a promising tool to facilitate anticancer drug development.

The functionalization of the side groups of the gelatin backbone is also a common crosslinking strategy that offers a higher degree of control over hydrogel design and

properties when compared to direct crosslinking approaches. Van Den Bulcke *et al.*[50] proposed for the first time the functionalization of gelatin with methacryloyl groups, by chemical reaction with MA, to prepare photo-crosslinkable gelatin hydrogels. The photo-initiated polymerization of methacrylated gelatin (GelMA) hydrogels occurs under mild conditions, enabling cell encapsulation, and provides good temporal and spatial control over the crosslinking process, which is crucial for the creation of architecturally complex tissue analogs. These features enabled Shim *et al.*[51] to develop cell encapsulating gelatin scaffolds with controlled porosity, by lithographical fabrication of GelMA hydrogel containing a liquid porogen (either gelatin or polyethylene glycol (PEG)) in a microfluidic channel, followed by porogen dissolution. The microporous structure plays a pivotal role in cell survival, growth, and function, by controlling the diffusion of soluble biochemical factors and oxygen through the scaffolds, as confirmed in the presented study, being observed that an increase of porosity enhanced the diffusivity and the viability of cells cultured within the GelMA hydrogels. The tunability of the mechanical properties of GelMA-based hydrogels by simply varying the experimental parameters, like the degree of functionalization, polymer and/or photo-initiator concentration, and photo-crosslinking time, is also a major advantage, conferring to GelMA biomaterials great versatility[46]. Li *et al.*[52] used GelMA hydrogels with different modification degrees to study the influence of matrix stiffness on the maintenance of chondrocyte phenotype. Chondrocytes encapsulated in high and low stiff hydrogels presented markedly distinct morphologies, indicating that cell morphology can be controlled by GelMA hydrogels stiffness emphasizing once more the importance of matrix stiffness on cell fate. Mechanical and chemical gradients also play a key role in cell migration, proliferation, and differentiation[53]. Therefore, 3D scaffolds in a gradient form are desirable platforms to mimic the heterogeneous structure of ECM. Ko *et al.*[54] proposed a simple layer-stacking technique to generate gradients of soluble proteins and mechanical stiffness inside GelMA hydrogels. Gradients profiles were tuned by varying UV intensity, the concentration of soluble proteins in the prehydrogel solution, and the concentration of the hydrogel itself in each layer. Fibroblasts culture put on evidence the importance of matrix gradients, being observed a directional migration towards gradient axis.

Other chemical modifications have also been tested for the preparation of gelatin-based biomaterials with superior properties. Liu *et al.*[55] combined dually-functionalized gelatin, with norbornene (NB) and hydroxyphenylacetic acid (HPA), and thiolated HA to

develop a pathophysiological relevant biomimetic hydrogel system of pancreatic ductal carcinoma (PDAC). The modular crosslinking of the gelatin, through thiol-NB photopolymerization, and the cell-laden hydrogels responsiveness to tyrosinase-triggered HPA dimerization, and therefore the physiologically relevant on-demand stiffening in the presence of PDAC cells, recapitulates what happens in PDAC microenvironment. More recently, Koivisto *et al.*[56] applied hydrazone chemistry to prepare gelatin-gellan gum hydrogels with tunable properties to develop cardiac disease models. By introducing hydrazide groups in the gelatin backbone and oxidizing gellan-gum, spontaneous hydrazone covalent bonds are formed between the two biopolymers, and therefore, hydrogels can be generated under physiological conditions, without the need to apply any external energy or add any crosslinkers or catalysts.

3. Elastin

Elastin is an ECM structural protein that confers stretch, flexibility, and strength to tissues and organs that undergo frequent cycles of stretch and recoil, such as ligaments, cartilage, blood vessels, skin, bladder, and lung[57]. Due to the high percentage of insoluble elastin that bovine and quine ligaments dry weight comprise, these are some of the commonest sources of elastin. Besides providing mechanical integrity, elastin also plays a crucial role in the modulation and regulation of cell behavior. By interacting with cells through membrane receptors such as glycosaminoglycans (GAGs), integrins, and elastin binding proteins, elastin participates in cell signaling and regulates intricate processes such as vascular morphogenesis and wound healing[58–60].

Elastic fibers, the functional units of elastin, consist of tropoelastin monomers covalently crosslinked and intertwined around a microfibrillar structure[61]. The mature fibers then assemble in complex hierarchical arrangements that can vary from branched networks in lungs, ligaments, and skin, to concentric sheets in blood vessels, depending on the function of the tissue in which they are embedded[62]. The microfibrillar structure of elastin comprises a complex array of macromolecules, including the structural glycoproteins fibrillin-1, fibrillin-2, and microfibril-associated glycoprotein-1, and serve as a scaffold for the alignment, deposition, and assembly of the tropoelastin monomers[63]. Tropoelastin, the soluble protein precursor of elastin, is a highly hydrophobic and non-glycosylated protein

secreted by various elastogenic cell types, including fibroblasts, endothelial cells (ECs), and smooth muscle cells[64]. Tropoelastin's primary structure is characterized by alternating hydrophilic and hydrophobic domains. The hydrophilic domains, mainly composed of alanine and lysine residues, are involved in tropoelastin monomers enzymatic cross-linking during the elastogenesis, and therefore are pivotal for elastin molecular stability[65]. On the other hand, the hydrophobic domains, composed of repeated motifs containing the non-polar residues glycine, valine, and proline, interact via hydrophobic interactions and are implied on the self-aggregation and elastic properties of elastin protein[66]. Furthermore, these hydrophobic domains are also thought to be the interaction sites with cells[67].

Elastin properties such as biological activity, elasticity, long-term stability, and self-assembling behavior, make this protein an attractive biomaterial for the development of elastin-based biomaterials, which find wide application in TE as biomimetic 3D scaffolds. In this sense, the combination of elastin with collagen is one of the commonest strategies to replicate the ECM of native tissues. Elastin is an essential element of the vascular wall ECM, providing it elasticity and dampening the pulsatile blood flow[68]. Thus, the combination of elastin with collagen, the major reinforcing ECM constituent of the vessel wall, appears as a promising strategy to fabricate purely natural composite scaffolds which better resemble the mechanical and biochemical properties of native cardiovascular tissue. In this regard, Ryan *et al.*[69] fabricated collagen-elastin composite scaffolds that resulted in a higher degree of creep resistance and critical strain recovery of the biomaterial and a more contractile phenotype of human smooth muscle cells (SMCs) cultured on them. In another work, Ghazanfari *et al.*[70] demonstrate that the mechanical properties, like extensibility and burst pressure, of decellularized tendon-derived collagen scaffolds, can be tuned through the crosslinking with bovine elastin. Furthermore, the preserved tendon architecture acted as a topological cue for SMCs cultured on the scaffolds, promoting their alignment along the fibers. The results presented thus support the assumption that collagen-elastin composites are of great value for cardiovascular TE.

Elastin-gelatin composites are another extensively exploited combination, that finds wide application in skin TE. In this regard, Khalili *et al.*[71] reported the addition of elastin to a blend of gelatin and cellulose acetate (CA) to fabricate nanofibrous scaffolds through electrospinning for skin regeneration purposes. The comparison of gelatin/CA and elastin/gelatin/CA scaffolds pointed out that elastin addition influenced the structural and

mechanical properties of the scaffolds, being observed that elastin/gelatin/CA scaffolds were characterized by increased fiber diameter and pore size and decreased swelling ratio and degradation rate. Additionally, the presence of elastin was shown to promote the interaction of fibroblasts with the scaffold. More recently, Cao *et al.*[72] proposed the covalent incorporation of elastin into a gelatin-PEG photopolymerizable hydrogel to construct a cellularized skin substitute that inherently regulates cell fate and behavior. Besides improving the elastic properties of the biomaterial and, therefore, better match skin mechanical properties, elastin also has shown to act as an instructive cue for the fibroblasts encapsulated within the hydrogel, promoting their adhesion and proliferation, and inducing morphological changes and ECM deposition.

Although the attractive mechanical and biological features that elastin offers as a biomaterial, its cross-linked and insoluble nature makes its processing challenging, limiting its wider application[73]. To obviate this drawback, researchers have been using recombinant DNA technologies to produce recombinant elastin-based polymers, named elastin-like polypeptides (ELPs)[74]. This class of genetically engineered proteins is bioinspired in the repetitive sequence Val-Pro-Gly-Xaa-Gly, where Xaa can be any naturally occurring amino acid except proline, that characterizes human elastin primary structure, retaining its inherent properties, such as the self-assembling ability, elastic mechanical behavior, hemocompatibility, and bioactivity, with the added advantage of solubility in aqueous medium[74]. Furthermore, as a product of recombinant protein engineering, ELPs present intrinsic advantages when compared to their natural counterparts, like the control over the amino acid sequence and peptide length, that by extension enables the design of the mechanical and biochemical properties of the materials, and limited inter- and intra-batch variability, and overcomes the transmission of potential pathogens related to polymers of animal origin[75].

The ability to design ELPs' primary structure enabled researchers to develop materials with selected and advanced properties that find varied applications. D'Andrea *et al.*[76] employed an ELP containing a repetitive hydrophilic sequence that accommodates lysine and glutamine residues, which can be enzymatically cross-linked by mTGase to give rise to hydrogel matrices, to study the physiological consequences of cell-biomaterial interactions. By comparing C2C21 cells behavior cultured in three different ELP substrates (non-crosslinked ELP adsorbed to glass coverslips and ELP hydrogels at two different monomer

concentrations, and by extension, with different stiffness degrees), differences in cell adhesion, morphology, proliferation, and differentiation among the cells cultured in the various ELP substrates were observed. In particular, ELP hydrogels with lower stiffness impaired myoblasts differentiation, and were proposed as 3D models to depict the molecular pathways that coordinate the transition of proliferating myoblasts to quiescent fusing myotubes. In another work, LeSavage *et al.*[77] reported the production of an ELP hydrogel with decoupled biochemical and biophysical properties that can be independently tuned for an optimal 3D culture of different cell types. The ELP presented includes three engineered domains: a tag that enables fluorescent labeling via tagged antibodies, the canonical elastin sequence repeated five times where four of the five Xaa amino acid sites are isoleucine and one is lysine and a bioactive region that encodes for cell-adhesive regions. The chosen Xaa residues, isoleucine and lysine, endows ELPs with lower critical solution temperature behavior, which can be exploited for simple post-expression purification of the peptides, and with reactive groups that could be crosslinked via reaction with the amine-reactive crosslinker tetrakis(hydroxymethyl)phosphonium chloride (THPC), respectively. By simply varying the concentration of the monomer and of the crosslinker, a plethora of hydrogels that span a physiologically relevant stiffness range can be easily obtained. Furthermore, by modulating the ratio of cell-adhesive and non-adhesive peptides, as the RGD motif, the ligand concentration, and the degradation profiles of the hydrogels can also be easily tuned.

ELPs have also been conjugated with other natural and synthetic polymers to fabricate composites with improved mechanical properties. Gurumurthy *et al.*[78] observed that the incorporation of ELP in a collagen hydrogel led to an increase in the tensile strength and elastic modulus of the composites, resultant from the extensive molecular entanglements and inter- and intra-molecular secondary bonding interactions between collagen and ELP. The increased stiffness of the composites with higher ELP concentrations favored the differentiation of human adipose stem cells (hASCs) along the osteoblastic lineage and the mineralization of the matrix, suggesting that the presented scaffold could be suitable for long-term 3D cell culture and guided bone regeneration applications. Almeida *et al.*[79] combined the biological potential of ELP with the nanotopography of continuous and aligned electrospun threads, based on a poly-ε-caprolactone/chitosan blend reinforced with cellulose nanocrystals, to develop tendon biomimetic scaffolds. The ELP coatings promoted stem cell differentiation toward the tenogenic lineage, being observed faster cell elongation

and the production of an elastin-rich tendon-like ECM by the differentiated cells. Due to the high level of mimicry of the biophysical and biochemical properties of tendons' microenvironment, the presented composites hold the potential to be used as 3D culture models to screen inflammatory responses and study the mechanisms that guide tenogenesis.

4. Keratin

Keratins are a group of insoluble cysteine-rich structural proteins that can either be found as the major cytoskeletal constituent of keratinocytes in the epidermis, in the form of "soft" keratins, or as fibrous extracellular proteins in epidermal appendageal, like hair, nails, feathers, beaks, horns, quills, hooves, and wool, in the form of "hard" keratins[80]. The characteristic amino acid composition of keratin polypeptide chains allows the formation of numerous intra- and inter-molecular disulfide bonds, which stabilize keratin molecules[81]. Furthermore, due to the higher cysteine content of "hard" keratins, such interactions are also responsible for the high mechanical strength of fibrous keratin structures. Besides, it has been reported that keratins derived from human hair contain numerous three amino acid residue motifs that are found in ECM proteins and that are known to promote cellular attachment and growth, like the RGD, Leu-Asp-Val (LDV), and Glu-Asp-Ser (EDS) motifs[82]. Hence, keratin-coated biomaterials have been tested for *in vitro* cell culture and when compared with standard controls, such as tissue culture plastics and collagen, keratin showed the better condition for cell groeth[83]. The inherent bioactivity of keratin biomaterials, therefore, eliminates the need for additional post-processing to incorporate binding motifs and, consequently, decreases the complexity of the manufacturing process. Moreover, keratins are not susceptible to rapid proteolytic breakdown once mammalian cells do not synthesize keratinases[84]. Adding to the relevant intrinsic biochemical properties, keratin is naturally abundant and can be readily extracted from renewable sources that are usually considered as a waste, like human hair and chicken feathers. Human hair keratins (HHK) have attracted particular interest due to the possible autogenous source, overcoming the risks of immunogenicity and pathogens transmission typically associated with other protein-based materials that have animal origin[85].

Owing to the innate propensity of keratins to spontaneously self-assemble into networks, as a result of disulfide bonding between the cysteine residues, keratin-based

hydrogels can be relatively easily fabricated[86]. Based on keratin flocculation, Wang *et al.*[87] developed and optimized a procedure to produce cell encapsulating HHK-based hydrogels. Protein concentration, pH, and temperature were identified as key factors in the flocculation process and can be easily adjusted to facilitate keratin gelation and cell encapsulation. L929 culture studies demonstrated that, when compared to collagen hydrogels, the fabricated keratin hydrogels presented a similar ability to promote cell proliferation and increased resistance to contraction, and hence have the potential to be exploited as alternative 3D cell culture systems. Wang *et al.*[88] described the preparation of feather keratin (FK)-based hydrogels through the crosslinking reaction of the thiol groups of lyophilized keratin with oxygenated water. Perming and dyeing are increasingly common practices that compromise the quality of HHK, therefore FK was here tested as an alternative keratin source that offers higher quality control. When compared with HHK hydrogels, FK hydrogels displayed comparable wound healing effects, biodegradation rates, and biocompatibility *in vivo*, suggesting that FK could be used as an alternative source of keratin to HHK, while maintaining the performance of the hydrogels.

Photochemical crosslinking has also been widely exploited for keratin-based hydrogels' fabrication. Placone *et al.*[89] reported the formulation of a keratin-based resin for the fabrication of HHK-based hydrogels through lithography-based 3D printing. The printing resin here presented couples keratin in the oxidized form and a photosensitive riboflavin-sodium persulfate-hydroquinone (initiator-catalyst-inhibitor) solution. Due to the chemical modification of cysteine residues, oxidized keratin cannot form disulfide bonds and therefore cannot self-assemble into a hydrogel network. Thus, hydrogel formation is directed by keratin entanglements and the tyrosine bonds formed upon UV exposure. The application of the developed UV-crosslinked keratin hydrogel as a permeable membrane for the regulation of molecular transport was then assessed by Navarro *et al.*[90]. The energy density was used as a design parameter to fine-tune the crosslinking degree of the membranes and hence control their microstructural properties, such as the mechanical features, degradation rate, swelling, and diffusion of molecules. Following a different approach, Barati *et al.*[91] proposed the chemical functionalization of FK through s-allyl modification of sulfhydryl groups present in cysteine residues, to fabricate photocrosslinkable keratin-based hydrogels for cell encapsulation. The synthesis of the keratin allyl thioether (KeratATE) macromer comprises two steps. First, the cysteine

sulfhydryl groups are converted to dehydroalanine by oxidative elimination reactions using O-(2,4,6-trimethylbenzenesulfonyl) hydroxylamine. Secondly, by the addition of allyl mercaptan, the dehydroalanine groups are converted to s-allyl cysteine to produce KeratATE. hMSCs encapsulated within KeratATE showed an elongated spindle-shape morphology with a higher number of focal adhesions and similar proliferation rates when compared to GelMA. Furthermore, KeratATE hydrogels presented low susceptibility to degradation by collagenase, unlike GelMA hydrogels that are degraded within a few days. The results thus suggest that KeratATE could be used in alternative to GelMA as a photo-polymerizable injectable hydrogel with controlled degradation for cell encapsulation.

Keratin-based scaffolds' poor mechanical properties and instability in aqueous environments have been limiting their application in the biomedical field. To overcome these limitations, Hartrianti *et al.*[92] proposed the chemical crosslinking of HHK with chitosan. Polymers combination resulted in porous and flexible sponges with improved mechanical properties and that support cellular infiltration, neovascularization, and neotissue formation *in vivo*. In another work, Kim *et al.*[93] also reported the blending of HHK with chitosan to fabricate electrospun nanofibers with improved mechanical properties. The HHK/chitosan nanofibrous mat was then combined with GelMA to develop a skin TE bi-layered scaffold. Normal human dermal fibroblasts and HaCaT cells co-cultured on the bi-layered scaffolds formed two distinct layers, a dermis-like cell-laden hydrogel on GelMA and an epidermis-like thin cell layer on HHK/chitosan nanofibrous mat, recapitulating the stratified architecture find in native skin. Aiming for the development of pure keratin scaffolds, Cui *et al.*[94] proposed the application of freeze-thaw cycles to lyophilized HHK scaffolds to enhance their mechanical properties. The freeze-thaw cycles promote the physical crosslinking of keratin molecules, primarily through the formation of hydrogen bonds among the -NH_2, -OH, and -C=O groups, and the oxidation of -SH groups into disulfide bonds. Therefore, the physical crosslinking degree and thus the properties of the scaffolds, including porosity, swelling ratio, compressive strength, and thermal stability, can be easily tuned by simply varying the number of freeze-thaw cycles. Furthermore, the ameliorated properties contribute to cell attachment, infiltration, and proliferation within the HHK scaffolds.

5. Blood plasma derivatives

The use of biomaterials from autologous sources for the development of scaffolds has become increasingly appealing as they present a diminished risk of rejection by the immune system and transference of disease-causing pathogens, follow the animal-free tendency, and include human-specific biochemical cues. Considering the limited resources of autologous tissues in the human body, blood-derived products gained a particular interest, since they can be obtained in a minimally invasive manner and can be readily replenished. Among them, albumin, fibrinogen, and platelet concentrates stand out, being extensively reported in the literature for their applications in the biomedical field[95].

5.1. Albumin

Albumin is the predominant plasmatic protein in mammals, accounting for 50% of blood's total protein content[96]. It is an endogenous, nonglycosylated, water-soluble, globular protein, predominantly produced by the liver and secreted into the bloodstream, where it plays numerous functions, including the transport of hydrophobic and charged endogenous (i.e., fatty acids, cholesterol, thyroxin, and bilirubin) or exogenous (i.e., toxins and drugs) molecules, and the maintenance of the pH, reducing power and osmotic pressure in the blood[97]. Albumin's primary structure contains large amounts of charged amino acid residues, including cysteine, glutamic acid, leucine, and lysine, that contributes to its high solubility and hydrophilicity. Moreover, albumin exhibit multiple ligand-binding sites and hydrophobic pockets and the innate ability to interact with different cellular receptors, which have rendered it wide application as a drug and biomolecule delivery platform[98]. Albumin has also been exploited for cell culture purposes, being used in cell culture media as a carrier protein for important biomolecules[99]. However, its application as a 2D culture matrix is limited due to inadequate cell attachment to albumin in the normal form. Approaches that have been applied on an attempt to overcome this limitation encompasses albumin's functionalization with glycoproteins or crosslinking/denaturation to fabricate 3D scaffolds[100,101]. Albumin presents some attractive features as a scaffolding material, such as the susceptibility to enzymatic breakdown by lysosomal proteins into non-toxic peptide intermediates and amino acids[102], the non-immunogenic profile[103], and the large amino acid

sequence, that offers numerous potential targets for modification or crosslinking reactions at different and specific residues[104,105]. In this scope, among the various types of albumin commonly used in scaffold fabrication, that encompass bovine serum albumin (BSA), human serum albumin (HSA), ovalbumin (OVA), and porcine serum albumin (PSA), HSA has been attracting particular attention[106]. Due to its abundance and ease of isolation from clinical samples, HSA presents a lower cost when compared to other commercially available human proteins and therefore constitutes an attractive autogenic biomaterial that has found increasing application in TE.

Albumin's chemical crosslinking is the commonest strategy to fabricate albumin-based 3D hydrogels and various crosslinkers have been used for such purpose conferring to the prepared materials distinct properties. Ma *et al.*[107] reported the fabrication of a BSA hydrogel with strong green and red autofluorescence through the intermolecular crosslinking of BSA with GTA. The autofluorescent hydrogel exhibit added value for biomedical applications, by enabling to non-invasively trace the *in vivo* degradation of the hydrogel using fluorescence images, without the drawbacks associated with fluorescent hydrogels synthesized by chemical or physical immobilization of the fluorophores. Bodenberger *et al.*[108] made use of THPC, an amine-reactive four-armed homotetra-functional crosslinking agent, to fabricate an HSA hydrogel with high chemical and mechanical stability for 3D cell culture purposes. The hydrogel formation is achieved within minutes and cells encapsulated within the 3D hydrogels revealed good viability. Furthermore, by simply varying the molar ratios of THPC to HSA concentration, they found out that Young's modulus can be adjusted, covering a range from 10 to 70 kPa, and thus hydrogels' mechanical properties could be tuned accordingly to the tissue being mimicked. Overby and Feldman[109], applied PEG functionalized with malonyl, succinimidyl succinate, or succinimidyl glutarate, as the crosslinking moiety to prepare PEG-albumin scaffolds. The functional end groups added to the PEG molecule can target and covalently bind to specific amino acid side groups, creating a network and limiting the mobility of albumin chains, which ultimately results in hydrogel formation. The chemistry of PEG functional end groups has proven to have great influence over gel's formation and properties, being observed that only the PEG-succinimidyl glutarate-albumin yielded stable hydrogels that could be further exploited as tissue scaffolding systems. As an alternative to the use of synthetic crosslinkers, to avoid the risk of immunogenicity associated and that raise some concern in biomedical applications, Bai

et al.[110] presented an approach to prepare injectable BSA hydrogels using only natural materials. For that, BSA was first exposed to urea, which denatures the protein conformation, and thus exposes intrachain non-crosslinking disulfide bonds, and secondly to glutathione, which breaks the non-crosslinking disulfide bonds by reducing them to thiol groups. The forces that guide hydrogel formation, namely urea-protein hydrogen bonds and disulfide-thiol, are both reversible equilibrium reactions and therefore by controlling the equilibrium extent, hydrogel's formation and its mechanical properties can be tuned to meet the demands for injectability. However, the change in albumin conformation to a non-native form during this process may result in altered protein binding affinity to cell membrane receptors and thus result in impaired cell attachment, as observed for other albumin-based materials prepared by thermal- or pH-induced gelation.

The albumin hydrogels prepared by chemical crosslinking or thermally- or pH-induced gelation usually demonstrate poor mechanical properties and stability in biological fluids[111]. As an alternative, photochemical crosslinking makes it possible to prepare albumin-based hydrogels with controlled spatial resolution, shape, and size, and tunable biological, chemical, and physical functions. For instance, Lantigua *et al.*[112] recently proposed the chemical modification of BSA with different volumes of glycidyl methacrylate (GMA) to prepare photocrosslinkable BSA hydrogels with tunable properties. The manipulation of the degree of functionalization of BSAGMA pre-polymers allowed to tune the degradation rate, pore structure, strength, and swelling properties of the hydrogels. NIH 3T3 fibroblasts encapsulated within the different BSAGMA hydrogels displayed distinct behaviors, emphasizing the influence of material's physical properties over cell response.

Albumin has also been proven to be a suitable raw material for the fabrication of fibrous scaffolds by electrospinning technology to recreate intricate tissue architectures. By the bottom-up assembly of multiple micropatterned electrospun albumin layers, Fleischer *et al.*[113] could recreate the anisotropic geometry and internal vasculature of the myocardium in a multifunctional cardiac patch. Cardiac cells cultured within the constructs assembled into aligned and elongated cardiac bundles, like in the native tissue. In another work carried out by Hsu *et al.*[114], electrospun albumin scaffolds coated with laminin, hemin, and basic fibroblast growth factor were designed for neural TE. The 3D fibrous structure of the electrospun albumin scaffold provides mechanical support and topographical guidance and the excellent ligand-binding capacity of albumin enabled the adsorption of the remaining

scaffold constituents, which confer electrical conductivity and increased bioactivity to the construct. The GFs release and the electrical stimulation were found to be crucial to support the culture and differentiation of human-induced pluripotent stem cell-derived populations.

5.2. Fibrinogen and fibrin

Fibrinogen is a soluble plasmatic glycoprotein with a dimeric structure, comprising two sets of Aα, Bβ, and γ polypeptide chains linked together by disulfide bridges, which plays a fundamental role in hemostasis, being a key intermediate of the coagulation cascade[115]. The coagulation cascade consists of a set of biochemical reactions that ultimately leads to the formation of a fibrin clot, which ceases the bleeding and acts as a provisional ECM, supporting cell adhesion and migration and promoting the regeneration of the injured tissue. In the last step of this intricate process, the fibrinopeptides A and B are enzymatically cleaved off, by the activated serine protease thrombin in the presence of calcium ions (Ca^{2+}), and fibrinogen is converted to fibrin monomers, which exhibit a high propensity to self-assemble and polymerize into protofibrils, forming an insoluble hydrogel of randomly arranged fibers that are held together by electrostatic interactions and non-covalent forces[116]. The fibrin 3D network is further stabilized by the activated factor XIII, which establishes intermolecular (γ-glutamyl)-lysine covalent bonds between lysine and glutamine residues from the various γ-chains[117]. The crosslinked fibrin matrix not only confers elasticity to the blood clot as also acts as a bioactive scaffold, binding to the GFs and cytokines released by the leukocytes and activated platelets entrapped within it, and establishing a spatial-temporal chemotactic gradient of these biomolecules which coordinates the migration of autologous cells involved in tissue healing, like fibroblasts, ECs, and MSCs, to the site of injury, ECM secretion, and angiogenesis, ultimately leading the way to tissue regeneration[118].

The physiological process of fibrin clot formation has been recapitulated *in vitro*, by adding thrombin and calcium chloride ($CaCl_2$) to fibrinogen solutions, to prepare fibrin-based biomaterials that have been applied in the clinic as emulsions to improve wound healing, adhesives for skin graft attachment, and hemostatic sealants in surgery[119]. The structural properties of these biomaterials, like density, permeability, and porosity, can be tuned *in vitro*, by controlling the ionic strength and pH of the medium, and the concentration of fibrinogen and thrombin, parameters that have great influence over the length and

thickness of the fibrin fibrils[120,121]. For example, lower concentrations of thrombin result in thick fibers and hydrogels with few branch points and large pores, while high thrombin concentrations originate thin fibers that result in hydrogels with many branch points and small pores[122]. Conversely, for Ca^{2+}, higher concentrations result in thicker and shorter fibers, while lower concentrations originate longer and thinner fibrils. In the case of fibrin sealants, due to the need for high tensile and adhesion strength in their applications, usually high concentrations of fibrinogen are used in their fabrication to match the mechanical needs[119].

Aiding to the tailorable mechanical properties and versatile molecular interactions already mentioned, fibrin also possesses the ability to promote cell adhesion, either directly, through integrin-interacting motifs such as RGD and AGDV, or indirectly, due to the ability to bind ECM proteins circulating in the blood[123]. Furthermore, fibrin hydrogels are readily degraded *in vivo*, through plasmin-mediated fibrinolysis, a physiological process that occurs in the last stages of wound healing, allowing the fibrin clot to be replaced by the ECM secreted by autologous cells and avoiding thrombosis[124]. All these properties have motivated the use of fibrin hydrogels as scaffolds for 3D cell culture and TE applications[125,126]. Moreover, fibrinogen is easy to blend with cells, polymerizes rapidly, and presents low viscosity, making it easy to use for conventional scaffolding, and when compared to the gold standard protein collagen, presents lower costs and can be readily isolated from the patient's blood, holding great promise as an autologous scaffolding biomaterial[119].

Despite the intrinsic bioactivity and biocompatibility of the fibrin hydrogels prepared by the traditional method previously described, they present some applicability constraints due to their limited mechanical strength, shrinkage upon gel formation, and mismatching degradation and tissue regeneration rates, precluding adequate tissue regeneration[127]. The combination of fibrin hydrogels with other natural or synthetic polymers and the application of chemical crosslinking techniques are the commonest strategies to overcome these drawbacks and fabricate constructs with appropriate mechanical properties. Zhang *et al.*[128] reported that the combination of disulfide crosslinked HA and fibrin hydrogels resulted in an interpenetrating network with increased stiffness and slower degradation rates *in vitro* when compared to pure fibrin hydrogels, that could be used as a stable platform for 3D cell culture. Furthermore, the developed composite hydrogel could also be used as an injectable scaffold for TE, since hydrogel formation occurs *in situ* upon the mixture of two solutions

containing the reactive macromolecular precursors. Keating *et al.*[129] proposed the use of a laser scanning confocal microscope to selectively pattern the crosslinking of fibrin hydrogels crosslinked via ruthenium-catalyzed photocrosslinking (RCP). In RCP, tyrosine residues are oxidized by a light-activated ruthenium compound in the presence of sodium persulfate, originating tyrosine radicals that can react and form dityrosine bonds among the peptide chains. The control over the spatial incidence of light within the 3D fibrin hydrogel enabled stiffness tuning at the micron level, which may be useful for mechanobiology studies. More recently, Yang *et al.*[130] blended polycaprolactone (PCL) with fibrin to fabricate small vascular scaffolds via electrospinning. The PCL/fibrin scaffolds presented larger fiber diameter, smaller aperture, slower degradation rates, and improved mechanical properties when compared to pure fibrin scaffolds. Furthermore, it was observed that the PCL/fibrin ratio influences the biological and mechanical properties, with 20/80 scaffolds presenting the best balance between both.

5.3. Platelet-rich plasma and platelet lysates

Platelets are blood figurative elements that play a key role in primary hemostasis and tissue regeneration. *In vivo*, when activated at tissue injury sites, platelets release the content of their α granules, which comprises multiple proteins, cytokines, and GFs[131]. These biomolecules initiate the physiologic wound healing cascade and tissue regeneration process, by interacting with transmembrane cell receptors and thus promoting the expression of genes that are involved in cell proliferation and differentiation, matrix synthesis, and angiogenesis. Platelets can be easily isolated from whole blood sampled through differential centrifugation, resulting in a plasma fraction with high platelet concentrations (at least $1x10^6$ platelets/μL in 5 mL of plasma), known as platelet-rich plasma (PRP)[132]. Therefore, PRP constitutes an important biological source of bioactive molecules, containing more than 300 GFs and cytokines, that can be harvested from autologous or allogeneic sources. Autologous sources have the main advantage of minimal immune response and diminished risk of disease-causing pathogens transference[133]. However, the number of platelets and their biochemical content is highly dependent on the donor's clinical condition. On the other hand, the commercially available allogenic sources are usually obtained from at least three distinct healthy blood donors to diminish the donor-dependent variability.

PRP has been used as an alternative cytokine supplement and GFs source for several clinical therapeutic applications, including musculoskeletal conditions, regeneration of bone and cartilage defects, and healing of damaged tissues[132]. PRP can be used directly in its liquid form, through injection, or in the form of a fibrin hydrogel rich in activated platelets, named platelet-rich fibrin (PRF), that is usually formed by the addition of thrombin and/or $CaCl_2$ to PRP, that leads to the polymerization of the fibrinogen from the plasma fraction and platelet activation[134]. The principle underlying the administration of PRP relies on the increase in the number of platelets, and hence, in the concentration of bioactive molecules at the injury site that activates and accelerate the physiological repair process. However, upon platelet activation, approximately 70% of the biomolecules are released in the first 10 minutes and after 1 hour full release is achieved[135]. Furthermore, GFs and cytokines present short half-life and circulation times, resulting in decreased PRP's bioavailability and compromising their regenerative potential. Additionally, PRP injections and PRF also fail to provide adequate structural and mechanical support for tissue regeneration.

To overcome the pointed shortcomings associated with current PRP and PRF application methods, these have been combined with other scaffolding materials and prepared by different biofabrication techniques. For example, Liu *et al.*[136] proposed the combination of autologous PRP with O-nitrobenzyl alcohol modified HA to prepare photocrosslinkable hydrogels with GFs-controlled release. Upon light irradiation, the modified HA generates aldehyde groups which in turn can react and form covalent bonds with the amino groups distributed within the PRP components, like fibrinogen, forming a robust hydrogel. The photoinduced imine crosslinking mechanism used allows *in situ* preparation of the hydrogels and confers to them strong tissue adhesiveness. Furthermore, the crosslinked network contributes to the controlled release of GFs, and the *in vivo* experiments demonstrated that the developed gels present a better regenerative effect on hyaline cartilage than PRF. Cheng *et al.*[137] reported the incorporation of PRP into silk fibroin/PCL nanofibrous scaffolds fabricated through coaxial electrospinning to increase their bioactivity. The scaffolds demonstrated to be able to sustain the release of PRP-derived GFs for 30 days, which were correlated with increased proliferation, migration, and differentiation into the osteogenic lineage of BM-MSCs *in vitro* and *in vivo*. Faramarzi *et al.*[138] described the development of an alginate-based bioink incorporating PRP to engineer scaffolds with healing-inducing ability. The bioink containing PRP presented a slightly

increased compressive modulus and a gradual release profile of GFs and multiple proteins for several days, which positively affected the cellular function of ECs and MSCs cultured on the constructs bioprinted with it. Amaral *et al.*[139] proposed the incorporation of PRP into collagen-GAG scaffolds as a simple and rapid strategy to combine the bioactivity of PRP-derived GFs and the mechanical stability of collagen-GAG scaffolds to obtain a composite scaffold with superior properties for wound healing applications. The obtained scaffold presented superior mechanical properties when compared to PRF and sustained GFs release for up to 14 days. Furthermore, the PRP-collagen-GAG scaffolds were able to support the co-culture of fibroblasts and keratinocytes *in vitro* and presented increased angiogenesis and vascularization *in vitro* and *in vivo*. Irmak *et al.*[140] choose microwave-induced GelMA to prepare photocrosslinkable and photoactivated PRP-based bioink. GelMA improved the mechanical properties of the bioink and the periodic application of near-infrared light allowed the controlled and long-term release of the GFs.

PRP can also be used to prepare platelet lysates (PL), through platelet membrane disruption, commonly via freeze-thaw cycles or ultrasounds[141]. The resulting solution presents a constant concentration of readily available platelet-derived GFs, cytokines, and other bioactive molecules. PL has been suggested as a viable humanized alternative to fetal bovine serum (FBS), the standard medium supplement, for cell and tissue culture practices, due to its unique and rich biochemical composition and the diminished risks of transmission of xenogeneic contaminants and antigens, following the tendency for animal product free conditions[142]. Moreover, PLs have also been explored as 3D cell culture platforms and for TE applications. Similarly to what is previously described for PRP, PL-based hydrogels can be prepared by the addition thrombin and/or $CaCl_2$, due to the presence of fibrinogen in their composition[143,144]. Despite their positive influence in cell expansion and their ability to support vascularization, these hydrogels are generally associated with weak mechanical properties and instability in cell culture conditions. Therefore, alternative fabrication methods have been tested for the fabrication of PL-based hydrogels as a way to improve their physical properties. In this sense, Santos *et al.*[145] reported the chemical modification of PL proteins with methacryloyl groups as a strategy to prepare PL-based photopolymerizable hydrogels for 3D cell culture. The mechanical and biochemical properties of the fabricated constructs can be easily tuned by varying the degree of modification and the concentration of methacrylated PL (PLMA). Furthermore, the hydrogels demonstrated the ability to

support the adhesion and proliferation of encapsulated cells and to be used as a spheroid invasion model[146]. The results suggest that the novel PLMA hydrogels could be used in alternative to the gold standards platforms collagen and Matrigel for 3D cell culture and drug screening, with the foremost advantages of being of human origin and offering the possibility of autologous source. Recently, mesoporous silica nanoparticles loaded with Dex and functionalized with calcium and phosphate ions were incorporated into PLMA hydrogels to create a composite material that could mimic bone ECM and promote the osteogenic differentiation of BM-MSCs[147].

6. Conclusions

The design of scaffolds is a growing field of research and the advancements made on this area have been the major contributors for the transition from the 2D to 3D cell culture as also for the progress made on TE. With the main goal to recapitulate native ECM, protein-based scaffolds hold great potential as they present high biochemical resemblance to the native ECM components. Furthermore, they present attractive features as biomaterials, due to their innate biocompatibility, biodegradability, and bioactivity. Among the myriad of proteins explored for scaffold development, the ones naturally occurring in the human body, including collagen, elastin, keratin, and blood plasma derived proteins, attract particular interest due their potential allogenic source, following the animal-free tendency. Notably, blood plasma derived proteins can be easily obtained from autologous samples through minimally invasive procedures and thus holding great potential for personalized medicine. Moreover, due their versatility, protein-based scaffolds have been prepared through different fabrication techniques, and so far, many protein-based scaffolds with distinct physical, mechanical, and topographical properties have been widely reported. In particular, photochemical crosslinking has been transversely used in the preparation of protein-based scaffolds, due to its recognized advantages, such as the ability of control over the degree of crosslinking and temporal and spatial polymerization. Therefore, protein-based scaffolds have been largely contributed to the further of our knowledge on scaffold-cell interactions and hold great potential for 3D cell culture and TE applications.

References

1. Hynes, R. O. The Extracellular Matrix: Not Just Pretty Fibrils. *Science (80-.).* **326**, 1216–1219 (2009).
2. Hinderer, S., Layland, S. L. & Schenke-Layland, K. ECM and ECM-like materials — Biomaterials for applications in regenerative medicine and cancer therapy. *Adv. Drug Deliv. Rev.* **97**, 260–269 (2016).
3. Wang, Y., Rudym, D. D., Walsh, A., Abrahamsen, L., Kim, H.-J., Kim, H. S., Kirker-Head, C. & Kaplan, D. L. In vivo degradation of three-dimensional silk fibroin scaffolds. *Biomaterials* **29**, 3415–3428 (2008).
4. Chien, K. B., Aguado, B. A., Bryce, P. J. & Shah, R. N. In vivo acute and humoral response to three-dimensional porous soy protein scaffolds. *Acta Biomater.* **9**, 8983–8990 (2013).
5. Lee, C. H., Singla, A. & Lee, Y. Biomedical applications of collagen. *Int. J. Pharm.* **221**, 1–22 (2001).
6. Altman, G. H., Diaz, F., Jakuba, C., Calabro, T., Horan, R. L., Chen, J., Lu, H., Richmond, J. & Kaplan, D. L. Silk-based biomaterials. *Biomaterials* **24**, 401–416 (2003).
7. Gomes, S., Leonor, I. B., Mano, J. F., Reis, R. L. & Kaplan, D. L. Natural and genetically engineered proteins for tissue engineering. *Progress in Polymer Science (Oxford)* **37**, 1–17 (2012).
8. Harkness, R. D. Biological functions of collagen. *Biol. Rev. Camb. Philos. Soc.* **36**, 399–463 (1961).
9. Shoulders, M. D. & Raines, R. T. Collagen structure and stability. *Annual Review of Biochemistry* **78**, 929–958 (2009).
10. Kadler, K. E., Baldock, C., Bella, J. & Boot-Handford, R. P. Collagens at a glance. *J. Cell Sci.* **120**, 1955–1958 (2007).
11. Veit, G., Kobbe, B., Keene, D. R., Paulsson, M., Koch, M. & Wagener, R. Collagen XXVIII, a Novel von Willebrand Factor A Domain-containing Protein with Many Imperfections in the Collagenous Domain. *J. Biol. Chem.* **281**, 3494–3504 (2006).
12. Brodsky, B. & Persikov, A. V. Molecular structure of the collagen triple helix. *Adv. Protein Chem.* **70**, 301–339 (2005).

13. Badylak, S. F. Xenogeneic extracellular matrix as a scaffold for tissue reconstruction. *Transpl. Immunol.* **12**, 367–377 (2004).
14. Lu, H., Hoshiba, T., Kawazoe, N., Koda, I., Song, M. & Chen, G. Cultured cell-derived extracellular matrix scaffolds for tissue engineering. *Biomaterials* **32**, 9658–9666 (2011).
15. Coelho, R. C. G., Marques, A. L. P., Oliveira, S. M., Diogo, G. S., Pirraco, R. P., Moreira-Silva, J., Xavier, J. C., Reis, R. L., Silva, T. H. & Mano, J. F. Extraction and characterization of collagen from Antarctic and Sub-Antarctic squid and its potential application in hybrid scaffolds for tissue engineering. *Mater. Sci. Eng. C* **78**, 787–795 (2017).
16. Yang, C., Hillas, P. J., Báez, J. A., Nokelainen, M., Balan, J., Tang, J., Spiro, R. & Polarek, J. W. The application of recombinant human collagen in tissue engineering. *BioDrugs* **18**, 103–119 (2004).
17. Pourjavadi, A. & Kurdtabar, M. Effect of different bases and neutralization steps on porosity and properties of collagen-based hydrogels. *Polym. Int.* **59**, 36–42 (2010).
18. Motte, S. & Kaufman, L. J. Strain stiffening in collagen I networks. *Biopolymers* **99**, 35–46 (2013).
19. Shahin-Shamsabadi, A. & Selvaganapathy, P. R. A rapid biofabrication technique for self-assembled collagen-based multicellular and heterogeneous 3D tissue constructs. *Acta Biomater.* **92**, 172–183 (2019).
20. Krishnakumar, G. S., Gostynska, N., Dapporto, M., Campodoni, E., Montesi, M., Panseri, S., Tampieri, A., Kon, E., Marcacci, M., Sprio, S. & Sandri, M. Evaluation of different crosslinking agents on hybrid biomimetic collagen-hydroxyapatite composites for regenerative medicine. *Int. J. Biol. Macromol.* **106**, 739–748 (2018).
21. Yan, L.-P., Wang, Y.-J., Ren, L., Wu, G., Caridade, S. G., Fan, J.-B., Wang, L.-Y., Ji, P.-H., Oliveira, J. M., Oliveira, J. T., Mano, J. F. & Reis, R. L. Genipin-cross-linked collagen/chitosan biomimetic scaffolds for articular cartilage tissue engineering applications. *J. Biomed. Mater. Res. Part A* **95A**, 465–475 (2010).
22. Rafat, M., Li, F., Fagerholm, P., Lagali, N. S., Watsky, M. A., Munger, R., Matsuura, T. & Griffith, M. PEG-stabilized carbodiimide crosslinked collagen–chitosan hydrogels for corneal tissue engineering. *Biomaterials* **29**, 3960–3972 (2008).
23. Chan, B. P., Hui, T. Y., Chan, O. C. M., So, K. F., Lu, W., Cheung, K. M. C.,

Salomatina, E. & Yaroslavsky, A. Photochemical cross-linking for collagen-based scaffolds: A study on optical properties, mechanical properties, stability, and hematocompatibility. in *Tissue Engineering* **13**, 73–85 (Tissue Eng, 2007).

24. Yang, K., Sun, J., Wei, D., Yuan, L., Yang, J., Guo, L., Fan, H. & Zhang, X. Photo-crosslinked mono-component type II collagen hydrogel as a matrix to induce chondrogenic differentiation of bone marrow mesenchymal stem cells. *J. Mater. Chem. B* **5**, 8707–8718 (2017).
25. Zhang, T., Chen, H., Zhang, Y., Zan, Y., Ni, T., Liu, M. & Pei, R. Photo-crosslinkable, bone marrow-derived mesenchymal stem cells-encapsulating hydrogel based on collagen for osteogenic differentiation. *Colloids Surfaces B Biointerfaces* **174**, 528–535 (2019).
26. Adamiak, K. & Sionkowska, A. Current methods of collagen cross-linking: Review. *International Journal of Biological Macromolecules* **161**, 550–560 (2020).
27. Nakada, A., Shigeno, K., Sato, T., Hatayama, T., Wakatsuki, M. & Nakamura, T. Optimal dehydrothermal processing conditions to improve biocompatibility and durability of a weakly denatured collagen scaffold. *J. Biomed. Mater. Res. Part B Appl. Biomater.* **105**, 2301–2307 (2017).
28. Zhao, X., Long, K., Liu, Y., Li, W., Liu, S., Wang, L. & Ren, L. To prepare the collagen-based artificial cornea with improved mechanical and biological property by ultraviolet-A/riboflavin crosslinking. *J. Appl. Polym. Sci.* **134**, 45226 (2017).
29. Zhao, L., Li, X., Zhao, J., Ma, S., Ma, X., Fan, D., Zhu, C. & Liu, Y. A novel smart injectable hydrogel prepared by microbial transglutaminase and human-like collagen: Its characterization and biocompatibility. *Mater. Sci. Eng. C* **68**, 317–326 (2016).
30. Chau, D. Y. S., Collighan, R. J., Verderio, E. A. M., Addy, V. L. & Griffin, M. The cellular response to transglutaminase-cross-linked collagen. *Biomaterials* **26**, 6518–6529 (2005).
31. Halloran, D. M. O., Collighan, R. J., Griffin, M. & Pandit, A. S. Characterization of a microbial transglutaminase cross-linked type II collagen scaffold. *Tissue Eng.* **12**, 1467–1474 (2006).
32. Collighan, R. J. & Griffin, M. Transglutaminase 2 cross-linking of matrix proteins: biological significance and medical applications. *Amino Acids* **36**, 659–670 (2009).
33. Jiang, H., Zheng, M., Liu, X., Zhang, S., Wang, X., Chen, Y., Hou, M. & Zhu, J.

Feasibility Study of Tissue Transglutaminase for Self-Catalytic Cross-Linking of Self-Assembled Collagen Fibril Hydrogel and Its Promising Application in Wound Healing Promotion. *ACS Omega* **4**, 12606–12615 (2019).

34. Eliaz, N. & Metoki, N. Calcium Phosphate Bioceramics: A Review of Their History, Structure, Properties, Coating Technologies and Biomedical Applications. *Materials (Basel).* **10**, 334 (2017).
35. Cox, R. F., Jenkinson, A., Pohl, K., O'Brien, F. J. & Morgan, M. P. Osteomimicry of Mammary Adenocarcinoma Cells In Vitro; Increased Expression of Bone Matrix Proteins and Proliferation within a 3D Collagen Environment. *PLoS One* **7**, e41679 (2012).
36. Barczyk, M., Carracedo, S. & Gullberg, D. Integrins. *Cell Tissue Res.* **339**, 269–280 (2010).
37. Jokinen, J., Dadu, E., Nykvist, P., Käpylä, J., White, D. J., Ivaska, J., Vehviläinen, P., Reunanen, H., Larjava, H., Häkkinen, L. & Heino, J. Integrin-mediated Cell Adhesion to Type I Collagen Fibrils. *J. Biol. Chem.* **279**, 31956–31963 (2004).
38. Rieu, C., Picaut, L., Mosser, G. & Trichet, L. From Tendon Injury to Collagen-based Tendon Regeneration: Overview and Recent Advances. *Curr. Pharm. Des.* **23**, (2017).
39. Giraud Guille, M. M., Mosser, G., Helary, C. & Eglin, D. Bone matrix like assemblies of collagen: From liquid crystals to gels and biomimetic materials. *Micron* **36**, 602–608 (2005).
40. Elamparithi, A., Punnoose, A. M. & Kuruvilla, S. Electrospun type 1 collagen matrices preserving native ultrastructure using benign binary solvent for cardiac tissue engineering. *Artif. Cells, Nanomedicine, Biotechnol.* **44**, 1318–1325 (2016).
41. Yang, S., Shi, X., Li, X., Wang, J., Wang, Y. & Luo, Y. Oriented collagen fiber membranes formed through counter-rotating extrusion and their application in tendon regeneration. *Biomaterials* **207**, 61–75 (2019).
42. Gomez-Guillen, M. C., Gimenez, B., Lopez-Caballero, M. E. & Montero, M. P. Functional and bioactive properties of collagen and gelatin from alternative sources: A review. *Food Hydrocolloids* **25**, 1813–1827 (2011).
43. Young, S., Wong, M., Tabata, Y. & Mikos, A. G. Gelatin as a delivery vehicle for the controlled release of bioactive molecules. in *Journal of Controlled Release* **109**, 256–

274 (Elsevier, 2005).

44. Van den Steen, P. E., Dubois, B., Nelissen, I., Rudd, P. M., Dwek, R. A. & Opdenakker, G. Biochemistry and Molecular Biology of Gelatinase B or Matrix Metalloproteinase-9 (MMP-9). *Crit. Rev. Biochem. Mol. Biol.* **37**, 375–536 (2002).
45. Lai, J.-Y. & Li, Y.-T. Functional Assessment of Cross-Linked Porous Gelatin Hydrogels for Bioengineered Cell Sheet Carriers. *Biomacromolecules* **11**, 1387–1397 (2010).
46. Van Den Bulcke, A. I., Bogdanov, B., De Rooze, N., Schacht, E. H., Cornelissen, M. & Berghmans, H. Structural and Rheological Properties of Methacrylamide Modified Gelatin Hydrogels. *Biomacromolecules* **1**, 31–38 (2000).
47. Yang, G., Xiao, Z., Long, H., Ma, K., Zhang, J., Ren, X. & Zhang, J. Assessment of the characteristics and biocompatibility of gelatin sponge scaffolds prepared by various crosslinking methods. *Sci. Rep.* **8**, 1616 (2018).
48. Echave, M. C., Pimenta-Lopes, C., Pedraz, J. L., Mehrali, M., Dolatshahi-Pirouz, A., Ventura, F. & Orive, G. Enzymatic crosslinked gelatin 3D scaffolds for bone tissue engineering. *Int. J. Pharm.* **562**, 151–161 (2019).
49. Sun, Y. J., Hsu, C. H., Ling, T. Y., Liu, L., Lin, T. C., Jakfar, S., Young, I. C. & Lin, F. H. The preparation of cell-containing microbubble scaffolds to mimic alveoli structure as a 3D drug-screening system for lung cancer. *Biofabrication* **12**, (2020).
50. Van Den Bulcke, A. I., Bogdanov, B., De Rooze, N., Schacht, E. H., Cornelissen, M. & Berghmans, H. Structural and Rheological Properties of Methacrylamide Modified Gelatin Hydrogels. *Biomacromolecules* **1**, 31–38 (2000).
51. Shim, K., Kim, S. H., Lee, D., Kim, B., Kim, T. H., Jung, Y., Choi, N. & Sung, J. H. Fabrication of micrometer-scale porous gelatin scaffolds for 3D cell culture. *J. Ind. Eng. Chem.* **50**, 183–189 (2017).
52. Li, X., Chen, S., Li, J., Wang, X., Zhang, J., Kawazoe, N. & Chen, G. 3D Culture of Chondrocytes in Gelatin Hydrogels with Different Stiffness. *Polymers (Basel).* **8**, 269 (2016).
53. Liu, Z., Meyers, M. A., Zhang, Z. & Ritchie, R. O. Functional gradients and heterogeneities in biological materials: Design principles, functions, and bioinspired applications. *Progress in Materials Science* **88**, 467–498 (2017).
54. Ko, H., Suthiwanich, K., Mary, H., Zanganeh, S., Hu, S. K., Ahadian, S., Yang, Y.,

Choi, G., Fetah, K., Niu, Y., Mao, J. J. & Khademhosseini, A. A simple layer-stacking technique to generate biomolecular and mechanical gradients in photocrosslinkable hydrogels. *Biofabrication* **11**, (2019).

55. Liu, H.-Y., Korc, M. & Lin, C.-C. Biomimetic and enzyme-responsive dynamic hydrogels for studying cell-matrix interactions in pancreatic ductal adenocarcinoma. *Biomaterials* **160**, 24–36 (2018).
56. Koivisto, J. T., Gering, C., Karvinen, J., Maria Cherian, R., Belay, B., Hyttinen, J., Aalto-Setälä, K., Kellomäki, M. & Parraga, J. Mechanically Biomimetic Gelatin–Gellan Gum Hydrogels for 3D Culture of Beating Human Cardiomyocytes. *ACS Appl. Mater. Interfaces* **11**, 20589–20602 (2019).
57. Daamen, W. F., Veerkamp, J. H., van Hest, J. C. M. & van Kuppevelt, T. H. Elastin as a biomaterial for tissue engineering. *Biomaterials* **28**, 4378–4398 (2007).
58. Jin, E., Lee, P. T., Jeon, W. B. & Li, W.-J. Effects of Elastin-Like Peptide on Regulation of Human Mesenchymal Stem Cell Behavior. *Regen. Eng. Transl. Med.* **2**, 85–97 (2016).
59. Karnik, S. K. A critical role for elastin signaling in vascular morphogenesis and disease. *Development* **130**, 411–423 (2003).
60. Almine, J. F., Wise, S. G. & Weiss, A. S. Elastin signaling in wound repair. *Birth Defects Res. Part C Embryo Today Rev.* **96**, 248–257 (2012).
61. Daamen, W. ., Hafmans, T., Veerkamp, J. . & van Kuppevelt, T. . Comparison of five procedures for the purification of insoluble elastin. *Biomaterials* **22**, 1997–2005 (2001).
62. Vrhovski, B. & Weiss, A. S. Biochemistry of tropoelastin. *Eur. J. Biochem.* **258**, 1–18 (1998).
63. Mithieux, S. M. & Weiss, A. S. Elastin. *Adv. Protein Chem.* **70**, 437–461 (2005).
64. Wise, S. G. & Weiss, A. S. Tropoelastin. *Int. J. Biochem. Cell Biol.* **41**, 494–497 (2009).
65. Le, D. H. T., Hanamura, R., Pham, D.-H., Kato, M., Tirrell, D. A., Okubo, T. & Sugawara-Narutaki, A. Self-Assembly of Elastin–Mimetic Double Hydrophobic Polypeptides. *Biomacromolecules* **14**, 1028–1034 (2013).
66. Li, B. & Daggett, V. Molecular basis for the extensibility of elastin. *Journal of Muscle Research and Cell Motility* **23**, 561–573 (2002).

67. Rodgers, U. R. & Weiss, A. S. Cellular interactions with elastin. *Pathol. Biol.* **53**, 390–398 (2005).
68. Patel, A., Fine, B., Sandig, M. & Mequanint, K. Elastin biosynthesis: The missing link in tissue-engineered blood vessels. *Cardiovasc. Res.* **71**, 40–49 (2006).
69. Ryan, A. J. & O'Brien, F. J. Insoluble elastin reduces collagen scaffold stiffness, improves viscoelastic properties, and induces a contractile phenotype in smooth muscle cells. *Biomaterials* **73**, 296–307 (2015).
70. Ghazanfari, S., Alberti, K. A., Xu, Q. & Khademhosseini, A. Evaluation of an elastic decellularized tendon-derived scaffold for the vascular tissue engineering application. *J. Biomed. Mater. Res. Part A* **107**, 1225–1234 (2019).
71. Khalili, S., Khorasani, S. N., Razavi, S. M., Hashemibeni, B. & Tamayol, A. Nanofibrous Scaffolds with Biomimetic Composition for Skin Regeneration. *Appl. Biochem. Biotechnol.* **187**, 1193–1203 (2019).
72. Cao, Y., Lee, B. H., Irvine, S. A., Wong, Y. S., Bianco Peled, H. & Venkatraman, S. Inclusion of Cross-Linked Elastin in Gelatin/PEG Hydrogels Favourably Influences Fibroblast Phenotype. *Polymers (Basel).* **12**, 670 (2020).
73. Pezzoli, D., Di Paolo, J., Kumra, H., Fois, G., Candiani, G., Reinhardt, D. P. & Mantovani, D. Fibronectin promotes elastin deposition, elasticity and mechanical strength in cellularised collagen-based scaffolds. *Biomaterials* **180**, 130–142 (2018).
74. MacEwan, S. R. & Chilkoti, A. Elastin-like polypeptides: biomedical applications of tunable biopolymers. *Biopolymers* **94**, 60–77 (2010).
75. Cai, L. & Heilshorn, S. C. Designing ECM-mimetic materials using protein engineering. *Acta Biomaterialia* **10**, 1751–1760 (2014).
76. D'Andrea, P., Civita, D., Cok, M., Ulloa Severino, L., Vita, F., Scaini, D., Casalis, L., Lorenzon, P., Donati, I. & Bandiera, A. Myoblast adhesion, proliferation and differentiation on human elastin-like polypeptide (HELP) hydrogels. *J. Appl. Biomater. Funct. Mater.* **15**, e43–e53 (2017).
77. LeSavage, B. L., Suhar, N. A., Madl, C. M. & Heilshorn, S. C. Production of Elastin-like Protein Hydrogels for Encapsulation and Immunostaining of Cells in 3D. *J. Vis. Exp.* **2018**, (2018).
78. Gurumurthy, B., Bierdeman, P. C. & Janorkar, A. V. Composition of elastin like polypeptide–collagen composite scaffold influences in vitro osteogenic activity of

human adipose derived stem cells. *Dent. Mater.* **32**, 1270–1280 (2016).

79. Almeida, H., Domingues, R. M. A., Mithieux, S. M., Pires, R. A., Gonçalves, A. I., Gómez-Florit, M., Reis, R. L., Weiss, A. S. & Gomes, M. E. Tropoelastin-Coated Tendon Biomimetic Scaffolds Promote Stem Cell Tenogenic Commitment and Deposition of Elastin-Rich Matrix. *ACS Appl. Mater. Interfaces* **11**, 19830–19840 (2019).
80. Hill, P., Brantley, H. & Van Dyke, M. Some properties of keratin biomaterials: Kerateines. *Biomaterials* **31**, 585–593 (2010).
81. McKittrick, J., Chen, P. Y., Bodde, S. G., Yang, W., Novitskaya, E. E. & Meyers, M. A. The structure, functions, and mechanical properties of keratin. *JOM* **64**, 449–468 (2012).
82. Rouse, J. G. & Van Dyke, M. E. A review of keratin-based biomaterials for biomedical applications. *Materials* **3**, 999–1014 (2010).
83. Yamauchi, K., Maniwa, M. & Mori, T. Cultivation of fibroblast cells on keratin-coated substrata. *J. Biomater. Sci. Polym. Ed.* **9**, 259–270 (1998).
84. Lange, L., Huang, Y. & Busk, P. K. Microbial decomposition of keratin in nature—a new hypothesis of industrial relevance. *Applied Microbiology and Biotechnology* **100**, 2083–2096 (2016).
85. Lee, H., Noh, K., Lee, S. C., Kwon, I. K., Han, D. W., Lee, I. S. & Hwang, Y. S. Human hair keratin and its-based biomaterials for biomedical applications. *Tissue Engineering and Regenerative Medicine* **11**, 255–265 (2014).
86. Silva, R., Fabry, B. & Boccaccini, A. R. Fibrous protein-based hydrogels for cell encapsulation. *Biomaterials* **35**, 6727–6738 (2014).
87. Wang, S., Wang, Z., Foo, S. E. M., Tan, N. S., Yuan, Y., Lin, W., Zhang, Z. & Ng, K. W. Culturing fibroblasts in 3D human hair keratin hydrogels. *ACS Appl. Mater. Interfaces* **7**, 5187–5198 (2015).
88. Wang, J., Hao, S., Luo, T., Cheng, Z., Li, W., Gao, F., Guo, T., Gong, Y. & Wang, B. Feather keratin hydrogel for wound repair: Preparation, healing effect and biocompatibility evaluation. *Colloids Surfaces B Biointerfaces* **149**, 341–350 (2017).
89. Placone, J. K., Navarro, J., Laslo, G. W., Lerman, M. J., Gabard, A. R., Herendeen, G. J., Falco, E. E., Tomblyn, S., Burnett, L. & Fisher, J. P. Development and Characterization of a 3D Printed, Keratin-Based Hydrogel. *Ann. Biomed. Eng.* **45**,

237–248 (2017).

90. Navarro, J., Swayambunathan, J., Lerman, M., Santoro, M. & Fisher, J. P. Development of keratin-based membranes for potential use in skin repair. *Acta Biomater.* **83**, 177–188 (2019).
91. Barati, D., Kader, S., Pajoum Shariati, S. R., Moeinzadeh, S., Sawyer, R. H. & Jabbari, E. Synthesis and Characterization of Photo-Cross-Linkable Keratin Hydrogels for Stem Cell Encapsulation. *Biomacromolecules* **18**, 398–412 (2017).
92. Hartrianti, P., Nguyen, L. T. H., Johanes, J., Chou, S. M., Zhu, P., Tan, N. S., Tang, M. B. Y. & Ng, K. W. Fabrication and characterization of a novel crosslinked human keratin-alginate sponge. *J. Tissue Eng. Regen. Med.* **11**, 2590–2602 (2017).
93. Kim, J. W., Kim, M. J., Ki, C. S., Kim, H. J. & Park, Y. H. Fabrication of bi-layer scaffold of keratin nanofiber and gelatin-methacrylate hydrogel: Implications for skin graft. *Int. J. Biol. Macromol.* **105**, 541–548 (2017).
94. Cui, X., Xu, S., Su, W., Sun, Z., Yi, Z., Ma, X., Chen, G., Chen, X., Guo, B. & Li, X. Freeze–thaw cycles for biocompatible, mechanically robust scaffolds of human hair keratins. *J. Biomed. Mater. Res. - Part B Appl. Biomater.* **107**, 1452–1461 (2019).
95. Burnouf, T., Goubran, H. A., Chen, T.-M., Ou, K.-L., El-Ekiaby, M. & Radosevic, M. Blood-derived biomaterials and platelet growth factors in regenerative medicine. *Blood Rev.* **27**, 77–89 (2013).
96. Elsadek, B. & Kratz, F. Impact of albumin on drug delivery — New applications on the horizon. *J. Control. Release* **157**, 4–28 (2012).
97. Fanali, G., di Masi, A., Trezza, V., Marino, M., Fasano, M. & Ascenzi, P. Human serum albumin: From bench to bedside. *Mol. Aspects Med.* **33**, 209–290 (2012).
98. Larsen, M. T., Kuhlmann, M., Hvam, M. L. & Howard, K. A. Albumin-based drug delivery: harnessing nature to cure disease. *Mol. Cell. Ther.* **4**, (2016).
99. Hirose, M., Tachibana, A. & Tanabe, T. Recombinant human serum albumin hydrogel as a novel drug delivery vehicle. *Mater. Sci. Eng. C* **30**, 664–669 (2010).
100. Fleischer, S., Shapira, A., Regev, O., Nseir, N., Zussman, E. & Dvir, T. Albumin fiber scaffolds for engineering functional cardiac tissues. *Biotechnol. Bioeng.* **111**, 1246–1257 (2014).
101. Amdursky, N., Mazo, M. M., Thomas, M. R., Humphrey, E. J., Puetzer, J. L., St-Pierre, J.-P., Skaalure, S. C., Richardson, R. M., Terracciano, C. M. & Stevens, M.

M. Elastic serum-albumin based hydrogels: mechanism of formation and application in cardiac tissue engineering. *J. Mater. Chem. B* **6**, 5604–5612 (2018).

102. Sun, Y. & Huang, Y. Disulfide-crosslinked albumin hydrogels. *J. Mater. Chem. B* **4**, 2768–2775 (2016).
103. Levitt, D. & Levitt, M. Human serum albumin homeostasis: a new look at the roles of synthesis, catabolism, renal and gastrointestinal excretion, and the clinical value of serum albumin measurements. *Int. J. Gen. Med.* **Volume 9**, 229–255 (2016).
104. Komatsu, T., Oguro, Y., Teramura, Y., Takeoka, S., Okai, J., Anraku, M., Otagiri, M. & Tsuchida, E. Physicochemical characterization of cross-linked human serum albumin dimer and its synthetic heme hybrid as an oxygen carrier. *Biochim. Biophys. Acta - Gen. Subj.* **1675**, 21–31 (2004).
105. Li, X.-Y., Li, T.-H., Guo, J.-S., Wei, Y., Jing, X.-B., Chen, X.-S. & Huang, Y.-B. PEGylation of bovine serum albumin using click chemistry for the application as drug carriers. *Biotechnol. Prog.* **28**, 856–861 (2012).
106. Li, P. S., -Liang Lee, I., Yu, W. L., Sun, J. S., Jane, W. N. & Shen, H. H. A novel albumin-based tissue scaffold for autogenic tissue engineering applications. *Sci. Rep.* **4**, (2014).
107. Ma, X., Sun, X., Hargrove, D., Chen, J., Song, D., Dong, Q., Lu, X., Fan, T.-H., Fu, Y. & Lei, Y. A Biocompatible and Biodegradable Protein Hydrogel with Green and Red Autofluorescence: Preparation, Characterization and In Vivo Biodegradation Tracking and Modeling. *Sci. Rep.* **6**, 19370 (2016).
108. Bodenberger, N., Paul, P., Kubiczek, D., Walther, P., Gottschalk, K.-E. & Rosenau, F. A Novel Cheap and Easy to Handle Protein Hydrogel for 3D Cell Culture Applications: A High Stability Matrix with Tunable Elasticity and Cell Adhesion Properties. *ChemistrySelect* **1**, 1353–1360 (2016).
109. Overby, R. & Feldman, D. Influence of Poly(Ethylene Glycol) End Groups on Poly(Ethylene Glycol)-Albumin System Properties as a Potential Degradable Tissue Scaffold. *J. Funct. Biomater.* **10**, 1 (2018).
110. Bai, Y., Li, S., Li, X., Han, X., Li, Y., Zhao, J., Zhang, J., Hou, X. & Yuan, X. An injectable robust denatured albumin hydrogel formed via double equilibrium reactions. *J. Biomater. Sci. Polym. Ed.* **30**, 662–678 (2019).
111. Rusu, A. G., Chiriac, A. P., Nita, L. E., Mititelu-Tartau, L., Tudorachi, N., Ghilan, A.

& Rusu, D. Multifunctional BSA Scaffolds Prepared with a Novel Combination of UV-Crosslinking Systems. *Macromol. Chem. Phys.* **220**, 1900378 (2019).

112. Lantigua, D., Nguyen, M. A., Wu, X., Suvarnapathaki, S., Kwon, S., Gavin, W. & Camci-Unal, G. Synthesis and characterization of photocrosslinkable albumin-based hydrogels for biomedical applications. *Soft Matter* **16**, 9242–9252 (2020).
113. Fleischer, S., Shapira, A., Feiner, R. & Dvir, T. Modular assembly of thick multifunctional cardiac patches. *Proc. Natl. Acad. Sci. U. S. A.* **114**, 1898–1903 (2017).
114. Hsu, C.-C., Serio, A., Amdursky, N., Besnard, C. & Stevens, M. M. Fabrication of Hemin-Doped Serum Albumin-Based Fibrous Scaffolds for Neural Tissue Engineering Applications. *ACS Appl. Mater. Interfaces* **10**, 5305–5317 (2018).
115. Mosesson, M. W. Fibrinogen and fibrin structure and functions. in *Journal of Thrombosis and Haemostasis* **3**, 1894–1904 (2005).
116. Weisel, J. W. & Litvinov, R. I. Mechanisms of fibrin polymerization and clinical implications. *Blood* **121**, 1712–1719 (2013).
117. De Willige, S. U., Standeven, K. F., Philippou, H. & Ariëns, R. A. S. The pleiotropic role of the fibrinogen γ′ chain in hemostasis. *Blood* **114**, 3994–4001 (2009).
118. Laurens, N., Koolwijk, P. & de Maat, M. P. Fibrin structure and wound healing. *Journal of thrombosis and haemostasis : JTH* **4**, 932–939 (2006).
119. de la Puente, P. & Ludeña, D. Cell culture in autologous fibrin scaffolds for applications in tissue engineering. *Exp. Cell Res.* **322**, 1–11 (2014).
120. Brown, A. C. & Barker, T. H. Fibrin-based biomaterials: Modulation of macroscopic properties through rational design at the molecular level. *Acta Biomater.* **10**, 1502–1514 (2014).
121. Davis, H. E., Miller, S. L., Case, E. M. & Leach, J. K. Supplementation of fibrin gels with sodium chloride enhances physical properties and ensuing osteogenic response. *Acta Biomater.* **7**, 691–699 (2011).
122. Weisel, J. W. Fibrinogen and fibrin. *Adv. Protein Chem.* **70**, 247–299 (2005).
123. Breen, A., O'Brien, T. & Pandit, A. Fibrin as a delivery system for therapeutic drugs and biomolecules. *Tissue Engineering - Part B: Reviews* **15**, 201–214 (2009).
124. Ahmann, K. A., Weinbaum, J. S., Johnson, S. L. & Tranquillo, R. T. Fibrin Degradation Enhances Vascular Smooth Muscle Cell Proliferation and Matrix

Deposition in Fibrin-Based Tissue Constructs Fabricated *In Vitro*. *Tissue Eng. Part A* **16**, 3261–3270 (2010).

125. Li, Y., Meng, H., Liu, Y. & Lee, B. P. Fibrin gel as an injectable biodegradable scaffold and cell carrier for tissue engineering. *Scientific World Journal* **2015**, (2015).
126. Rajangam, T. & An, S. S. A. Fibrinogen and fibrin based micro and nano scaffolds incorporated with drugs, proteins, cells and genes for therapeutic biomedical applications. *International Journal of Nanomedicine* **8**, 3641–3662 (2013).
127. Ahmed, T. A. E., Dare, E. V. & Hincke, M. Fibrin: A Versatile Scaffold for Tissue Engineering Applications. *Tissue Eng. Part B Rev.* **14**, 199–215 (2008).
128. Zhang, Y., Heher, P., Hilborn, J., Redl, H. & Ossipov, D. A. Hyaluronic acid-fibrin interpenetrating double network hydrogel prepared in situ by orthogonal disulfide cross-linking reaction for biomedical applications. *Acta Biomater.* **38**, 23–32 (2016).
129. Keating, M., Lim, M., Hu, Q. & Botvinick, E. Selective stiffening of fibrin hydrogels with micron resolution via photocrosslinking. *Acta Biomater.* **87**, 88–96 (2019).
130. Yang, L., Li, X., Wang, D., Mu, S., Lv, W., Hao, Y., Lu, X., Zhang, G., Nan, W., Chen, H., Xie, L., Zhang, Y., Dong, Y., Zhang, Q. & Zhao, L. Improved mechanical properties by modifying fibrin scaffold with PCL and its biocompatibility evaluation. *J. Biomater. Sci. Polym. Ed.* **31**, 658–678 (2020).
131. Golebiewska, E. M. & Poole, A. W. Platelet secretion: From haemostasis to wound healing and beyond. *Blood Rev.* **29**, 153–162 (2015).
132. Santos, S. C. N. da S., Sigurjonsson, Ó. E., Custódio, C. de A. & Mano, J. F. C. da L. Blood Plasma Derivatives for Tissue Engineering and Regenerative Medicine Therapies. *Tissue Eng. Part B Rev.* **24**, 454–462 (2018).
133. Hesler, M., Kohl, Y., Wagner, S. & von Briesen, H. Non-pooled Human Platelet Lysate: A Potential Serum Alternative for *In Vitro* Cell Culture. *Altern. to Lab. Anim.* **47**, 116–127 (2019).
134. Velier, M., Magalon, J., Daumas, A., Cassar, M., Francois, P., Ghazouane, A., Philandrianos, C., Bertrand, B., Frere, C., Bernot, D., Villani, P., George, F. D. & Sabatier, F. Production of platelet-rich plasma gel from elderly patients under antithrombotic drugs: Perspectives in chronic wounds care. *Platelets* **29**, 496–503 (2018).
135. Foster, T. E., Puskas, B. L., Mandelbaum, B. R., Gerhardt, M. B. & Rodeo, S. A.

Platelet-rich plasma: From basic science to clinical applications. *American Journal of Sports Medicine* **37**, 2259–2272 (2009).

136. Liu, X., Yang, Y., Niu, X., Lin, Q., Zhao, B., Wang, Y. & Zhu, L. An in situ photocrosslinkable platelet rich plasma – Complexed hydrogel glue with growth factor controlled release ability to promote cartilage defect repair. *Acta Biomater.* **62**, 179–187 (2017).
137. Cheng, G., Ma, X., Li, J., Cheng, Y., Cao, Y., Wang, Z., Shi, X., Du, Y., Deng, H. & Li, Z. Incorporating platelet-rich plasma into coaxial electrospun nanofibers for bone tissue engineering. *Int. J. Pharm.* **547**, 656–666 (2018).
138. Faramarzi, N., Yazdi, I. K., Nabavinia, M., Gemma, A., Fanelli, A., Caizzone, A., Ptaszek, L. M., Sinha, I., Khademhosseini, A., Ruskin, J. N. & Tamayol, A. Patient-Specific Bioinks for 3D Bioprinting of Tissue Engineering Scaffolds. *Adv. Healthc. Mater.* **7**, 1701347 (2018).
139. do Amaral, R. J. F. C., Zayed, N. M. A., Pascu, E. I., Cavanagh, B., Hobbs, C., Santarella, F., Simpson, C. R., Murphy, C. M., Sridharan, R., González-Vázquez, A., O'Sullivan, B., O'Brien, F. J. & Kearney, C. J. Functionalising Collagen-Based Scaffolds With Platelet-Rich Plasma for Enhanced Skin Wound Healing Potential. *Front. Bioeng. Biotechnol.* **7**, (2019).
140. Irmak, G. & Gümüşderelioğlu, M. Photo-activated platelet-rich plasma (PRP)-based patient-specific bio-ink for cartilage tissue engineering. *Biomed. Mater.* **15**, 065010 (2020).
141. Fekete, N., Gadelorge, M., Fürst, D., Maurer, C., Dausend, J., Fleury-Cappellesso, S., Mailänder, V., Lotfi, R., Ignatius, A., Sensebé, L., Bourin, P., Schrezenmeier, H. & Rojewski, M. T. Platelet lysate from whole blood-derived pooled platelet concentrates and apheresis-derived platelet concentrates for the isolation and expansion of human bone marrow mesenchymal stromal cells: production process, content and identification of active components. *Cytotherapy* **14**, 540–554 (2012).
142. Burnouf, T., Strunk, D., Koh, M. B. C. & Schallmoser, K. Human platelet lysate: Replacing fetal bovine serum as a gold standard for human cell propagation? *Biomaterials* **76**, 371–387 (2016).
143. Walenda, G., Hemeda, H., Schneider, R. K., Merkel, R., Hoffmann, B. & Wagner, W. Human Platelet Lysate Gel Provides a Novel Three Dimensional-Matrix for Enhanced

Culture Expansion of Mesenchymal Stromal Cells. *Tissue Eng. Part C Methods* **18**, 924–934 (2012).

144. Robinson, S. T., Douglas, A. M., Chadid, T., Kuo, K., Rajabalan, A., Li, H., Copland, I. B., Barker, T. H., Galipeau, J. & Brewster, L. P. A novel platelet lysate hydrogel for endothelial cell and mesenchymal stem cell-directed neovascularization. *Acta Biomater.* **36**, 86–98 (2016).
145. Santos, S. C., Custódio, C. A. & Mano, J. F. Photopolymerizable Platelet Lysate Hydrogels for Customizable 3D Cell Culture Platforms. *Adv. Healthc. Mater.* **7**, 1800849 (2018).
146. Monteiro, C. F., Santos, S. C., Custódio, C. A. & Mano, J. F. Human Platelet Lysates-Based Hydrogels: A Novel Personalized 3D Platform for Spheroid Invasion Assessment. *Adv. Sci.* **7**, 1902398 (2020).
147. Tavares, M. T., Santos, S. C., Custódio, C. A., Farinha, J. P. S., Baleizão, C. & Mano, J. F. Platelet Lysates-based Hydrogels Incorporating Bioactive Mesoporous Silica Nanoparticles for Stem Cell Osteogenic Differentiation. *Mater. Today Bio* 100096 (2021).

Chapter III

Materials and methods

1. Chemicals and biologicals

Regarding the ABS phase-forming compounds, the glycine-betaine analogues ionic liquids (AGB-ILs) tri(n-butyl)[4-ethoxy-4-oxobutyl]ammonium bromide ([Bu_3NC_4]Br) and tri(n-butyl)[2-ethoxy-2-oxoethyl]phosphonium bromide ([Bu_3PC_2]Br), were synthesized by us according to previously reported protocols (≥97% pure)[1]. The commercial IL tetrabutylphosphonium bromide ([P_{4444}]Br, ≥ 96% pure) was purchased from Iolitec. The chemical structure of the synthesized and commercial ILs are depicted in Figure III.1.

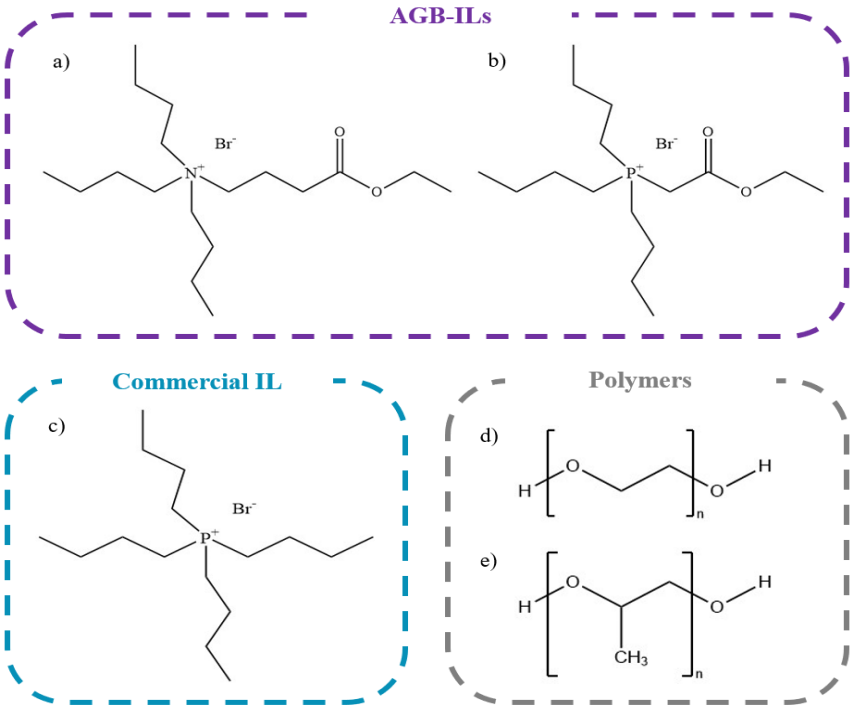

Figure III.1 Chemical structure of the phase ILs and polymers investigated: a) [Bu_3NC_4]Br, b) [Bu_3PC_2]Br, c) [P_{4444}]Br, d) PEG, and e) PPG

The polymers polyethylene glycols (PEGs) with 400, 1000, and 2000 Da molecular weight (PEG 400, PEG 1000, and PEG 2000, respectively) were purchased from Fluka and PPG with 400 Da molecular weight (PPG 400) was obtained from Sigma-Aldrich. The salts, potassium phosphate monobasic (KH_2PO_4, ≥ 98% pure) was acquired from Honeywell, di-potassium hydrogen phosphate trihydrate ($K_2HPO_4 \cdot 3H_20$, extra pure) was obtained from Scharlau, tri-potassium citrate monohydrate ($K_3C_6H_5O_7 \cdot H_2O$, ≥ 99% pure) and cholinium

chloride (ChCl, ≥ 98% pure) were purchased from Acros Organics, and citric acid monohydrate ($C_6H_8O_7 \cdot H_2O$, ≥ 99.5% pure) was obtained from Panreac.

PL and lyophilized HSA (>97% pure) were purchased from STEMCELL Technologies and Sigma-Aldrich, respectively. Phosphate buffered saline solution (PBS, pH=7.4) pellets were acquired from Sigma Aldrich and the water used in PL dilution and systems preparation was treated with a water purification system Milli-Q® Integral (Merck Millipore).

2. Platelet lysates

Platelets are natural reservoirs of growth factors (GFs), cytokines, adhesive and structural proteins, and other bioactive molecules, that are essential for their role in hemostasis, wound healing, and tissue regeneration[2]. Platelet-rich plasma (PRP) is a portion of blood plasma with high platelet concentration (≥ $1x10^6$ platelets/µL in 5 mL of plasma) that is collected from a whole blood sample after differential centrifugation[3]. PRP may subsequently be subjected to freeze-thaw cycles to disrupt the membrane and obtain a protein-rich mixture comprising the intramembrane platelet content, known as platelet lysates (PL)[4]. Due to its remarkable biochemical composition and allogeneic source, PL has been used as an alternative cell culture supplement to the animal-derived serum[5] and, more recently, have also been proposed as a biomaterial for the development of three dimensional (3D) *in vitro* cell culture platforms[6]. The PL used in this work were stored at -20°C. Before use, PL was thawed in a 37°C water bath with slow agitation.

3. Huma serum albumin removal from PL using aqueous biphasic systems-based three-phase partitioning systems

Recently, researchers of the spin-off METATISSUE developed novel photopolymerizable PL-based hydrogels for three-dimensional (3D) cell culture[7]. The exceptional cell encapsulation performance of the methacrylated platelet lysates (PLMA) hydrogels is largely due to the unique biochemical composition of PL, which comprises a variety of bioactive molecules, like GFs, cytokines, and adhesion proteins, that are essential for cell growth and proliferation. Nonetheless, PL encompasses other biomolecules that

perform mainly structural functions, like human serum albumin (HSA) which accounts for approximately 41% of the protein content of PL. Albumin in its normal form have been associated with low cell adhesion ability[8] and thus the high levels of HSA are thought to be related to the low cell adhesion observed on cells seeded on the top of PLMA hydrogels. Therefore, it was hypothesized that the removal of HSA from the PL protein mixture will improve the bioactivity of the resulting biomaterials, due to the decrease in HSA and the consequent relative increase in bioactive molecules content, thus representing the target of this work.

3.1. ABS/TPP systems preparation

The selective partition of a target molecule to one of the phases in ABS is ruled by several properties of the system and the target molecule, as well as by the chemical and physical interactions established between the system components and the target molecule[12]. Therefore, the affinity of a target molecule for one of the phases or even its precipitation at the interface between the two aqueous phases, i.e. for the three-phase partitioning (TPP) systems, could be adjusted by manipulating ABS's composition. In this sense, in a preliminary part of this work, a screening of six ABS comprising different phase-forming compounds was performed to access their ability to be used as TTP systems for the selective removal of HSA from PL, either by HSA precipitation at the interphase and partitioning of the remaining proteins for one of the aqueous phases or preferential partition of HSA for one of the aqueous phases and precipitation of the remaining proteins at the interphase. The mixture point of each system was chosen based on the ternary phase diagrams and information already reported in the literature[13–16] and are specified in Table III.1. Since high amounts of PL are needed to be processed for the final application, minimal PL dilutions were tested in the preparation of the ABS. PL were used with no dilution and diluted in deionized water, 2- to 5- fold. Considering the results from the screening, two more ABS formed by PEGs with different molecular weights, namely PEG 1000 and PEG 2000, and citrate buffer were additionally tested using PL with no dilution. The mixture point of the systems was chosen based on the ternary phase diagrams and information reported in the literature[17] and are specified in Table III.2.

Systems with 2.0 g of total weight were prepared by weighing the proper amount of each component, and each mixture was stirred until total dissolution of the phase-forming components, centrifuged for 10 min at 3500 rpm, and left to equilibrate for 10 min at 25°C. The volume of the phases and the macroscopic aspect were registered, and both phases were carefully separated. In the cases in which an interphase precipitate was observed, i.e., for the TPP systems, the precipitate was completely isolated from the remaining phases and resuspended in 1.0 mL of PBS. The best identified TPP system to remove HSA from PL was then scaled-up to a system with 52.0 g of total weight, to meet the amounts of albumin-depleted PL (AD-PL) needed for the modification step. The 52.0 g system was prepared as aforementioned for the 2.0 g systems, only differing the volume of PBS used for precipitate resuspension, that in this case was 26.0 mL. The pH values of each phase at 25 (±1) °C were determined using a Mettler Toledo U402-M3-S7/200 microelectrode, showing that a pH 6.9 ± 0.3 was maintained in all systems.

Blank systems, without biological sample, with 2.0 g of total weight were also prepared to address the interference of the ABS phase forming compounds with the analytical methods and to guarantee that the interphase precipitate only forms in the presence of PL.

Table III.1 Composition of the ABS used in the initial screening and correspondent mixture point

	Component	**Mixture point (wt%)**
System 1	$[Bu_3NC_4]Br$	40
	KH_2PO_4	15
	K_2HPO_4	
	H_2O	7.5
	PL	37.5
System 2	$[Bu_3PC_2]Br$	40
	KH_2PO_4	15
	K_2HPO_4	
	H_2O	7.5
	PL	37.5

System 3	$[P_{4444}]Br$	40
	KH_2PO_4	15
	K_2HPO_4	
	H_2O	7.5
	PL	37.5
System 4	$[P_{4444}]Br$	30
	$K_3C_6H_5O_7$	30
	$C_6H_8O_7$	
	PL	40
System 5	PEG 400	25
	$K_3C_6H_5O_7$	25
	$C_6H_8O_7$	
	PL	50
System 6	ChCl	25
	PPG 400	30
	PL	45

Table III.2 Composition of the two polymer-nased ABS additionally tested and corresponding mixture point

	Component	**Mixture point (wt%)**
System 7	PEG 1000	20
	$K_3C_6H_5O_7$	25
	$C_6H_8O_7$	
	H_2O	15
	PL	40
System 8	PEG 2000	20
	$K_3C_6H_5O_7$	25
	$C_6H_8O_7$	
	H_2O	15
	PL	40

3.2. Protein quantification

To evaluate ABS performance and thus understand HSA and total protein partition and identify the best system to selectively remove HSA from PL, HSA and total protein were quantified as described in the next sections.

3.2.1. Size-exclusion high-performance liquid chromatography

Size-exclusion high-performance liquid chromatography (SE-HLPC) employs porous particles on the stationary phase to separate biomolecules accordingly to their size in solution. In this work, SE-HPLC was used to quantify HSA in each ABS phase and thus understand HSA partition in the ABS studied. Samples were conveniently diluted in an aqueous potassium phosphate buffer solution (100 mmol/L, pH 7.0, with NaCl 0.3 mol/L), which was also used as the mobile phase. The equipment used was a Chromaster HPLC system (VWR Hitachi) equipped with a binary pump, column oven (operating at 40 °C), temperature-controlled auto-sampler (operating at 10 °C), DAD detector, and a column Shodex Protein KW-802.5 (8 mm x 300 mm). The mobile phase was run isocratically with a flow rate of 0.5 mL/min and the injection volume was 25 µL. The wavelength was set at 280 nm. The calibration curve was established with commercial HSA from 2.5 to 1500 mg/L. The percentage of HSA in each phase was calculated accordingly to the following equation:

$$\%HSA = \frac{[HSA]_{phase} \times v_{phase}}{[HSA]_{PL} \times v_{PL}} \times 100 \quad (1)$$

where $[HSA]_{phase}$ and $[HSA]_{PL}$ represent the concentration of HSA in the phase analyzed and concentration of HSA on the PL added to the ABS, respectively, and v_{phase} and v_{PL} correspond to the volume of the phase analyzed and the volume of PL added to the system, respectively.

3.2.2. Pierce™ BCA protein assay kit

Since PL is a complex mixture of proteins, the total protein content of each ABS phase was determined with the Pierce™ BCA protein assay kit (Thermo Fisher Scientific). The Pierce BCA protein assay is a colorimetric technique used for the detection and quantification of total protein and relies on the ability of proteins in an alkaline environment to reduce Cu^{2+} to Cu^{1+}, which in turn reacts with bicinchoninic acid (BCA) and generate a

purple-colored product. The percentage of total protein in each phase was calculated accordingly to the following equation:

$$\%Total\ protein = \frac{[Total\ protein]_{phase} \times v_{phase}}{[Total\ protein]_{PL} \times v_{PL}} \times 100 \quad (2)$$

where $[Total\ protein]_{phase}$ and $[Total\ protein]_{PL}$ represent the concentration of total protein in the phase analyzed and concentration of total protein on the PL added to the ABS, respectively, and v_{phase} and v_{PL} correspond to the volume of the phase analyzed and the volume of PL added to the system, respectively.

3.3. Protein profile determination

For the albumin depleted PL (AD-PL) fraction obtained from the best-identified system to remove HSA from PL it is important to confirm that beyond the decrease in HSA, a protein profile similar to that of the original PL is maintained. Sodium dodecyl sulfate-polyacrylamide gel electrophoresis (SDS-PAGE) separate proteins based on their molecular weight and was used in this work to infer the protein profile of each fraction of the best identified TPP system for HSA removal from PL. The samples, previously diluted in PBS, were diluted at 1:1 in sample buffer containing 4% (w/v) of SDS, 20% (w/v) of glycerol, 120 mM of Tris-HCl, pH 6.8, and 0.02% (w/v) bromophenol blue under reducing conditions with 200 mM dithiothreitol (DTT) and then denatured by incubation at 95°C for 5 min. The samples were then injected in the polyacrylamide gel (Precast Gel SDS-PAGE 4-12%, Expedeon). Lastly, protein staining was achieved by incubation with BlueSafe (NZYTech) under mild agitation for 1 h.

4. Phase-forming compounds removal from AD-PL

The phase-forming compounds could interfere with the following methacrylation and/or polymerization reactions. Therefore, the AD-PL fraction obtained from the scale-up of the best-identified system to remove HSA from PL was purified by an additional ultrafiltration step using an ultrafiltration system (Laborspirit) equipped with a 5 kDa filter

(regenerated cellulose Merck) and passing a volume of PBS equivalent to three times the volume of the AD-PL fraction. The ultrafiltrate AD-PL was then frozen with liquid nitrogen, lyophilized (LyoQuestPlusEco, Telstar, Spain) for 3 days and stored at 4°C until further use.

5. Chemical modification of lyophilized AD-PL

The insertion of chemical moieties into natural polymers backbone is a common approach to increase the control over the mechanical properties of the biomaterial and to make it stimuli responsive. Chemical modification of proteins with methacryloyl groups, photoresponsive moieties that undergo covalent crosslinking by free-radical polymerization in the presence of a photoinitiator and upon exposure to UV radiation, have been commonly explored for the fabrication of photopolymerizable protein-based hydrogels[18–20] and was the strategy adopted by METATISSUE researchers to develop PL-based photopolymerizable hydrogels[7]. In this work, to make AD-PL photoresponsive, 630 mg of lyophilized AD-PL were dissolved in 10 mL of PBS (pH 7.4, Sigma Aldrich), to obtain a solution with a similar protein concentration to PL, and then chemically modified with MA 94% (Sigma-Aldrich, USA), as previously reported for PLMA synthesis[7]. Briefly, 100 or 300 µL of MA were added, to synthesize AD-PLMA 100 (low-degree of modification) and AD-PLMA 300 (high-degree of modification). The reaction occurred under constant stirring for 4 hours at room temperature. The pH was checked and maintained within a 6-8 range by adding 5M sodium hydroxide (NaOH) (AkzoNobel USA) to neutralize the acid produced during the reaction and thus prevent protein precipitation due to pH decrease. After 4 hours of reaction, the synthesized AD-PLMAs were purified by dialysis with Float-a-Lyzer G2 Dialysis Devices 3.5-5 kDa (Spectrum, USA) against deionized water for 24 hours. The AD-PLMA solutions were then sterilized by filtering with a 0.2 µm low protein retention filter (Enzymatic S.A., Portugal), frozen with liquid nitrogen, lyophilized (LyoQuestPlusEco, Telstar, Spain) and stored at 4°C until further use.

6. Hydrogel formation

Photocrosslinking is a cost-effective and simple technique that allows the rapid fabrication of easy-to-handle hydrogels with great control over their mechanical properties,

size, and shape. Furthermore, it can be carried out under mild conditions enabling cell encapsulation and allows trans-tissue *in situ* polymerization. Therefore, photocrosslinkable hydrogels are a growing class of biomaterials that can be easily fabricated from photorresponsive polymers in the presence of a photoinitiator and upon exposure to ultraviolet (UV) irradiation. Therefore, in this work, hydrogel precursor solutions were prepared by dissolving lyophilized AD-PLMA, a photoresponsive polymer, in a solution of 0.5% (w/v) 2-hydroxy-4'-(2-hydroxyethoxy)-2-methylpropiophenone (Irgacure 2959, Sigma-Aldrich) in PBS to final concentrations of 7.5%, 10%, and 15% (w/v) AD-PLMA. Hydrogels were fabricated by pipetting 10 µL of the precursor solutions into polydimethylsiloxane (PDMS, Dow Corning) molds with 3.5 mm diameter followed by UV irradiation (Omnicure-S2000, Excelitas Technologies Corp.) for 60 s with an output intensity of 1.54 W/cm^2.

References

1. Pereira, M. M., Pedro, S. N., Gomes, J., Sintra, T. E., Ventura, S. P. M., Coutinho, J. A. P., Freire, M. G. & Mohamadou, A. Synthesis and characterization of analogues of glycine-betaine ionic liquids and their use in the formation of aqueous biphasic systems. *Fluid Phase Equilib.* **494**, 239–245 (2019).
2. Piccin, A., Di Pierro, A. M., Canzian, L., Primerano, M., Corvetta, D., Negri, G., Mazzoleni, G., Gastl, G., Steurer, M., Gentilini, I., Eisendle, K. & Fontanella, F. Platelet gel: A new therapeutic tool with great potential. *Blood Transfusion* **15**, 333–340 (2017).
3. Foster, T. E., Puskas, B. L., Mandelbaum, B. R., Gerhardt, M. B. & Rodeo, S. A. Platelet-Rich Plasma. *Am. J. Sports Med.* **37**, 2259–2272 (2009).
4. Frese, L., Sasse, T., Sanders, B., Baaijens, F. P. T., Beer, G. M. & Hoerstrup, S. P. Are adipose-derived stem cells cultivated in human platelet lysate suitable for heart valve tissue engineering? *J. Tissue Eng. Regen. Med.* **11**, 2193–2203 (2017).
5. Mojica-Henshaw, M. P., jacobson, P., Morris, J., Kelley, L., Pierce, J., Boyer, M. & Reems, J.-A. Serum-converted platelet lysate can substitute for fetal bovine serum in human mesenchymal stromal cell cultures. *Cytotherapy* **15**, 1458–1468 (2013).
6. Robinson, S. T., Douglas, A. M., Chadid, T., Kuo, K., Rajabalan, A., Li, H., Copland, I. B., Barker, T. H., Galipeau, J. & Brewster, L. P. A novel platelet lysate hydrogel for endothelial cell and mesenchymal stem cell-directed neovascularization. *Acta Biomater.* **36**, 86–98 (2016).
7. Santos, S. C., Custódio, C. A. & Mano, J. F. Photopolymerizable Platelet Lysate Hydrogels for Customizable 3D Cell Culture Platforms. *Adv. Healthc. Mater.* **7**, 1800849 (2018).
8. Ong, J., Zhao, J., Levy, G. K., Macdonald, J., Justin, A. W. & Markaki, A. E. Functionalisation of a heat-derived and bio-inert albumin hydrogel with extracellular matrix by air plasma treatment. *Sci. Rep.* **10**, 12429 (2020).
9. Bridges, N. J., Gutowski, K. E. & Rogers, R. D. Investigation of aqueous biphasic systems formed from solutions of chaotropic salts with kosmotropic salts (salt–salt ABS). *Green Chem.* **9**, 177–183 (2007).
10. Phong, W. N., Show, P. L., Chow, Y. H. & Ling, T. C. Recovery of biotechnological

products using aqueous two phase systems. *J. Biosci. Bioeng.* **126**, 273–281 (2018).

11. Freire, M. G., Cláudio, A. F. M., Araújo, J. M. M., Coutinho, J. A. P., Marrucho, I. M., Lopes, J. N. C. & Rebelo, L. P. N. Aqueous biphasic systems: a boost brought about by using ionic liquids. *Chem. Soc. Rev.* **41**, 4966 (2012).
12. Rosa, P. A. J., Ferreira, I. F., Azevedo, A. M. & Aires-Barros, M. R. Aqueous two-phase systems: A viable platform in the manufacturing of biopharmaceuticals. *Journal of Chromatography A* **1217**, 2296–2305 (2010).
13. Mondal, D., Sharma, M., Quental, M. V., Tavares, A. P. M., Prasad, K. & Freire, M. G. Suitability of bio-based ionic liquids for the extraction and purification of IgG antibodies. *Green Chem.* **18**, 6071–6081 (2016).
14. Capela, E. V., Santiago, A. E., Rufino, A. F. C. S., Tavares, A. P. M., Pereira, M. M., Mohamadou, A., Aires-Barros, M. R., Coutinho, J. A. P., Azevedo, A. M. & Freire, M. G. Sustainable strategies based on glycine–betaine analogue ionic liquids for the recovery of monoclonal antibodies from cell culture supernatants. *Green Chem.* **21**, 5671–5682 (2019).
15. Pereira, M. M., Pedro, S. N., Quental, M. V., Lima, Á. S., Coutinho, J. A. P. & Freire, M. G. Enhanced extraction of bovine serum albumin with aqueous biphasic systems of phosphonium- and ammonium-based ionic liquids. *J. Biotechnol.* **206**, 17–25 (2015).
16. Pereira, M. M., Cruz, R. A. P., Almeida, M. R., Lima, Á. S., Coutinho, J. A. P. & Freire, M. G. Single-step purification of ovalbumin from egg white using aqueous biphasic systems. *Process Biochem.* **51**, 781–791 (2016).
17. Lu, Y.-M., Yang, Y.-Z., Zhao, X.-D. & Xia, C.-B. Bovine serum albumin partitioning in polyethylene glycol (PEG)/potassium citrate aqueous two-phase systems. *Food Bioprod. Process.* **88**, 40–46 (2010).
18. Van Den Bulcke, A. I., Bogdanov, B., De Rooze, N., Schacht, E. H., Cornelissen, M. & Berghmans, H. Structural and Rheological Properties of Methacrylamide Modified Gelatin Hydrogels. *Biomacromolecules* **1**, 31–38 (2000).
19. Yang, K., Sun, J., Wei, D., Yuan, L., Yang, J., Guo, L., Fan, H. & Zhang, X. Photo-crosslinked mono-component type II collagen hydrogel as a matrix to induce chondrogenic differentiation of bone marrow mesenchymal stem cells. *J. Mater. Chem. B* **5**, 8707–8718 (2017).

20. Lantigua, D., Nguyen, M. A., Wu, X., Suvarnapathaki, S., Kwon, S., Gavin, W. & Camci-Unal, G. Synthesis and characterization of photocrosslinkable albumin-based hydrogels for biomedical applications. *Soft Matter* **16**, 9242–9252 (2020).

Chapter IV

HSA removal from PL using TPP systems for the fabrication of PL-based hydrogels for 3D cell culture

HSA removal from PL using TPP systems for the fabrication of PL-based hydrogels for 3D cell culture

Abstract

The design of scaffolds has been proven to be fundamental for the advances made on three-dimensional (3D) cell culture and thus there is an ongoing effort to develop new scaffolds or improve the properties of the existing ones. Photopolymerizable hydrogels prepared from human platelet lysates (PL) were developed and hold great potential to be used as a 3D cell culture platform. However, these hydrogels exhibit low cell attachment for seeded cells, and it was hypothesized this drawback could be overcome by removing human serum albumin (HSA) from PL. Herein, a three-phase partitioning (TPP) approach using aqueous biphasic systems (ABS) was investigated for the processing of PL to obtain an albumin-depleted PL (AD-PL) fraction that could be further used for hydrogel formation. A screening of eight different ABS was performed to access their ability to be used as TPP systems for the removal of HSA from PL. Two approaches were investigated, selective precipitation of HSA at the ABS interphase and the precipitation of the remaining proteins at the interphase with HSA being selectively extracted to one of the ABS phases. The depletion performance of each system was characterized by quantification of the total protein and HSA content in each phase. PEG 1000/citrate buffer TPP system showed a preferential partition of HSA for the PEG-rich phase and the precipitation of the remaining PL proteins at the interphase, corresponding to an AD-PL fraction with less 53% of HSA. The system was then scaled-up and the AD-PL fraction recovered was successfully used for hydrogel formation.

1. Introduction

Scaffold-based models have been the major contributors to the transition from 2D to 3D cell culture and, therefore, the design of scaffolds is a growing field of research. Scaffolds are designed to act as a provisional extracellular matrix (ECM) and thus provide structural support for the cellular constituents and biochemical and biophysical cues that guide cellular development[1]. Currently, collagen type I and solubilized basement membrane of Engelbreth-

Holm-Swarm mouse sarcoma cells gels are considered the gold-standard platforms for 3D cell culture. However, despite their ability to conduct cellular self-organization and complex morphogenetic processes, these materials go against the current animal-free tendency and are difficult to handle, reinforcing an ongoing research to find 3D cell culture platforms that can overcome such limitations and could be implement for routinely lab use[2]. Santos *et al.*[3] proposed a novel human based alternative by conjugating platelet lysates (PL) proteins with methacryloyl groups (PLMA) to fabricate photocrosslinkable human PL hydrogels. PL can be easily obtained through freeze-thaw cycles of a platelet-rich plasma (PRP) fraction harvested by differential centrifugation of a whole blood sample, presenting as a cost-effective human source of fibrous and adhesive proteins, cytokines, growth factors, and other bioactive molecules that are involved in numerous cellular functions and tissue development[4]. By combining the rich biochemical composition of human PL with the highly tunable mechanical properties of photocrosslinkable materials, the developed PLMA hydrogel provide a humanized physiologically relevant tissue-like microenvironment, holding great potential as a scaffold for 3D cell culture[3]. Despite the ability to support the growth and migration of human derived cells encapsulated within them, PLMA hydrogels did not promote the proper adhesion of seeded cells. Looking for a possible explanation, the biochemical composition of PL may represent the answer. Human serum albumin (HSA) accounts for circa 41% of the total protein content of PL[3]. As reported in studies that make use of albumin-based scaffolds, albumin in its normal form could not promote adequate cell attachment[5,6] and therefore, despite the presence of adhesive proteins and other biomolecules that promote cell adhesion in PLMA hydrogels, the higher amounts of HSA may mask their activity and thus explain the low cell adhesion in PLMA hydrogels. In this sense, the removal of HSA from PL protein mixture presents as a reliable strategy to increase the cell adhesion ability of PLMA hydrogels.

Aqueous biphasic systems (ABS) are typically ternary mixtures of two polymers, a polymer and a salt, or two salts dissolved in an aqueous media, that above a certain concentration undergo separation and form two coexisting immiscible phases, which are enriched in each one of the phase-forming compounds[7]. ABS were first proposed by Albertson *et al.*[8] as liquid-liquid extraction/purification techniques and rapidly gained considerable attention for the extraction of bioactive molecules as they offer a biocompatible environment, due to their high-water content and avoiding the use of hazardous volatile

organic solvents, and allow the purification and concentration in a single-step[9]. Furthermore, they can be easily scaled-up and are cost effective if properly designed. The partitioning of a target protein on ABS depends on its surface properties, on the physicochemical properties of the two aqueous phases, and on the interactions established between the protein and the phase forming components. Therefore, by tailoring the type and concentration of the phase forming components, pH, and temperature of the ABS it is possible to manipulate the protein partition[10]. Polymer-polymer and polymer-salt ABS have been widely exploited for the extraction of proteins[11]. However, this type of ABS, especially polymer-polymer systems, presents some constraints such as the high viscosity, that may hinder mass transfer and lead to slower phase separation, and the restricted range of polarity, limiting the selectivity of the systems. Ionic liquids (ILs) have been later proposed as alternative ABS phase-forming components by Rogers *et al.*[12] bringing the possibility to tailor the affinities and polarities of the phases, through the proper anion/cation design, and thus overcome the limited polarity range associated with traditional polymer-based systems. Within the field of IL-based ABS, Alvarez *et al.*[13] recently proposed the concept of IL-based three-phase partitioning (ILTPP) for the recovery of proteins. Traditional TPP systems have been widely reported for the concentration and purification of proteins, involving, the recovery of a target protein as a precipitate formed at the interphase between a *tert*-butanol organic phase and an ammonium sulphate phase[14]. However, ILTTP sharing the advantage of both ABS and ILs is a less investigated approach[15]. Furthermore, ILTPP is a hybrid technique that combines the advantages of ABS with the ease of isolation of proteins without the need of back-extraction steps of TPP if the target protein is the precipitated one.

Herein, eight ABS composed of different phase-forming compounds, were tested for their ability to be used as TPP systems for the removal of HSA from PL, either by precipitation of HSA at the interphase and partition of the remaining PL proteins for one of the phases, or by HSA partition for one of the phases and precipitation of the remaining proteins at the interphase, to obtain an albumin-depleted PL (AD-PL) fraction. The AD-PL fraction was then functionalized with methacryloyl groups (AD-PLMA) and photocrosslinked to prepare hydrogels for 3D cell culture.

2. Materials and methods

2.1. Chemicals and biologicals

Regarding the ABS phase forming components, the betaine glycine analogues ILs (AGB-ILs) tri(n-butyl)[4-ethoxy-4-oxobutyl]ammonium bromide ([Bu_3NC_4]Br) and tri(n-butyl)[2-ethoxy-2-oxoethyl]phosphonium bromide ([Bu_3PC_2]Br), were synthetized by us according to previously reported protocols (≥97% pure)[16]. The commercial IL tetrabutylphosphonium bromide ([P_{4444}]Br, ≥ 96% pure) was purchased from Iolitec. The chemical structure of the synthetized and commercial ILs are depicted in Figure IV.1. The polymers, polyethylene glycols (PEGs) with 400, 1000, and 2000 Da molecular weight (PEG 400, PEG 1000, and PEG 2000, respectively) were purchased from Fluka, and PPG with 400 Da molecular weight (PPG 400) was obtained from Sigma-Aldrich. The salts, potassium phosphate monobasic (KH_2PO_4, ≥ 98% pure) was acquired from Honeywell, di-potassium hydrogen phosphate trihydrate ($K_2HPO_4 \cdot 3H_20$, extra pure) was obtained from Scharlau, tri-potassium citrate monohydrate ($K_3C_6H_5O_7 \cdot H_2O$, ≥ 99% pure) and cholinium chloride (ChCl, ≥ 98% pure) were purchased from cros Organics, and citric acid monohydrate ($C_6H_8O_7 \cdot H_2O$, ≥ 99.5% pure) was obtained from Panreac.

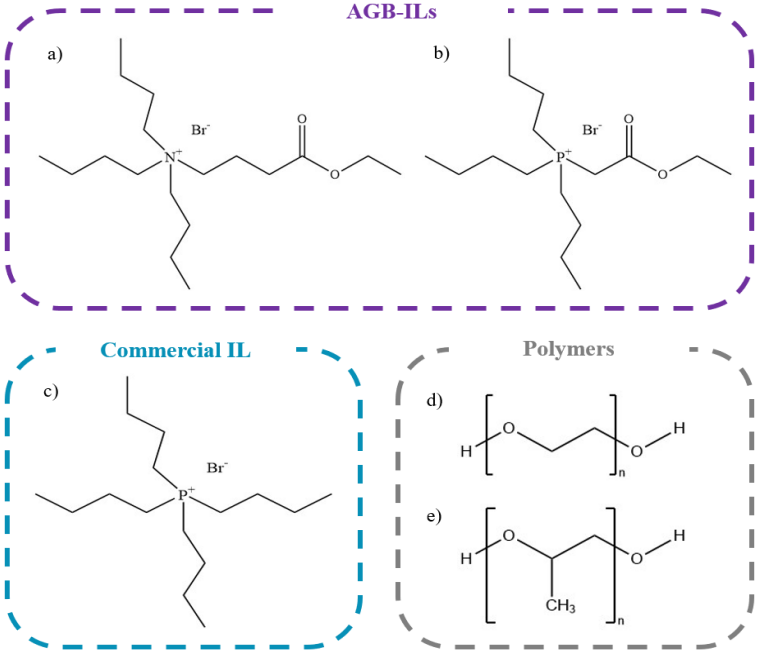

Figure IV.1 Chemical structure of the investigated ILs and polymers: a) [Bu_3NC_4]Br, b) [Bu_3PC_2]Br, c) [P_{4444}]Br, d) PEG, and e) PPG.

PL and lyophilized HSA (>97% pure) were purchased from STEMCELL Technologies and Sigma-Aldrich, respectively. Phosphate buffered saline solution (PBS, pH=7.4) pellets were acquired from Sigma Aldrich and the water used in PL dilution and systems preparation was treated with a water purification system Milli-Q® Integral (Merck Millipore).

2.2. HSA removal from PL using ABS-based TPP systems

2.2.1. ABS/TPP systems preparation

Since ABS phase-forming components have a high influence over target molecules partition between the two phases or even on their precipitation at the interphase, i.e. for the TPP systems, a preliminary screening was carried out. Accordingly, six ABS comprising different phase-forming compounds at a given mixture point based in the ternary phase diagrams and information already reported in the literature[15,17–19] were prepared to access their ability to be used as TTP systems for the selective removal of HSA from PL. Each system was prepared with original PL and PL diluted in deionized water, from 2- to 5-fold. Additionally, two more ABS at a given mixture point based in the ternary phase diagrams already reported in the literature[20], formed by PEGs with different molecular weights, namely PEG 1000 and PEG 2000, were tested. Each system was prepared with original PL. The systems and corresponding mixture points tested were as follows:

1) 40 wt% $[Bu_3NC_4]Br$ + 15 wt% KH_2PO_4/ K_2HPO_4 + 7.5 wt% H_2O + 37.5 wt% PL
2) 40 wt% $[Bu_3PC_2]Br$ + 15 wt% KH_2PO_4/ K_2HPO_4 + 7.5 wt% H_2O + 37.5 wt% PL
3) 40 wt% $[P_{4444}]Br$ + 15 wt% KH_2PO_4/ K_2HPO_4 + 7.5 wt% H_2O + 37.5 wt% PL
4) 30 wt% $[P_{4444}]Br$ + 30 wt% $K_3C_6H_5O_7/C_6H_8O_7$ + 40 wt% PL
5) 25 wt% PEG 400 + 25 wt% $K_3C_6H_5O_7/C_6H_8O_7$ + 50 wt% PL
6) 25 wt% ChCl + 30 wt% PPG + 45 wt% PL
7) 20 wt% PEG 1000 + 25 wt% $K_3C_6H_5O_7/C_6H_8O_7$ + 15 wt% H_2O + 40 wt% PL
8) 20 wt% PEG 2000 + 25 wt% $K_3C_6H_5O_7/C_6H_8O_7$ + 15 wt% H_2O + 40 wt% PL

Systems with 2.0 g of total weight were prepared by weighting the proper amount of each component. Each mixture was stirred until total dissolution of the solid components, centrifuged for 10 min at 3500 rpm, and left to equilibrate for 10 min at 25°C. The volume of the phases and the macroscopic aspect were registered, and both phases were carefully separated. In the cases in which an interphase precipitate was observed, i.e., for the TPP systems, the precipitate was completely isolated from the remaining phases and resuspended in 1.0 mL of PBS. Then, the best identified TPP system to remove HSA from PL was scaled-up to a system with 52.0 g of total weight to meet the amounts of AD-PL needed for the modification step and prepared as aforementioned for the 2.0 g systems, only differing the volume of PBS used for precipitate resuspension, that in this case was 26.0 mL. The pH values of each phase at 25 (±1) °C were determined using a Mettler Toledo U402-M3-S7/200 micro electrode, showing that a pH 6.9 ± 0.3 was maintained in all systems.

Blank systems, without biological sample, with 2.0 g of total weight were also prepared to address the interference of the ABS phase-forming compounds with the analytical methods subsequently used for protein quantification and guarantee that the interphase precipitate only occurs in the presence of PL, which was verified.

2.2.2. Protein quantification

2.2.2.1. Size-exclusion high-performance liquid chromatography

The HSA content in each ABS phase was determined by size-exclusion high-performance liquid chromatography (SE-HPLC). Samples were conveniently diluted in an aqueous potassium phosphate buffer solution (100 mmol/L, pH 7.0, whith NaCl 0.3 mol/L) that was used as the mobile phase. The equipment used was a Chromaster HPLC system (VWR Hitachi) equipped with a binary pump, column oven (operating at 40 °C), temperature controlled auto-sampler (operating at 10°C), DAD detector and a column Shodex Protein KW-802.5 (8 mm x 300 mm). The mobile phase was run isocratically with a flow rate of 0.5 mL/min and the injection volume was 25 µL. The wavelength was set at 280 nm. The calibration curve was established with commercial HSA from 2.5 to 1500 mg/L (Supporting information – Figure S.1). The percentage of HSA in each phase was calculated accordingly to the following equation:

$$\%HSA = \frac{[HSA]_{phase} \times v_{phase}}{[HSA]_{PL} \times v_{PL}} \times 100 \quad (1)$$

where $[HSA]_{phase}$ and $[HSA]_{PL}$ represent the concentration of HSA in the phase analyzed and concentration of HSA in the PL added to the ABS, respectively, and v_{phase} and v_{PL} correspond to the volume of the phase analyzed and the volume of PL added to the system, respectively.

2.2.2.2. Pierce™ BCA protein assay kit

The total protein content in each ABS phase was determined with the Pierce™ BCA protein assay kit (Thermo Fisher Scientific). The percentage of total protein in each phase was calculated accordingly to the following equation:

$$\%Total\ protein = \frac{[Total\ protein]_{phase} \times v_{phase}}{[Total\ protein]_{PL} \times v_{PL}} \times 100 \quad (2)$$

where $[Total\ protein]_{phase}$ and $[Total\ protein]_{PL}$ represent the concentration of total protein in the phase analyzed and concentration of total protein on the PL added to the ABS, respectively, and v_{phase} and v_{PL} correspond to the volume of the phase analyzed and the volume of PL added to the system, respectively.

2.2.3. Protein profile determination

To infer the protein profile of each phase and precipitate of the best identified TPP system for HSA removal from PL, a sodium dodecyl sulfate-polyacrylamide gel electrophoresis (SDS-PAGE) analysis was performed. The samples, previously diluted in PBS, were then diluted at 1:1 in sample buffer containing 4% (w/v) of SDS, 20% (w/v) of glycerol, 120 mM of Tris-HCl, pH 6.8, and 0.02% (w/v) bromophenol blue under reducing conditions with 200 mM dithiothreitol (DTT) and then denatured by incubation at 95°C for 5 min. The samples were then injected in the polyacrylamide gel (Precast Gel SDS-PAGE

4-12%, Expedeon). Lastly, protein staining was achieved by incubation with BlueSafe (NZYTech) under mild agitation for 1 h.

2.3. Phase-forming components removal from AD-PL

The AD-PL fraction obtained from the scale-up of the best identified system to remove HSA from PL was purified by ultrafiltration using an ultrafiltration system (Laborspirit) equipped with a 5 kDa filter of regenerated cellulose (Merck) and passing a volume of PBS equivalent to three times the volume of the AD-PL fraction. The ultrafiltrate AD-PL was then frozen with liquid nitrogen, lyophilized (LyoQuestPlusEco, Telstar, Spain) for 3 days and stored at 4°C until further use.

2.4. Chemical modification of lyophilized AD-PL

The photocrosslinkable AD-PL (AD-PLMA) were synthetized by reaction with methacrylic anhydride (MA), as previously reported for PLMA[3]. First, two solutions with similar protein concentration to original PL (Stemcell Technologies) (≈ 63 mg/mL) were prepared by dissolving 630 mg of lyophilized AD-PL in 10 mL of PBS. Then, either 100 or 300 µL of MA, in order to synthetize AD-PLMA 100 (low-degree of modification) and AD-PLMA 300 (high-degree of modification) were added to the AD-PL solution. The reaction occurred under constant stirring during 4 hours at room temperature. The pH was checked and maintained within a 6-8 range by adding 5M sodium hydroxide (NaOH) (AkzoNobel USA) to neutralize the acid produced during the reaction and thus prevent protein precipitation due to pH decrease. After 4 hours of reaction, the synthetized AD-PLMAs were purified by dialysis with Float-a-Lyzer G2 Dialysis Devices 3.5-5 kDa (Spectrum, USA) against deionized water for 24 hours. The AD-PLMA solutions were then sterilized by filtering with a 0.2 µm low protein retention filter (Enzymatic S.A., Portugal), frozen with liquid nitrogen, lyophilized for 3 days and stored at 4°C until further use.

2.5. Hydrogel formation

Hydrogel precursor solutions were prepared by dissolving lyophilized AD-PLMA in a solution of 0.5% (w/v) 2-hydroxy-4'-(2-hydroxyethoxy)-2-methylpropiophenone (Irgacure 2959, Sigma-Aldrich) in PBS to final concentrations of 7.5%, 10%, and 15% (w/v) AD-PLMA. Hydrogels were fabricated by pipetting 10 µL of the precursor solutions into polydimethylsiloxane (PDMS, Dow Corning) molds with 3.5 mm diameter followed by UV irradiation (Omnicure-S2000, Excelitas Technologies Corp.) for 60 s with an output intensity of 1.54 W/cm^2.

3. Results and discussion

3.1. HSA removal from PL using TPP systems

The application of ABS-based TPP systems for the removal of HSA from PL, to the best of our knowledge, has never been exploited. Therefore, an initial screening of different types of ABS, including IL-salt, IL-polymer, and polymer-salt ABS, previously reported for the extraction of other proteins[15,17–19], were investigated to access their ability to form TPP systems in the presence of PL. Ideally, due to the high amounts of AD-PL needed for the methacrylation reaction and hydrogel formation, the use of PL with no dilution for ABS formation would be the ideal condition to take advantage of the concept of molecular crowding[21] and since higher amounts of the biological matrix could be processed in a single step. Due to the high protein content in PL, the use of PL with no dilution could, on the other hand, hamper proper phase separation. Furthermore, the protein load introduced in the system could also influence the protein partition and therefore PL dilutions from 2- to 5-fold were tested.

From the ABS macroscopic observation, all systems formed a precipitate between the two aqueous phases, i.e. behave as TPP systems, with all PL dilutions, except system 5, which interphase precipitate was not significant when the system was prepared with PL diluted 3-, 4-, and 5-fold, and for system 6. Furthermore, the extent of the precipitation was different from system to system, suggesting that the system composition influences the protein solubility and partition, as expected, and that the protein load is also an important

factor, as for system 5, the formation of a TPP was only achieved with higher concentrations of PL. Moreover, the blank systems did not show any precipitate at the interphase, confirming that the TPP only occurs in the presence of PL.

The top and bottom phases were separated, and the precipitates resuspended in PBS. However, the top phase separation from the precipitates of system 4, prepared with PL with no dilution and 2-fold diluted and precipitates resuspension was not achieved, except for the precipitates from system 5. Furthermore, for systems 2 and 4 prepared with PL diluted 3-, 4-, and 5-fold, and system 3 prepared with PL diluted 4- and 5-fold, the top phases precipitated on the vial upon the addition of the phosphate buffer, and therefore the respective analysis by SE-HPLC was not possible, being discarded for further studies. This suggests that the phase forming components exerted a deleterious effect on protein structure and seems to be common for the TPP systems containing ILs with phosphonium-based cations. Similarly, Pereira *et al.*[18] have previously reported total precipitation of bovine serum albumin (BSA) in an ABS composed by $[P_{4444}]$Br and suggested that the alterations in protein conformation could be due to interactions between the protein and the IL.

The remaining top and bottom phases were analyzed by SE-HPLC and Pierce BCA to quantify the HSA and total protein mass (Supporting information – Table S.1), respectively, and thus their percentage in each phase accordingly to equations 1 and 2. Since precipitates resuspension in PBS was not completely achieved in some cases, its composition was calculated through the difference between the mass of HSA quantified for the amount of PL added to the system and the sum of the masses of HSA quantified for top and bottom phases, and likewise for total protein. The results obtained are depicted in Figure IV.2.

It should be remarked that, for some phases the mass of HSA is higher than the mass of total protein (Supporting information – Table S.1). It should be however remarket that the first was quantified by an analytical method (SE-HPLC), that relies on protein molecular weight, and the latter quantified by a colorimetric method (Pierce), and thus, less sensitive and more prone to interferences of the ABS constituents.

From Figure IV.2, it is clear that for system 6, regardless of the amount of PL added to the system, all PL proteins have preferential partition for the bottom phase, which corresponds to the ChCl-rich phase, similar to the findings reported by Quental *et al.*[22] and that was attributed to the hydrogen bonding and dispersive interactions between the IL and the protein. However, in this case, no precipitation was observed in the presence of PL,

contrary to what was described for BSA extraction studies that made use of the same type of ABS[22,23]. Therefore, system 6 was discarded due to its inability to act as a TPP system in the presence of PL. Likewise, system 2 and 3 were also discarded, since it was observed total protein precipitation for both, independently on PL concentration (Figure IV.2), confirming once again the idea that phosphonium-based ILs have a deleterious effect over proteins structure, as previously discussed, and thus are not suitable for the goal of this work.

For system 1, it could be depicted a preferential HSA partition for the top phase (IL-rich phase), in accordance to was previously described by Capela *et al.*[15], and a tendency for its increase with the decrease of PL concentration (Figure IV.2). Such behavior could be indicative that HSA partition, that is negatively charged at the pH of the system (isoelectric point of HSA is *c.a.* 4.7), could be mainly ruled by the electrostatic interactions established with the IL cation, since for lower concentrations of PL, fewer HSA molecules are introduced in the system and therefore more IL molecules are free to interact. Looking at the results, the system prepared with PL diluted 5-fold presents the most significative percentage removal of HSA from the remaining PL proteins, which precipitate at the interphase. However, despite no deleterious effects are observed for the proteins in suspension at the top phase, the interphase precipitate could not be resuspended, suggesting that the protein precipitation could be associated with strong protein-protein interactions and/or conformational changes that are irreversible, and thus this system was also discarded for further studies.

For system 5 prepared with non-diluted PL a preferential partition of HSA for the top phase (PEG-rich phase) was also observed and is in agreement with the results obtained for the extraction of ovalbumin (OVA) from egg white reported by Pereira *et al.*[17], suggesting that there is a tendency for the most abundant proteins of biological matrices to be retained at the polymer-rich phase. Nevertheless, the system presented a different degree of selectivity between the two studies, being observed that in the study of OVA removal from egg white only OVA was extracted for the PEG-rich phase, while in the present work other proteins were also present at the PEG-rich phase, as other peaks besides the HSA peak were present at the chromatograms (Supporting Information – Figure S.2). Therefore, the precipitate obtained from system 5 prepared with non-diluted PL consists of an AD-PL fraction that could be isolated without the need of back-extraction steps, once precipitates obtained for the PEG-salt systems could be easily recovered and resuspended in PBS.

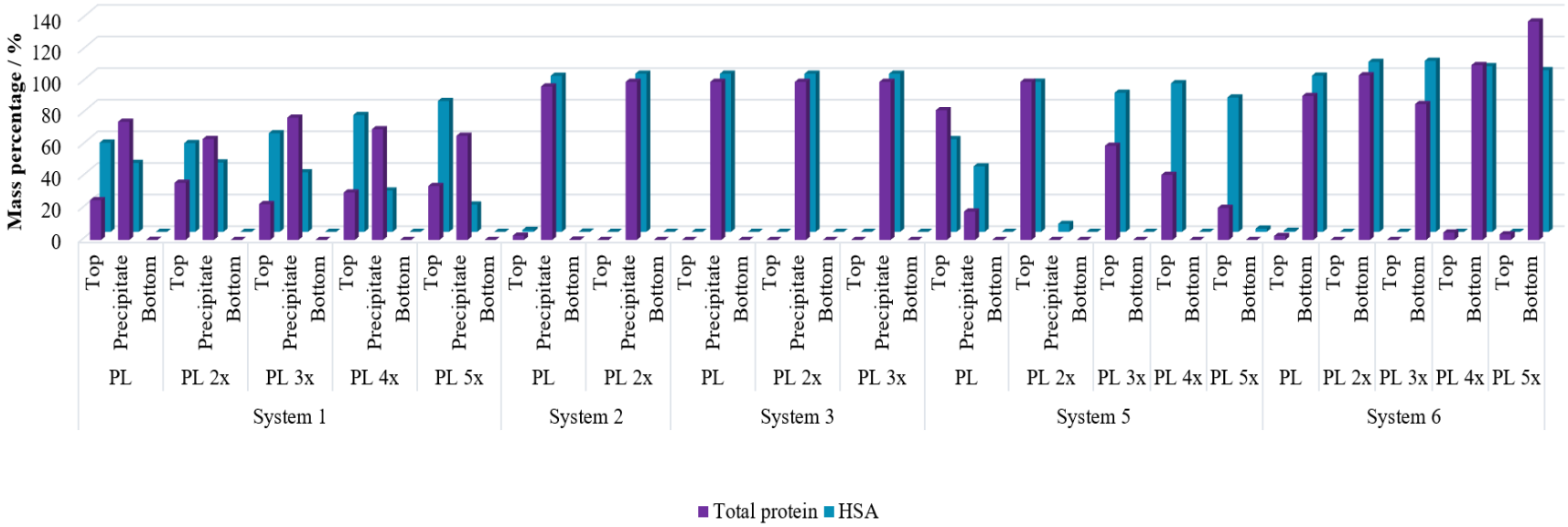

Figure IV.2 Total protein and HSA mass percentage for top phase, interphase precipitate (calculated through the difference between the total protein mass added to the system and the total protein mass quantified for top and bottom phases), and bottom phase for the various systems prepared with different PL dilution factors.

The partition of proteins in PEG-citrate buffer systems seems to be governed by the salting-out effect of the citrate-based salt and the hydrophobic interactions of proteins with PEG molecules. Due to the promising results obtained with system 5 but aiming to improve the selectivity for HSA, two additional systems composed of PEG with different molecular weights, namely PEG 1000 and PEG 2000, and citrate buffer were tested using PL with no dilution, and both formed a TPP system. Regarding the chromatographic profiles, it could be noticed that the partition of HSA for the top phase is more selective in the system 7 when compared to the system 5 (Supporting information – Figure S.2 and Figure S.3), and for system 8 no peaks were observed in any of the phases, suggesting that the higher hydrophobicity of the PEG-rich phase could induce irreversible protein precipitation, and therefore the system 8 was discarded for further studies. The results for the PEG-citrate buffer TPP systems prepared with no diluted PL (Figure IV.3) indicate that an increase in the hydrophobicity of the PEG-rich phase to a certain extent improve the selectivity of the phase for HSA and that above a given point have a deleterious effect over PL proteins.

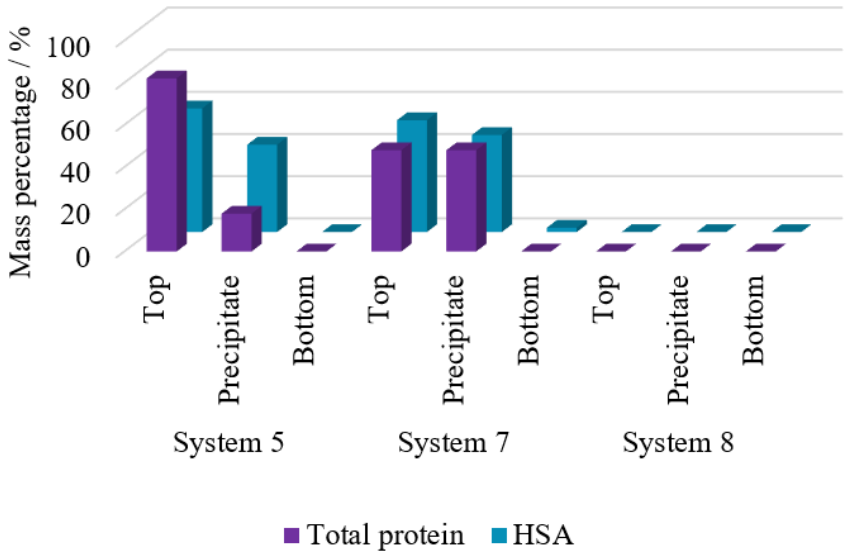

Figure IV.3 Total protein and HSA mass percentage for top phase, interphase precipitate (calculated through the difference between the total protein mass added to the system and the total protein mass quantified for top and bottom phases), and bottom phase for the PEG-citrate buffer TPP systems prepared with PL with no dilution.

Although total and selective removal of HSA from PL was not achieved for any of the systems tested, the TPP system 7 presents the best results, allowing the recovery at the interphase a precipitate of an AD-PL fraction, which retains the majority of PL proteins and contains approximately less 53% of HSA than original PL.

3.1.1. Scale-up

TPP system 7 was the best identified system for the removal of HSA from PL and therefore it was scaled-up to process the amount of PL needed to obtain an AD-PL fraction containing sufficient protein mass for the modification reaction. The system phases were analyzed by SDS-PAGE to ascertain their protein profile, and as can be seen from Figure IV.4 the only protein present at the top phase of system 7 is HSA whereas other PL-proteins precipitate. The electrophoretic protein profile for the AD-PL fraction, which corresponds to the precipitate, is similar to the electrophoretic PL profile, varying the intensity of the band corresponding to HSA.

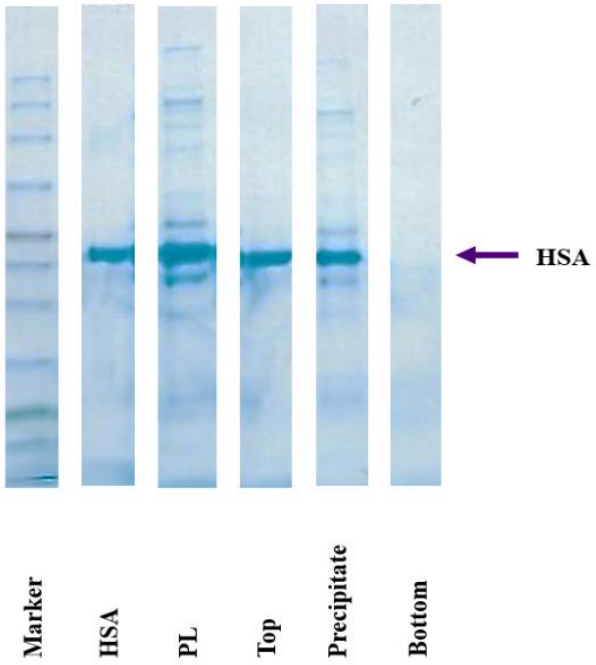

Figure IV.4 SDS-PAGE analysis of the phases of system 7 scaled-up prepared with no diluted PL.

From the SE-HPLC chromatograms used for HSA quantification (Figure IV.5), it can be concluded that the top phase contains majorly HSA and that the remaining proteins are retained at the interphase precipitate. Moreover, it could be also confirmed that no significant aggregation or fragmentation of the proteins occurred, since no other peaks at lower retention times were identified and thus the system provides a biocompatible environment for protein extraction.

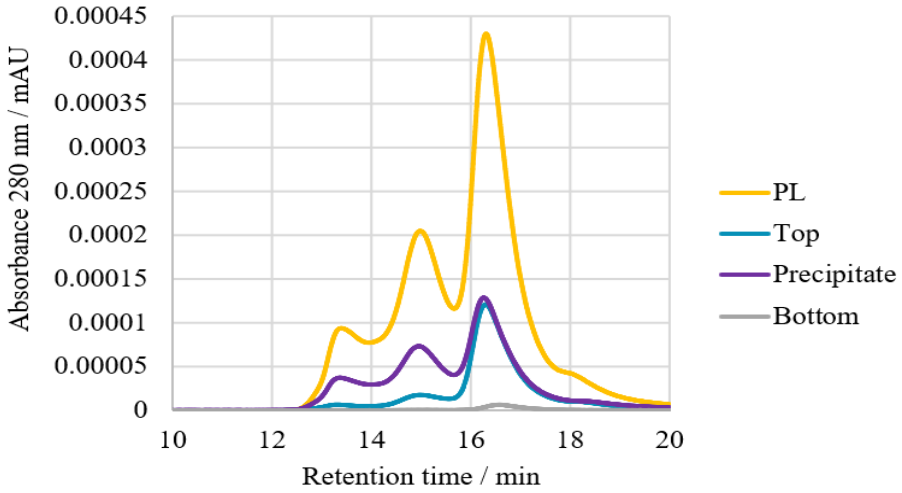

Figure IV.5 Size exclusion chromatograms of PL and top, precipitate, and bottom phases of the scale-up of system 7.

Despite a similar chromatographic profile was observed for the screening and scaled-up systems, i.e., the top phase contains majorly HSA, some differences were observed between the total protein and HSA mass percentage in each phase (Table IV.1). These results suggest that the optimization of steps that may influence mass transfer and phase separation processes, such as the centrifugation conditions and the time for equilibrium after centrifugation, its acritical request. Moreover, as reference for the following steps, the AD-PL as a result of the scaled-up system present 25% less HSA when compared to original PL.

Table IV.1 Total protein and HSA mass percentage for the screening and scale-up systems.

	Total protein (%)		**HSA (%)**	
	Screening system (2g)	Scale-up (52g)	Screening system (2g)	Scale-up (52g)
Top	48	19	53	25
Precipitate	48	59	46	55
Bottom	0	0	2	0

3.2. Synthesis of AD-PLMA and hydrogel formation

To guarantee that the remaining phase-forming components did not interfere with the methacrylation reaction or AD-PLMA photocrosslinking, an additional step of ultra-filtration was performed for the AD-PL fraction recovered from the scale-up of system 7. AD-PLMA hydrogels with different degrees of modification and concentrations were successfully formed by photopolymerization upon exposure of an AD-PLMA solution to UV irradiation (Figure IV.6), in the same conditions used for PLMA hydrogels fabrication, suggesting that the methacrylation reaction occurred. However, H^1-NMR analysis will be necessary to confirm the conjugation of AD-PL proteins with methacryloyl groups. Furthermore, a characterization of AD-PL, AD-PLMA100, and AD-PLMA300 by mass spectrometry will be useful to better understand the alterations in protein composition between PL and AD-PL and if the removal of HSA has influence over the degree of modification as also as the main modified protein.

The solubility of AD-PLMA and the viscosity of its aqueous solutions have shown similar to those of PLMA and therefore AD-PLMA could also be exploited as an injectable hydrogel. However, further characterization of AD-PLMA hydrogels, including mechanical tests, determination of water uptake, evaluation of porosity, *in vitro* cell culture studies, and i*n vitro* protein release studies, will be needed to understand the effect of HSA removal from PL in the overall performance of the hydrogels.

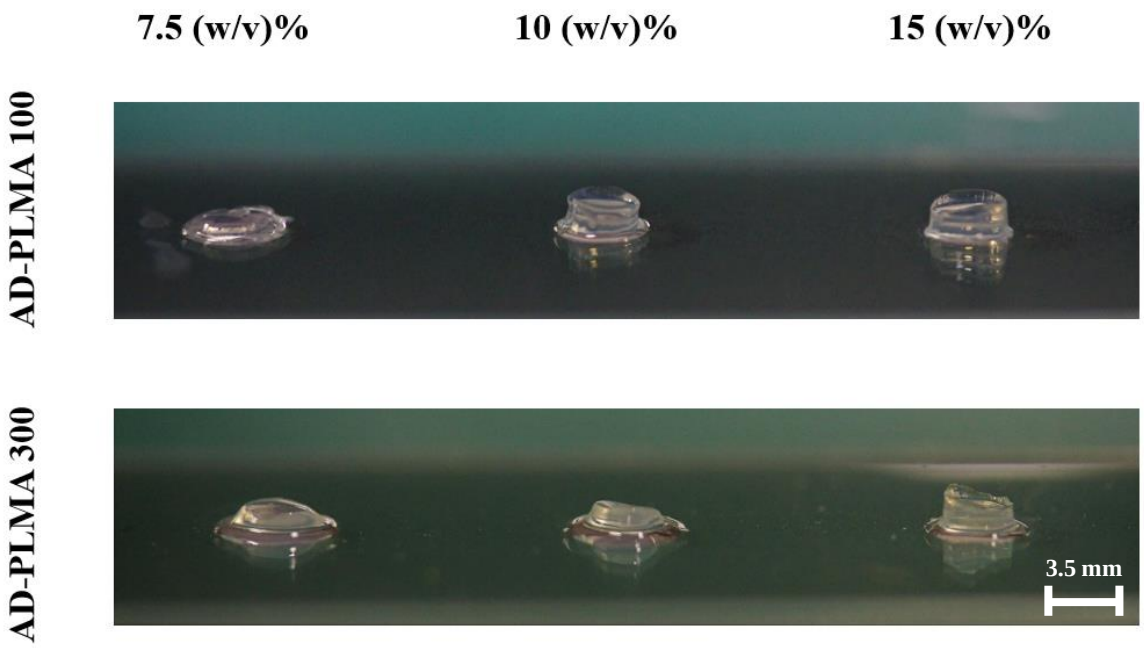

Figure IV.6 Crosslinked AD-PLMA hydrogels formed from PLMA100 and PLMA300 at 7.5%, 10%, and 15% (w/v).

4. Conclusions and future work

The removal of HSA from PL using TPP systems was here proposed and evaluated for the first time. To this end, a screening of eight ABS, including IL-salt, IL-polymer, and polymer-salt, were investigated for their ability to be used as TPP systems for the removal of HSA from PL, either by preferential partition of HSA at the interphase or by its selective partition to one of the phases. Among the different systems tested, PEG 1000/citrate buffer showed the best profit for the end application. Some differences were observed on the percentage of HSA removal between the screening (2g) and the scaled-up (52g) systems, meaning that experimental optimizations are still needed to improve the HSA removal at a larger scale. The processing of PL using ABS-TPP seems to do not affect the methacrylation reaction and hydrogel formation; however, further studies are needed to better understand the effect of HSA removal from PL in the hydrogel mechanical and biological performance. Also, despite the insights that the present work gives into PL-protein partition in TPP systems, replicates are needed to confirm some results. Although additional experiments are

still required, it was here demonstrated that the application of ABS-TPP is a successful technique for HSA removal from PL for further hydrogel fabrication.

References

1. Custódio, C. A., Reis, R. L. & Mano, J. F. Engineering Biomolecular Microenvironments for Cell Instructive Biomaterials. *Adv. Healthc. Mater.* **3**, 797–810 (2014).
2. Zhu, J. & Marchant, R. E. Design properties of hydrogel tissue-engineering scaffolds. *Expert Review of Medical Devices* **8**, 607–626 (2011).
3. Santos, S. C., Custódio, C. A. & Mano, J. F. Photopolymerizable Platelet Lysate Hydrogels for Customizable 3D Cell Culture Platforms. *Adv. Healthc. Mater.* **7**, 1800849 (2018).
4. Santos, S. C. N. da S., Sigurjonsson, Ó. E., Custódio, C. de A. & Mano, J. F. C. da L. Blood Plasma Derivatives for Tissue Engineering and Regenerative Medicine Therapies. *Tissue Eng. Part B Rev.* **24**, 454–462 (2018).
5. Lantigua, D., Nguyen, M. A., Wu, X., Suvarnapathaki, S., Kwon, S., Gavin, W. & Camci-Unal, G. Synthesis and characterization of photocrosslinkable albumin-based hydrogels for biomedical applications. *Soft Matter* **16**, 9242–9252 (2020).
6. Ong, J., Zhao, J., Levy, G. K., Macdonald, J., Justin, A. W. & Markaki, A. E. Functionalisation of a heat-derived and bio-inert albumin hydrogel with extracellular matrix by air plasma treatment. *Sci. Rep.* **10**, 12429 (2020).
7. Freire, M. G., Cláudio, A. F. M., Araújo, J. M. M., Coutinho, J. A. P., Marrucho, I. M., Lopes, J. N. C. & Rebelo, L. P. N. Aqueous biphasic systems: a boost brought about by using ionic liquids. *Chem. Soc. Rev.* **41**, 4966 (2012).
8. Albertsson, P.-Å. Partition of Proteins in Liquid Polymer–Polymer Two-Phase Systems. *Nature* **182**, 709–711 (1958).
9. Rosa, P. A. J., Ferreira, I. F., Azevedo, A. M. & Aires-Barros, M. R. Aqueous two-phase systems: A viable platform in the manufacturing of biopharmaceuticals. *Journal of Chromatography A* **1217**, 2296–2305 (2010).
10. Asenjo, J. A. & Andrews, B. A. Aqueous two-phase systems for protein separation: Phase separation and applications. *J. Chromatogr. A* **1238**, 1–10 (2012).
11. Castro, L. S., Pereira, P., Passarinha, L. A., Freire, M. G. & Pedro, A. Q. Enhanced performance of polymer-polymer aqueous two-phase systems using ionic liquids as adjuvants towards the purification of recombinant proteins. *Sep. Purif. Technol.* **248**,

117051 (2020).

12. Gutowski, K. E., Broker, G. A., Willauer, H. D., Huddleston, J. G., Swatloski, R. P., Holbrey, J. D. & Rogers, R. D. Controlling the Aqueous Miscibility of Ionic Liquids: Aqueous Biphasic Systems of Water-Miscible Ionic Liquids and Water-Structuring Salts for Recycle, Metathesis, and Separations. *J. Am. Chem. Soc.* **125**, 6632–6633 (2003).
13. Alvarez-Guerra, E. & Irabien, A. Ionic Liquid-Based Three Phase Partitioning (ILTPP) for Lactoferrin Recovery. *Sep. Sci. Technol.* **49**, 957–965 (2014).
14. Dennison, C. & Lovrien, R. Three Phase Partitioning: Concentration and Purification of Proteins. *Protein Expr. Purif.* **11**, 149–161 (1997).
15. Capela, E. V., Santiago, A. E., Rufino, A. F. C. S., Tavares, A. P. M., Pereira, M. M., Mohamadou, A., Aires-Barros, M. R., Coutinho, J. A. P., Azevedo, A. M. & Freire, M. G. Sustainable strategies based on glycine–betaine analogue ionic liquids for the recovery of monoclonal antibodies from cell culture supernatants. *Green Chem.* **21**, 5671–5682 (2019).
16. Pereira, M. M., Pedro, S. N., Gomes, J., Sintra, T. E., Ventura, S. P. M., Coutinho, J. A. P., Freire, M. G. & Mohamadou, A. Synthesis and characterization of analogues of glycine-betaine ionic liquids and their use in the formation of aqueous biphasic systems. *Fluid Phase Equilib.* **494**, 239–245 (2019).
17. Pereira, M. M., Cruz, R. A. P., Almeida, M. R., Lima, Á. S., Coutinho, J. A. P. & Freire, M. G. Single-step purification of ovalbumin from egg white using aqueous biphasic systems. *Process Biochem.* **51**, 781–791 (2016).
18. Pereira, M. M., Pedro, S. N., Quental, M. V., Lima, Á. S., Coutinho, J. A. P. & Freire, M. G. Enhanced extraction of bovine serum albumin with aqueous biphasic systems of phosphonium- and ammonium-based ionic liquids. *J. Biotechnol.* **206**, 17–25 (2015).
19. Mondal, D., Sharma, M., Quental, M. V., Tavares, A. P. M., Prasad, K. & Freire, M. G. Suitability of bio-based ionic liquids for the extraction and purification of IgG antibodies. *Green Chem.* **18**, 6071–6081 (2016).
20. Ferreira, A. M., Faustino, V. F. M., Mondal, D., Coutinho, J. A. P. & Freire, M. G. Improving the extraction and purification of immunoglobulin G by the use of ionic liquids as adjuvants in aqueous biphasic systems. *J. Biotechnol.* **236**, 166–175 (2016).

21. Bharmoria, P., Mondal, D., Pereira, M. M., Neves, M. C., Almeida, M. R., Gomes, M. C., Mano, J. F., Bdikin, I., Ferreira, R. A. S., Coutinho, J. A. P. & Freire, M. G. Instantaneous fibrillation of egg white proteome with ionic liquid and macromolecular crowding. *Commun. Mater.* **1**, 1–13 (2020).
22. Quental, M. V., Caban, M., Pereira, M. M., Stepnowski, P., Coutinho, J. A. P. & Freire, M. G. Enhanced extraction of proteins using cholinium-based ionic liquids as phase-forming components of aqueous biphasic systems. *Biotechnol. J.* **10**, 1457–1466 (2015).
23. Taha, M., Quental, M. V., Correia, I., Freire, M. G. & Coutinho, J. A. P. Extraction and stability of bovine serum albumin (BSA) using cholinium-based Good's buffers ionic liquids. *Process Biochem.* **50**, 1158–1166 (2015).

Chapter V

Conclusions and future perspectives

Conventional two-dimensional (2D) cell culture assays have been routinely used as *in vitro* models by researchers to study fundamental mechanisms underlying cell behavior and tissue development and by pharmaceutical industries in drug development. Despite the ease of use and well-established protocols offered by 2D cell culture methodologies, 2D platforms lack important features of the physiological cellular microenvironment and, therefore, 2D cultured cells behave differently from *in vivo* growing cells and the results obtained from such assays could be misleading and non-predictive. On an attempt to overcome 2D cell culture shortcomings and increase the reliability of cell-based assays, three-dimensional (3D) cell culture models have emerged, providing a cellular microenvironment that better resembles the extracellular matrix (ECM), and thus bridge the gap between 2D models and *in vivo* tissues.

In this transition from the second to the third dimension, scaffolds have been playing a major role, since their biochemical and biophysical properties could be manipulated to create physiological relevant *in vitro* cellular microenvironments. The materials and fabrication techniques dictate the features of the scaffold and therefore the design of scaffolds is fundamental for the advances in 3D cell culture practices and tissue engineering (TE) applications. Proteins have been attracting considerable attention as biomaterials for the development of scaffolds, due to their inherent biocompatibility, biodegradability, bioactivity, and biochemical resemblance with native ECM, being their major constituents. In particular, proteins naturally occurring in the human body, including collagen and its derivative gelatin, elastin, keratin, and blood plasma derived proteins, have been widely explored in combination with various fabrication techniques, of which stand out electrospinning, chemical, biological, and photochemical crosslinking, and a plethora of scaffolds with distinct mechanical, structural and biological properties is described on the literature. The ability to precisely manipulate scaffolds properties and the continuous research have allowing not only to further our knowledge on the influence of cell microenvironment on cell behavior and tissue development as also to recreate the ECM *in vitro* with higher mimicry levels.

Currently, collagen type I and solubilized basement membrane of Engelbreth-Holm-Swarm mouse sarcoma cells gels have been routinely used as platforms for 3D cell culture include the and collagen type I. However, despite their reported ability to recapitulate complex cellular processes, the difficult in its handling and xenogeneic origin have been

raising some concerns and limit their clinical application. In this sense, METATISSUE have proposed a novel photopolymerizable hydrogel derived from human platelet lysates (PL) proteins that overcome the drawbacks presented for the previous mentioned platforms. Furthermore, they have tunable mechanical properties and their allogenic origin makes it of great interest for personalized medicine. However, the PL-based hydrogels seeded cells do not adhere properly to the hydrogel. The high amounts of human serum albumin (HSA) in PL was hypothesized as a possible explanation for such results and therefore its removal presents as a reliable strategy to improve the bioactivity of PL-based hydrogels. Therefore, the main goal of the presented work was the removal of HSA from PL.

Aqueous biphasic systems (ABS) have been attracting considerable attention for the extraction of biomolecules, since they offer a biocompatible environment due to the high-water content, are considered an environmentally friendly technique, can be easily scaled-up and are cost-effective, if well designed. More recently, the ability of ABS to form three phase partitioning (TPP) systems have been attracting considerable attention for the purification proteins from biological matrices. Herein, ABS-based TPP systems were explored to remove HSA from PL for the first time, either through the precipitation of HSA or preferential partition of HSA for one of the phases. A screening of eight ABS with different phase-forming components was performed, comprising IL-salt, IL-polymer, and polymer-salt systems. The results demonstrate that the protein partition in ABS-TPP systems is a complex process that is not only dependent on the system properties as also on the composition of the biological matrix. Furthermore, the PEG 1000/citrate buffer ABS-TPP system was the best identified system for HSA removal from PL, being observed a preferential partition of HSA for the PEG-rich phase and the precipitation of the remaining PL proteins at the interphase. These could be easily isolated and used as an albumin-depleted PL (AD-PL) fraction for the fabrication of hydrogels. The obtained AD-PL fraction from the scale-up system was methacrylated following the same procedure proposed for the PL-based hydrogel fabrication and hydrogels were successfully photopolymerized. However, further assays are needed to: (i) optimize the HSA removal in the scale-up system; (ii) to characterize the formed AD-PL-based hydrogels and determine their properties, namely by ^{1}H NMR, mass spectrometry, mechanical tests, scanning electron microscopy, water up-take, proteins and growth factors release assays, *in vitro* cell seeding and encapsulation; and (iii) to address if the step of removal of ABS phase-forming components from the AD-PL is

required or if these could improve the hydrogels properties, while avoiding the use of an extra step.

Supporting information

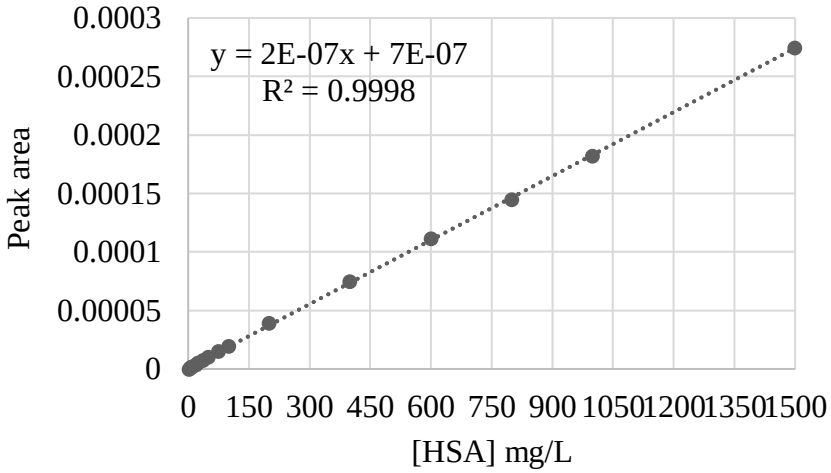

Figure S.1 Calibration curve used for HSA quantification by SE-HPLC obtained from commercial HSA solutions with 2.5-1500 mg/L.

Table S.1 Total protein and HSA mass quantified by Pierce BCA and SE-HPLC, respectively, for top phase, interphase precipitate (calculated through the difference between the total protein mass added to the system and the total protein mass quantified for top and bottom phases), and bottom phase for the various systems prepared with different PL dilutions factors. Top – Top phase; P – Interphase precipitate; Bot – Bottom phase; TP – Total protein.

		System 1 [$BuNC_4$]Br + KH_2PO_4/K_2HPO_4				**System 2** [$BuPC_2$]Br + KH_2PO_4/K_2HPO_4				**System 3** [P_{4444}]Br + KH_2PO_4/K_2HPO_4				**System 4** [P_{4444}]Br + $K_3C_6H_5O_7$/$C_6H_8O_7$				**System 5** PEG 400 + $K_3C_6H_5O_7$/$C_6H_8O_7$				**System 6** ChCl + PPG 400		
		PL mg	Top mg	P mg	Bot mg	PL mg	Top mg	P mg	Bot mg	PL mg	Top mg	P mg	Bot mg	PL mg	Top mg	P mg	Bot mg	PL mg	Top mg	P mg	Bot mg	PL mg	Top mg	Bot mg
PL	TP	38.63	9.71	28.90	0.02	38.94	1.10	37.74	0.10	38.56	0.00	38.46	0.10	39.35	-	-	0.20	49.88	40.90	8.98	0.00	46.20	1.10	42.10
	HSA	34.12	19.25	14.87	0.00	34.39	0.42	33.95	0.02	34.06	0.00	34.06	0.00	34.75	-	-	0.00	44.06	25.81	18.25	0.00	40.81	0.25	40.33
PL 2x	TP	16.21	5.86	10.35	0.00	16.22	0.00	16.22	0.00	16.24	0.00	16.24	0.00	16.60	-	-	0.00	21.09	21.20	-0.11	0.00	19.66	0.00	20.50
	HSA	16.10	9.03	7.07	0.00	16.11	0.00	16.11	0.00	16.14	0.00	16.14	0.00	16.49	-	-	0.00	20.95	19.98	0.97	0.00	19.53	0.00	21.00
PL 3x	TP	13.25	3.00	10.25	0.00	13.20	-	-	0.00	13.20	0.00	13.20	0.01	13.90	-	-	0.00	17.01	10.13	-	0.00	15.93	0.00	13.69
	HSA	11.88	7.42	4.46	0.00	11.83	-	-	0.00	11.83	0.00	11.83	0.00	12.46	-	-	0.00	15.24	13.43	-	0.00	14.28	0.00	15.45
PL 4x	TP	8.33	2.50	5.83	0.00	8.47	-	-	0.03	8.36	-	-	0.02	8.48	-	-	-	10.82	4.46	-	0.00	10.01	0.47	11.07
	HSA	9.85	7.28	2.57	0.00	10.01	-	-	0.00	9.88	-	-	0.00	10.00	-	-	0.00	12.78	11.98	-	0.00	11.82	0.00	12.39
PL 5x	TP	5.84	1.99	3.85	0.00	5.76	-	-	0.00	5.81	-	-	0.01	6.07	-	-	0.00	7.52	1.53	-	0.00	6.93	0.24	9.57
	HSA	7.25	6.01	1.24	0.00	7.16	-	-	-	7.22	-	-	0.00	7.55	-	-	-	9.34	7.92	-	0.16	8.61	0.00	8.80

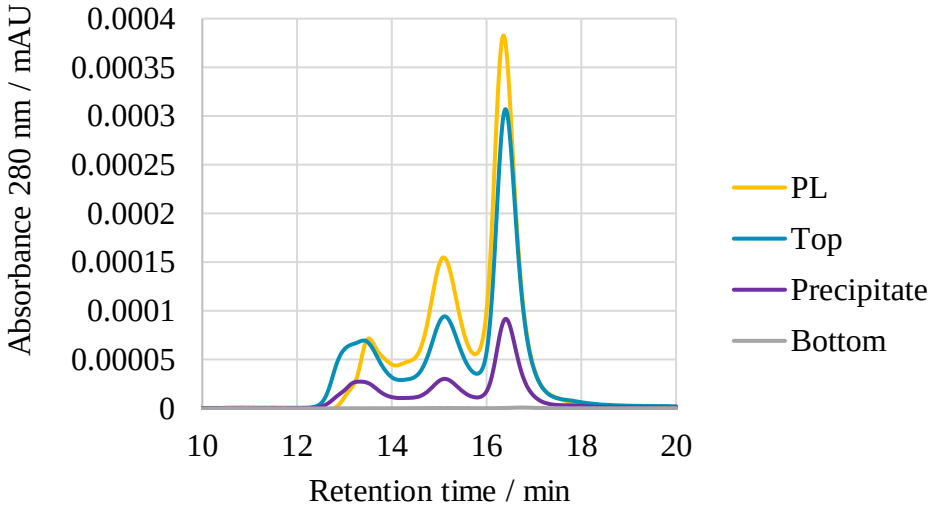

Figure S.2 Size exclusion chromatograms of PL and top, precipitate, and bottom phases of system 5.

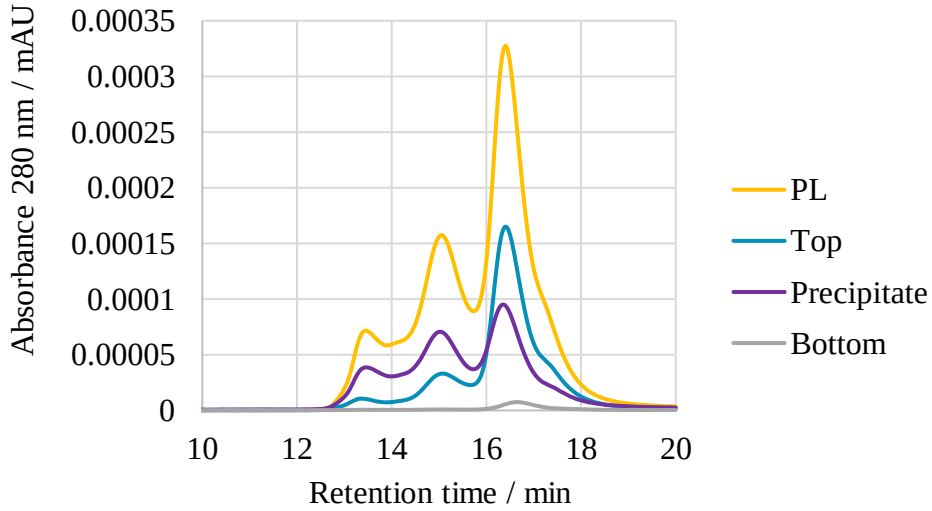

Figure S.3 Size exclusion chromatograms of PL and top, precipitate, and bottom phases of system 7.